Neuroimaging Study of Prenatal Alcohol Exposure Effects on Structural and Functional Connectivity in Children

Jia Fan

Thesis Presented for the Degree of

DOCTOR OF PHILOSOPHY

in the Department of Human Biology

UNIVERSITY OF CAPE TOWN

March, 2015

Declaration

I, ***Jia Fan***, hereby declare that the work on which this thesis is my own unaided work both in concept and execution, and that apart from the normal guidance from my supervisors, I have received no assistance.

This thesis has been presented by me for examination for the degree of *Doctor of Philosophy* in Medicine in Biomedical Engineering.

_____

Signature

_____

Date

Abstract

Neuroimaging Study of Prenatal Alcohol Exposure Effects on Structural and Functional Connectivity in Children

Jia Fan March, 2015

Fetal alcohol spectrum disorders (FASD) describe the spectrum of cognitive, behavioural and neurological impairments associated with prenatal alcohol exposure (PAE). Diffusion tensor imaging (DTI) and resting-state functional MRI (rs-fMRI) were used to assess effects of PAE on microstructural integrities of cerebellar and cerebral white matters (WM) and on resting-state functional connectivity (RSFC) in gray matter (GM) in children with varying degrees of FASD severity (fetal alcohol syndrome (FAS) and partial FAS (PFAS)), as well as nonsyndromal heavily exposed (HE) children. Children with FAS revealed lower fractional anisotropy (FA) bilaterally in the superior peduncles. Mean diffusivity (MD) was higher in the left middle peduncle in children with FAS or PFAS (FAS/PFAS). Mediation of effects of PAE on eyeblink conditioning (EBC) provided statistical evidence that poorer microstructural integrity in these regions may play an important role in the EBC deficit observed in children with FASD. The FAS/PFAS children also revealed lower FA and/or higher MD in 7 cortical WM regions and lower RSFC in 5 GM regions within 5 networks. Four of the 7 WM and 3 of the 5 GM regions also showed alterations in HE children, providing evidence that alterations in nonsyndromal children are less extensive and that some regions appear to be relatively spared. Alterations in DTI parameters (FA and MD) were dose dependent in many, but not all, of the regions where group differences were detected, specifically in the left (L) and right (R) superior peduncles, L middle peduncle, L inferior longitudinal fasciculus, medial (M) splenium of the corpus callosum (CC), and M isthmus of the CC. The WM deficits were attributable to increased radial diffusivity (RD) rather than decreased axial diffusivity (AD), suggesting poorer axon packing density and/or myelination. Increasing alcohol exposure was associated with reduced fractional amplitude of low frequency fluctuations (fALFF), indicating changes in functional connectivity in the default mode, salience, and dorsal attention networks. The locations of the WM alterations found with DTI suggest that the compromised RSFC found in 3 of the 5 networks could be attributable to WM deficits in tracts providing intra-network connections.

Acknowledgements

I would like to express my sincere thanks to the following people or institutes who assisted with the work presented in this thesis:

- First and foremost, my supervisor, Professor Ernesta M. Meintjes, for her input, guidance and advice throughout this project;
- My co-supervisor, Dr Paul A. Taylor, for always making time when needed, ideas, motivation, and assistance;
- All other co-authors of my article, especially to Professors Sandra and Joseph Jacobson and Dr Bruce Spottiswoode, for their input and suggestions;
- My colleagues, Dr Ali Alhamud, Muhammad Saleh, Dr Daniel Auger, Dr Ian Burger, and others from my research group, for the useful discussions on research related topics;
- The following organisations that provided the funding and/or the resources used in this work:
    - National Institutes of Health/National Institute on Alcohol Abuse and Alcoholism (NIAAA) grants R01AA016781, R21AA017410, U01-AA014790;
    - South African Research Chairs Initiative of the Department of Science and Technology and National Research Foundation of South Africa;
    - Medical Research Council of South Africa;
    - CUBIC radiographers Marie-Louise de Villiers and Nailah Maroof, and our UCT and WSU research staff Nicolette Hamman, Mariska Pienaar, Maggie September, Emma Makin, and Renee Sun;
    - The three dysmorphologists H.E. Hoyme, L.K. Robinson, and N. Khaole, for the dysmorphology examinations of the children in conjunction with the NIAAA Collaborative Initiative on Fetal Alcohol Spectrum Disorders;
- All mothers and children who have participated in our Cape Town research program.

List of Abbreviations

Abbreviation	Description
3D	three dimensional
AA	absolute alcohol
AA/day	absolute alcohol consumed per day across pregnancy
AA/occasion	absolute alcohol consumed per occasion across pregnancy
AD	axial diffusivity
ALFF	amplitude of low-frequency fluctuation
ANCOVA	analysis of covariance
AP-PA	anterior-posterior and posterior-anterior
ARND	alcohol-related neurodevelopmental disorders
BCC	body of corpus callosum
BOLD	blood oxygenation level dependent
C	carbon
CC	corpus callosum
CNS	central nervous system
Cr	crus
CTLS	Cape Town Longitudinal Study
CS	conditioned stimulus
CSF	cerebrospinal fluid
CST	corticospinal tracts
Ctl	control
CUBIC	Cape Universities Brain Imaging Center
days/week	drinking days per week across pregnancy
D-Att	dorsal attention

Abbreviation	Description
DM	default mode
DMN	default mode network
DT	diffusion tensor
DTI	diffusion tensor imaging
DWI	diffusion weighted image
EBC	eyeblink conditioning
EPI	echo planar imaging
Exe	executive control
FA	fractional anisotropy
fALFF	fractional amplitude of low-frequency fluctuations
FAS	fetal alcohol syndrome
FAS/PFAS	combined FAS and PFAS group
FASD	fetal alcohol spectrum disorder
FCP	Functional Connectome Project
fMRI	functional magnetic resonance imaging
FOV	field of view
FWHM	full-width at half maximum
GCC	genu of corpus callosum
GM	gray matter
HE	heavily exposed
Hz	hertz
IC	independent component
ICA	independent component analysis
ICC	isthmus of corpus callosum
ILF	inferior longitudinal fasciculus

Abbreviation	Description
IOM	Institute of Medicine
IQ	intelligence quotient
JSAIS	Junior South African Intelligence Scale
L	left
LFF	low-frequency fluctuation
M	medial
M_0	initial net magnetization
M_{xy}	transverse magnetic component
M_z	longitudinal magnetic component
MD	mean diffusivity
MFG	medial frontal gyrus
MNI	Montreal Neurological Institute
MPRAGE	magnetization-prepared rapid gradient echo
MRI	magnetic resonance imaging
oz	ounces
PAE	prenatal alcohol exposure
PET	positron emission tomography
PFAS	partial fetal alcohol syndrome
POG	postcentral gyrus
PRG	precentral gyrus
R	right
ReHo	regional homogeneity
RD	radial diffusivity
RSFC	resting-state functional connectivity
rs-fMRI	resting-state function magnetic resonance imaging

Abbreviation	Description
RF	radiofrequency
ROI	region of interest
RSN	resting-state network
Sal	salience
SCC	splenium of corpus callosum
SD	standard deviation
SES	socioeconomic status
SLF	superior longitudinal fasciculus
T1W	T1-weighted
TBSS	tract-based spatial statistics
TE	echo time
TI	inversion time
TR	repetition time
TT	Talairach-Tournoux
UCT	University of Cape Town
US	unconditioned stimulus
V-Att	ventral attention
WISC-IV	Wechsler Intelligence Scale for Children-IV
WM	white matter
WSU	Wayne State University
yr	year

Table of Contents

List of Figures

List of Tables

Preface

This thesis presents a neuroimaging study using magnetic resonance imaging (MRI) to noninvasively assess the impacts of prenatal alcohol exposure (PAE) on the developing brains of school-age children with fetal alcohol spectrum disorders (FASD). Two MRI modalities, diffusion tensor imaging (DTI) and resting-state functional MRI (rs-fMRI), were used to examine the microstructural properties of white matter (WM) and functional connectivity in gray matter (GM), respectively. The cohort in whom this data were collected is unique as mothers were recruited during pregnancy and their drinking histories were recorded at regular intervals during that time, along with supplementary information of potential control factors such as cigarette smoking and other substance usage.

The content of this thesis includes three independent articles that are presented in chapters 2, 3 and 4. While all of these chapters are related to the central theme of associating alcohol exposure with structural and functional brain connectivity, each has been prepared as an independent manuscript and as such includes its own introduction, methodology, results, discussion and conclusion. Since each chapter provides the necessary background, procedures, and key findings of that individual study, we note that this format of the thesis does necessarily lead to repetition of some information.

The content of each chapter is as follows:

- **Chapter 1** contains a brief introduction of the overall purpose and scope of this thesis, as well as an overview of basic MRI physics and the neuroimaging methods employed in this study – DTI and rs-fMRI, as well as an in-depth literature review of structural, DTI and rs-fMRI studies that have been conducted on individuals with FASD.
- **Chapter 2** describes the WM deficits in the cerebellar peduncles in children with FASD, as well as the mediation of effects of PAE on eyeblink conditioning by these deficits. This article, which has been accepted for publication in Human Brain Mapping, was co-authored by Ernesta M. Meintjes, Christopher D. Molteno, Bruce S. Spottiswoode, Neil C. Dodge, Alkathafi A. Alhamud, Mark E. Stanton, Bradley S. Peterson, Joseph L. Jacobson,

Figureand Sandra W. Jacobson. My major contributions to the article were assistance with data acquisition, as well as primary responsibility for data analyses, interpretation of the findings and the writing of the article.

- **Chapter 3** contains another DTI study, which localizes and quantitatively assesses the adverse impacts of PAE on cortical WM. We investigate how the effects of PAE vary with severity of FASD and how the effects relate to the extent of maternal drinking.
- **Chapter 4** describes the results of a rs-fMRI study assessing the effects of PAE on multiple resting state networks (RSNs) across the brain, again as a function of both diagnosis and extent of alcohol exposure.
- **Chapter 5** provides a comprehensive discussion of the three studies, summarizes the main findings of the individual articles and highlights the structure-function relations associated with PAE.
- **Chapter 6** presents the conclusions of the study.

The majority of this work has been presented at conferences and appears in the following proceedings:

- Jia Fan, Joseph L. Jacobson, Alkathafi A. Alhamud, Roland V. Baasch, Christopher D. Molteno, Bradley S. Peterson, Sandra W. Jacobson, Bruce S. Spottiswoode, and Ernesta M. Meintjes, 'DTI Study of the Cerebellar Peduncles in Children with Fetal Alcohol Spectrum Disorder', 17th OHBM, Beijing, China, June 2012.
- Jia Fan, Sandra W. Jacobson, Christopher D. Molteno, Bruce S. Spottiswoode, Joseph L. Jacobson, and Ernesta M. Meintjes, 'DTI study of white matter abnormalities in children with fetal alcohol spectrum disorders', 18th OHBM, Seattle, USA, June 2013.
- Jia Fan, Paul A. Taylor, Christopher D. Molteno, Suril Gohel, Bharat B. Biswal, Sandra W. Jacobson, Joseph L. Jacobson, and Ernesta M. Meintjes, 'Changes in resting-state functional connectivity in children with prenatal alcohol exposure', 19th OHBM, Hamburg, Germany, June 2014.
- Jia Fan, Paul A. Taylor, Sandra W. Jacobson, Christopher D. Molteno, Suril Gohel, Bharat B. Biswal, Joseph L. Jacobson, and Ernesta M. Meintjes, 'Changes in resting-state functional

connectivity in children with fetal alcohol spectrum disorders', 20th OHBM, Hawaii, USA, June 2015.

- Jia Fan, Sandra W. Jacobson, Christopher D. Molteno, Bruce S. Spottiswoode, Neil C. Dodge, Alkathafi A. Alhamud, Mark E. Stanton, Bradley S. Peterson, Joseph L. Jacobson, and Ernesta M. Meintjes, 'White matter integrity of the cerebellar peduncles as a mediator of effects of prenatal alcohol exposure on eyeblink conditioning', 12th SONA, Durban, South Africa, March 2015.

Additionally, the following article (comprising the contents of Chapter 2) has been accepted for publication in the journal Human Brain Mapping:

- Jia Fan, Ernesta M. Meintjes, Christopher D. Molteno, Bruce S. Spottiswoode, Neil C. Dodge, Alkathafi A. Alhamud, Mark E. Stanton, Bradley S. Peterson, Joseph L. Jacobson, and Sandra W. Jacobson (2015): White matter integrity of the cerebellar peduncles as a mediator of effects of prenatal alcohol exposure on eyeblink conditioning. Human Brain Mapping, 36(7):2470-2482.

Chapter 1

Introduction

1.1 Project Purpose and Scope

Prenatal alcohol exposure (PAE) has numerous adverse consequences on fetal development, which are often encompassed under an umbrella term, fetal alcohol spectrum disorder (FASD). As detailed below, these include the following clinical categories (in decreasing order of severity): fetal alcohol syndrome (FAS), partial FAS (PFAS) and alcohol-related neurodevelopmental disorder (ARND). There are also children with confirmed prenatal alcohol exposure who do not exhibit the FAS facial phenotype or meet criteria for a clinical diagnosis. In our studies these children have been termed nonsyndromal heavily exposed (HE). The number of children with FASD in the Cape Coloured population in South Africa is among the highest in the world (May et al., 2000), due to very heavy maternal drinking during pregnancy in this community. In this work we use noninvasive neuroimaging of children from this community to study the effects of PAE on both the structural and functional connectivity properties of the brain during pediatric development.

The participants in this study had been recruited as part of the Cape Town Longitudinal Study (CTLS) (Jacobson et al., 2008) during the period from 1999 to 2002 at an antenatal clinic in Cape Town in an area where there is known to be heavy alcohol consumption. Each mother was interviewed regarding her alcohol consumption using a timeline follow-back approach to determine incidence and amount of drinking on a day-by-day basis during a typical 2-week period both at time of conception and time of recruitment (Jacobson et al., 2002). Each of the alcohol-exposed children was clinically diagnosed for FASD by expert dysmorphologists. Several other characteristics were also recorded, such as the numbers of cigarettes smoked per day and any drug usage, which represent additional factors that may contribute to alterations in brain development. Magnetic resonance imaging (MRI) of each child included both resting state functional MRI (rs-fMRI) and diffusion tensor imaging (DTI), which yield information on brain

functional and structural connectivity, respectively. In addition, participants performed some behavioral tasks, such as eyeblink conditioning (EBC) and IQ tests, during separate laboratory visits providing measures of neurocognitive abilities. In total, this dataset provides a unique opportunity to study abnormalities in brain development in relation to both diagnosis and the specific degree of alcohol exposure in a cohort of well-characterised school-age children with varying degrees of FASD severity.

Eyeblink conditioning (EBC), a cerebellar mediated Pavlovian conditioning paradigm between an auditory tone and the application of a small air puff, has been shown to be a remarkably sensitive marker of alcohol exposure (Jacobson et al., 2008, 2011). Typically, children with more severe FASD diagnoses are less likely to meet the conditioning criterion. Even nonsyndromal heavily exposed children who do not meet clinical criteria for an FASD diagnosis, have been shown to exhibit EBC deficits similar to those of the more severely affected syndromal children, making EBC potentially a very sensitive marker of prenatal alcohol exposure (Jacobson et al., 2008, 2011; Coffin et al. 2005). Since the cerebellar peduncles constitute the principal white matter (WM) tracts that transmit the different signals required for successful conditioning (Christian and Thompson, 2003), examing the integrity of these tracts using DTI were a key focus of this study.

DTI yields useful measures of white matter (WM) properties, with parameters such as fractional anisotropy (FA) and mean diffusivity (MD) often associated with fiber integrity, density and maturation. A previous cerebellar DTI study in a small pilot sample found greater radial diffusivity (RD) and lower FA in the left middle cerebellar peduncle in children with FAS or PFAS compared to healthy controls (Spottiswoode et al., 2011). Lower FA in this region was associated with poorer performance on trace EBC, but the study lacked power to investigate the association with short delay EBC. These results require validation in a larger sample, as well as an extension to cortical WM.

Rs-fMRI is a popular methodology to identify several networks of regions in the brain that are functionally correlated while no explicit task is being performed (Biswal et al., 1995). Many of the observed rs-fMRI networks have been shown to correspond to those seen previously during

individual task-based fMRI sessions, but rs-fMRI has the advantage of allowing one to study several networks from a single acquisition. Few studies have previously examined resting state functional connectivity (RSFC) in FASD (Wozniak et al., 2011, 2013; Kim et al., 2014; Santhanam et al., 2011). Our study is the first to quantitatively assess PAE effects on *multiple* resting state networks (RSNs) in children with FASD. In combination with DTI results, we additionally investigated whether regions exhibiting decreased functional connectivity with alcohol exposure were connected by tracts in which we found regions showing exposure-related WM differences.

The main aims of this study were: (1) to investigate the effects of alcohol exposure on DTI measures in the cerebellar peduncles, as well as associations of DTI measures in regions showing PAE effects with EBC performance; (2) to assess the extent and locations of effects of PAE on cortical WM; (3) to assess the effects of PAE on multiple resting state networks (RSNs) throughout the brain; and (4) to combine rs-fMRI and DTI results in order to investigate whether local RSFC changes may be due to changes in WM tracts connecting affected regions.

1.2 Background and Literature Review

1.2.1 Prenatal Alcohol Exposure

FASD refers to the spectrum of disorders that result from PAE. These include life-long cognitive and behavioural impairments, as well as potential structural damage to the brain (Jacobson and Jacobson, 2002; Burden et al., 2005; Kalberg et al., 2006; Mukherjee et al., 2006; Spadoni et al., 2007). While PAE does not always result in FASD for a child, there is no medical guideline for safe levels of alcohol consumption during pregnancy (Barr and Streissguth, 2001; Mattson and Riley, 1998; Spadoni et al., 2007).

Due to increased public attention, the US Center for Disease Control and Prevention (2012) reported that, among a sample of 13,880 pregnant women in the USA between 2006 and 2010, 7.6% admitted to consuming alcohol during the prior 30 days and 1.4% to binge drinking. The

prevalence of FASD in the US is estimated to be as high as 2-5% of the total population (May et al., 2009) and has been identified in all racial and ethnic groups (Abel, 1995).

An unusually high incidence of alcohol abuse has been reported in the Cape Colored community in the Western Cape Province of South Africa, with the incidence of FAS being 18 to 141 times higher than in the United States (May et al., 2000). The Cape Colored population is a mixed ancestry group, originally from Africa, Europe and Malaysia. Children with FASD are very prevalent in this community (Croxford and Viljoen, 1999) due both to poor psychosocial circumstances and the residual impact of the now-outlawed *dop* system whereby labourers were paid in part with wine.

Several specific criteria for FASD diagnosis have been established. Two diagnostic sets, the 1996 Institute of Medicine (IOM) criteria (Stratton et al., 1996) and the Washington criteria (Astley and Clarren, 2000), are commonly used for evaluation of FASD (Hoyme et al., 2005). However, both have significant drawbacks in their practical application. The 1996 IOM criteria are very ambiguous since there are no specific parameters for each diagnostic category. Although the Washington criteria (Astley and Clarren, 2000) are quite specific in placing each child into a given diagnostic category, they are not restricted to fetal development effects of only PAE since the focus is on encephalopathy and neurobehavioural disorders, which may be caused genetically or by other developmental disorders. To address these concerns, Hoyme and colleagues (2005) defined a complete and more accurate IOM method applicable for clinical pediatric practice.

The first modern description of recognizable malformations associated with prenatal alcohol exposure was reported in 1968 (Lemoine et al., 1968), while fetal alcohol syndrome (FAS), the most severe categorization of FASD, was first introduced in 1973 (Jones and Smith, 1973) and can be defined by three criteria: central nervous system dysfunction, pre- and postnatal growth deficiencies, and specific craniofacial features (short palpebral fissures, indistinct philtrum, and thin vermillion) (Hoyme et al., 2005; Stratton et al., 1996). These facial features (Figure 1.1) are indicative of brain damage and are caused by developmental changes between the 10^{th} and 20^{th} weeks of pregnancy (Renwick and Asker, 1983). Partial fetal alcohol syndrome (PFAS) is the

term applied to a child who shows two of the three alcohol-related facial anomalies and at least one of either small head circumference or growth retardation (< 10th percentile) (Hoyme et al., 2005). Children with confirmed prenatal exposure to alcohol who do not show all diagnostic criteria but still exhibit neurobehavioral deficits, are diagnosed as having alcohol-related neurodevelopmental disorder (ARND).

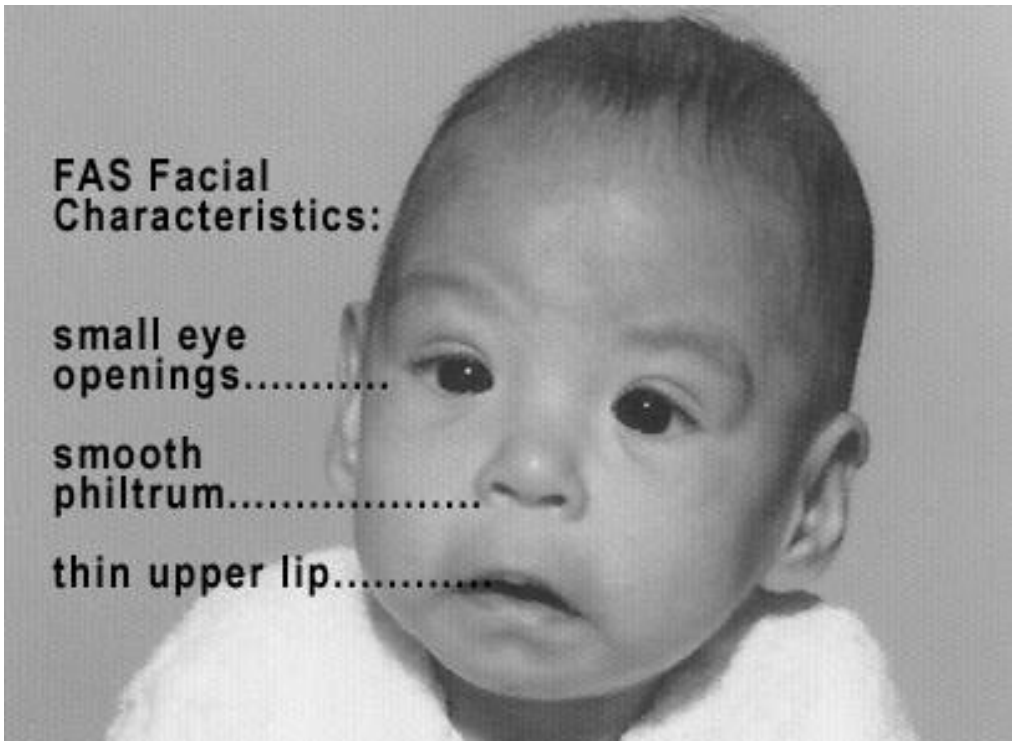

Figure 1.1 Baby with fetal alcohol syndrome showing the characteristic facial dysmorphology.

Both FAS (Mattson et al., 1997) and ARND (Jacobson et al., 2004) have adverse effects on the intelligence quotient (IQ). Since the central nervous system (CNS), especially the brain, is permanently damaged by the alcohol that crosses the placental barrier, children with FASD often have motor delays and deficits in attention (Burden et al., 2005; Coles et al., 2002; Jacobson et al., 1993; Kalberg et al., 2006; Streissguth et al., 1990), verbal learning and memory (Kaemingk et al., 2003; Mattson et al., 1996), executive function (Coles et al., 1997; Kodituwakku et al., 1995), mathematics and language (Jacobson and Jacobson, 2002). The diagnosis of FASD in childhood is difficult due to the occasional absence of facial anomalies and

inaccurate maternal drinking histories. Furthermore, most neuropsychological tests provide little information about the specific aspects of CNS structure and function that are affected by PAE.

Brain abnormalities in children with FASD reported from early autopsy studies have included agenesis of the corpus callosum, microcephaly, ventriculomegaly, a small brain, and a variety of other malformations caused by neuronal and glial migration errors (Jones and Smith, 1973; Clarren et al., 1978; Peiffer et al., 1979; Wisniewski et al., 1983). These earliest autopsy studies did not show an identifiable pattern of brain abnormalities. Further, they represented the most severely affected individuals rather than a spectrum of individuals in whom alterations may be less severe but have significant implications for neurodevelopment and future quality of life. Attention has recently turned to neuroimaging in order to identify brain regions most sensitive to prenatal alcohol exposure and the range of alterations that may result from different levels and timing of alcohol exposure.

1.2.2 Eyeblink Conditioning

Eyeblink conditioning (EBC) is a cerebellar mediated Pavlovian conditioning paradigm that involves contingent temporal pairing of a conditioned stimulus (CS, auditory tone) with an unconditioned stimulus (US, air puff). A brief air puff to the eye will cause a reflexive blink. After repeated pairing of a pure tone and a brief air puff to the eye, the conditioning criterion is that the subject learns to blink in anticipation of the air puff. In short delay conditioning, the tone and the air puff end at the same time. The interval between the onset of the tone and the onset of the air puff is of the order of 650 ms. In trace conditioning, there is an interval of approximately 500 ms after the termination of the tone and the onset of the air puff. Figure 1.2 shows an experimental EBC setup.

Figure 1.2 Experimental EBC step-up.

The neural pathway of EBC has been extensively studied in animal models (Christian and Thompson, 2003). Figure 1.3 illustrates the parts of the cerebellar circuit involved in EBC. The cerebellar peduncles, which are large bundles of myelinated nerve fibers that connect the cerebellum to the brainstem, constitute the principal white matter elements of the EBC circuit. The tone (CS) is conveyed from the pontine nucleus in the brainstem to the cerebellum via the middle cerebellar peduncle; information about the air puff (US) is transmitted from the inferior olive via the inferior peduncle. Both inputs reach Purkinje cells in the cerebellar cortex and send signals to the cerebellar deep nuclei. Neural plasticity in these cerebellar regions produced by appropriately timed CS and US inputs underlies EBC. The essential efferent pathway signal for the conditioned response is transmitted via the superior cerebellar peduncle to the red nucleus, where the conditioned response is projected to motor neurons that generate the conditioned eyeblinks. Although the brainstem-cerebellar circuitry described here is sufficient for short-delay conditioning, trace conditioning also engages the hippocampus (Cheng et al., 2008; Woodruff-Pak and Disterhoft, 2008; Tran and Thomas, 2007).

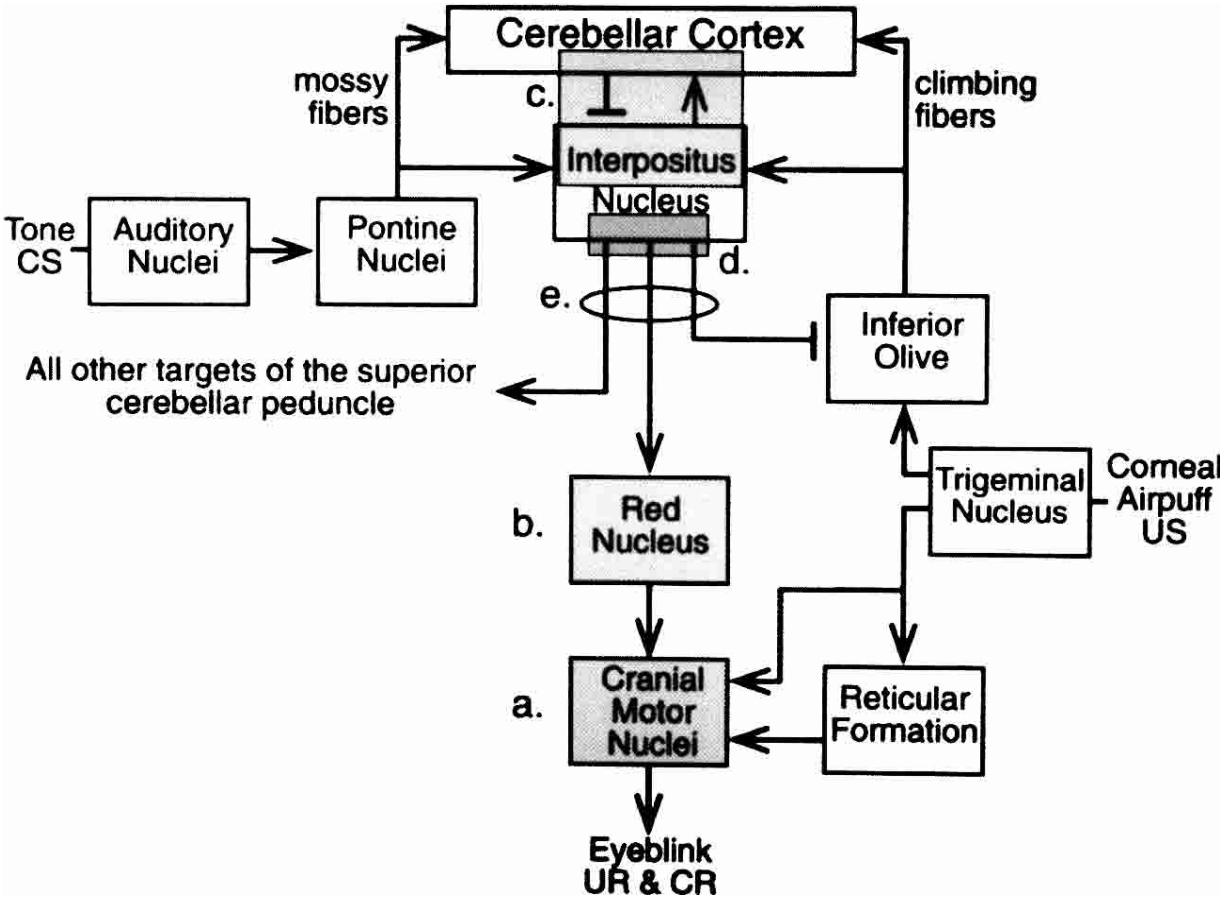

Figure 1.3 Schematic of the cerebellar circuit responsible for the EBC response: (a) motor nuclei; (b) red nucleus; (c) interpositus nucleus and cerebellar cortex; (d) only interpositus; (e) superior cerebellar peduncle. (Figure from Christian and Thompson, 2003)

The effect of prenatal alcohol exposure on the EBC response has also been studied in animal models. Impairment of EBC in weanling and adult rats was found by heavy alcohol exposure during the equivalent of the third trimester of pregnancy in humans (Stanton and Goodlett, 1998). Even a single heavy dose to a rat results in apoptosis of Purkinje cells and reduced neuronal density in the cerebellar deep nuclei (Dikranian et al., 2005; Green, 2004).

EBC is remarkably sensitive to prenatal alcohol exposure (Jacobson et al., 2008, 2011), and was first assessed in children with FASD as part of a 5-year follow up study of a cohort with heavy

prenatal alcohol exposure in the CTLS (Jacobson et al., 2008). Not a single child with full FAS met criterion for conditioning, compared to 75% of controls who were successful; 72.3% of the other children with prenatal alcohol exposure also failed to meet criterion for conditioning (Jacobson et al., 2008). By contrast, 75% of microcephalic children whose IQ values were in the same range as the children with FAS did meet criterion for conditioning. As such, EBC has the potential to be a remarkably sensitive biomarker of fetal alcohol exposure. These findings were corroborated by a report of poorer EBC in a small sample of school-aged, alcohol-exposed children (Coffin et al., 2005) and were replicated in a cross-sectional sample of school-age Cape Town children at 11 years of age (Jacobson et al., 2011).

1.2.3 Magnetic Resonance Imaging

We present a very brief introduction to the physics of MRI. MRI has been used to noninvasively and efficiently study both brain development and brain abnormalities in individuals and groups. MRI uses the magnetic dipole moments associated with the spinning charged particles in an atom's nucleus and relies on elements which have an odd number of protons plus neutrons in order to possess a non-zero nuclear spin angular momentum. The most commonly used nucleus, which is also used in this study, is hydrogen (^{1}H), both because of its high natural abundance (99.98%) and abundance in biological tissue (about 62% of all atoms in the human body are hydrogen). Since ^{1}H contains only a single proton in its nucleus and electron effects are negligible, ^{1}H MRI is often called 'proton MRI'. Other atoms with more complicated nuclear structures that occur in biological tissues and possess isotopes with non-zero angular momentum include carbon (^{13}C), fluorine (^{19}F), sodium (^{23}Na) and phosphorus (^{31}P). These are, however, far less abundant in biological tissue and the MR-active isotopes often have low natural abundances. For instance, only 12% of the atoms in the body are carbon and of these only about 1% are ^{13}C.

When a powerful external magnetic field (B_0) is applied, the dipole moments associated with the protons start to precess around the axis of that magnetic field at a frequency (ω) given by the Larmor equation (Equation 1.1, Figure 1.4)

$$\omega = \gamma B_0, \qquad \textbf{Equation 1.1}$$

where ω is the Larmor frequency or angular precession, γ is the gyromagnetic ratio (42.6 MH_z/T for ^1H), and B_0 is the strength of the external magnetic field. The ideal B_0 field is static and homogeneous; the field strength used in human MRI experiments and medical applications is typically 1.5T or 3T. B_0 is applied in the *z*-direction of the scanner coordinates (usually corresponding to a foot-to-head, or inferior-superior, orientation of the subject), known as the longitudinal direction, and the orthogonal *xy*-plane represents the transverse plane. The precessions of millions of dipole moments in a region give rise to a local net magnetization vector M, initially parallel to the main magnetic field B_0.

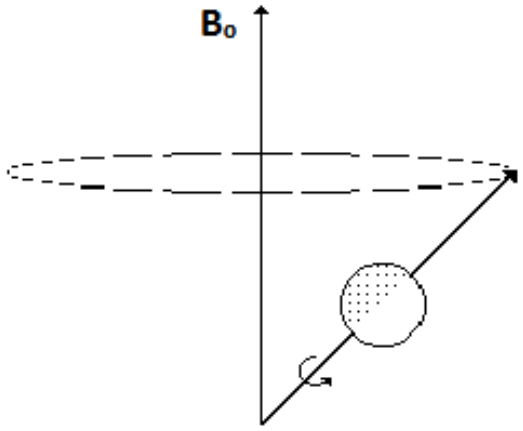

Figure 1.4 The dipole moment associated with a spinning proton precesses about B_0.

In order to create a signal, a radiofrequency (RF) pulse (electromagnetic wave) is applied briefly so as to create an alternating magnetic field B_1 perpendicular to B_0. In order to achieve resonance, the frequency of the RF pulse must match the Larmor precession frequency of the spins. If this condition is met, the application of this alternating B_1 field causes the initial net magnetization M_0 to precess also around B_1, so that the magnetization vector is flipped towards the *xy*-plane in a spiralling motion. How far the magnetization gets flipped into the transverse plane depends on the duration of the application of the RF pulse. After application of the RF pulse, the magnetization is described by its transverse (M_{xy}) and longitudinal (M_z) components. After termination of the RF pulse, atoms begin to relax back to their equilibrium state aligned with B_0 through two independent processes. Firstly, energy transmitted to the protons during

excitation is released back to the lattice. This process is known as longitudinal (or spin-lattice) relaxation and is characterised by the time constant T1, which is defined as the time it takes for M_z to recover to roughly 63% of its maximum value (Equation 1.3). Simultaneously the transverse component of the magnetization decreases exponentially with a time constant T2 defined as the time it takes M_{xy} to decrease by roughly 63% (Equation 1.2). The loss of the transverse signal is called spin-spin relaxation and results from the dephasing that occurs due to protons in different chemical environments experiencing slightly different effective magnetic fields (due to differences in electron shielding) causing their associated dipole moments to precess at slightly different frequencies around B_0.

$$M_{xy}(t) = M_0 e^{-t/T2}, \qquad \textbf{Equation 1.2}$$

$$M_z(t) = M_0 (1-e^{-t/T1}). \qquad \textbf{Equation 1.3}$$

For each type of tissue and field strength, T1 and T2 are approximately constant. T2 contrast is determined by the echo time (TE), which is the time between excitation and signal readout; T1 contrast is determined by the repetition time (TR), which is the time between successive RF pulses. Due to the combined effect of molecular interactions (spin-spin relaxation) and local magnetic field inhomogeneities, signal decay actually occurs faster than it would due to T2 decay only. T2* is the time constant that defines the rate at which the signal decays and is shorter than T2.

Three magnetic field gradients are used to spatially encode the signal. During the RF pulse, the slice encoding gradient (G_Z) is applied perpendicular to the imaging plane to ensure that only spins within a narrow band of tissue (slice) satisfy the resonance condition and are excited. The width of the slice depends on the strength of G_z and the bandwidth of the RF pulse. During signal acquisition, the frequency encoding gradient (G_x) is applied in one of the in-plane directions. This gradient causes the precessional frequencies of the spins to vary with position, so that the signal frequency is spatially encoded. The phase encoding gradient (G_Y) is applied between the RF pulse (excitation) and signal readout and creates a linear variation in spin phase. This step is repeated for different strengths of the phase encoding gradient to encode the phase pattern of every pixel in the y-direction. The number of repetitions of G_y is determined by

the number of rows in the image. The digitised data of the MR signal for each of the different phase encode gradients are recorded in a 2x2 matrix known as k-space. Once k-space has been filled, the MR image is generated by performing a 2D Fourier Transform.

1.2.4 Diffusion Tensor Imaging

DTI is a magnetic resonance imaging technique that uses the random motion of water molecules to infer local structural properties of tissue (Basser et al., 1994). Essentially, the MRI signal is attenuated more in regions where diffusion is high along the direction of an applied diffusion gradient. By repeating the acquisition with the diffusion gradient applied in at least six different directions, the direction of diffusion can be inferred. DTI is most often used to study the location, density and integrity of WM, which provides the anatomical links and fibre pathways between brain regions. The method is based on the fact that white matter tract structure is highly directional (anisotropic), which in turn leads to highly directional water diffusion. For example, in the basic model water molecules more easily diffuse along a tract bundle direction than perpendicular to it, due largely to cell membranes and myelin insulation. In contrast, diffusion is mainly isotropic in gray matter (GM) and cerebrospinal fluid (CSF). A second rank tensor D (Equation 1.4) is used to characterize the diffusion in white matter:

$$D = \begin{pmatrix} D_{xx} & D_{xy} & D_{xz} \\ D_{yx} & D_{yy} & D_{yz} \\ D_{zx} & D_{zy} & D_{zz} \end{pmatrix} \qquad \textbf{Equation 1.4}$$

D has the properties of being real, symmetric and having positive definite eigenvalues, which means that it corresponds geometrically to the surface of an ellipsoid. The principal parameters provided by DTI are fractional anisotropy (FA) and mean diffusivity (MD), given by Equations 1.5 and 1.6. FA is the normalised variance of diffusion tensor eigenvalues and represents the degree to which water diffuses preferentially parallel to the axonal axis rather than perpendicular to it. MD, the average diffusivity of water in a voxel, is commonly separated into eigenvalues that are parallel (e1) and perpendicular (e2 and e3) to the white matter tracts. These components are described as parallel or axial diffusivity (AD = e1), and perpendicular or radial diffusivity (RD = (e2 + e3)/2). FA, MD, AD and RD maps obtained from a control subject

from this study are show in Figure 1.5a. High FA and low MD values are often assumed to be indicative of healthy or highly organised white matter. FA values in human adult (and late adolescent) parenchymal white matter are typically ≥ 0.2 (Mori and van Zijl, 2002).

$$FA = \sqrt{\frac{(e_1 - e_2)^2 + (e_1 - e_3)^2 + (e_2 - e_3)^2}{2(e_1 + e_2 + e_3)}} \qquad \textbf{Equation 1.5}$$

$$MD = \frac{e_1 + e_2 + e_3}{3} \qquad \textbf{Equation 1.6}$$

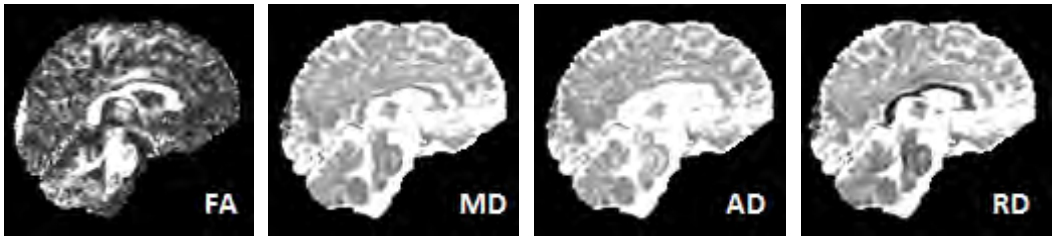

(a)

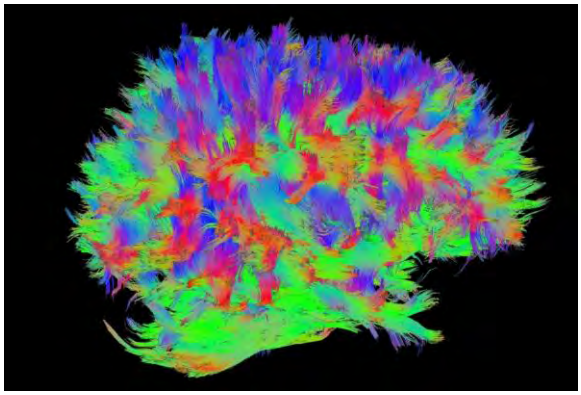

(b)

Figure 1.5 (a) FA, MD, AD and RD maps from a control subject; (b) A DTI tractography image, where red indicates tract directions along the *x*-axis (right-left); green indicates directions along the *y*-axis (posterior-anterior); and blue indicates directions along the *z*-axis (inferior-superior). (Figure from the AFNI_FATCAT Demo)

The principal barriers to water diffusion in white matter are the cellular membrane structures and myelin sheaths of axons. Fiber tracts, bundles of axons, create an environment where water diffuses more parallel than perpendicular to the tracts. Tractography is a modelling technique that combines the principal diffusion eigenvectors in regions where diffusion is

anisotropic to estimate the extended locations of major WM tracts throughout the brain (Figure 1.5b). Tractography is ideal for studies of populations with potentially heterogeneous structural development for whom standard atlases may not be appropriate.

1.2.5 Resting-state fMRI

FMRI is used to measure hemodynamic responses related to neural activity in the brain (Ogawa et al., 1990). The blood oxygen level dependent (BOLD) signal results from increases in local blood perfusion and oxygen consumption during neural activation due to the different magnetic properties of oxy- and deoxyhemoglobin–oxyhemoglobin is diamagnetic while deoxyhemoglobin is paramagnetic–causing different signal intensities on T2*-weighted images. Since there is far more energy metabolism and vascularisation in grey matter (GM) than in white matter, fMRI largely reveals information about brain function in GM (Cole et al., 2010; Logothetis and Wandell, 2004).

Rs-fMRI is a relatively new method based on the identification of reliable and consistent temporal correlations in the spontaneous BOLD signal fluctuations of different brain regions in the absence of a task. Biswal et al. first demonstrated in 1995 that rs-fMRI could be used to investigate functional connectivity in a meaningful way. In that study the subjects were asked not to perform any task. Despite the absence of a task, high correlation was found between the time series of the left and right motor cortices in nearly the exact same regions that are activated and reveal functional connectivity during a finger-tapping task. The 'task-free' nature of the technique makes it ideal for pediatric fMRI studies, since subject task performance and attention is known to be a significant concern in children, as well as reducing the potential for task-induced motion (Stevens et al., 2009; Supekar et al., 2009).

Resting state functional connectivity (RSFC) has been used to identify and quantify several functional networks, many of which have been recognizable from task-based functional studies. These networks are generally referred to as resting state networks (RSNs). About 15 to 20 RSNs have been identified with reliability, reproducibility, and consistency across subjects (Beckmann

et al., 2005; Damoiseaux et al., 2006; De Luca et al., 2006; Fox and Raichle, 2007; Smith et al., 2009), stages of cognitive development (Fair et al., 2007; Fransson et al., 2007), degree of consciousness (Boly et al., 2008; Greicius et al., 2008), and even species (Vincent et al., 2007). Rs-fMRI allows us to examine the intrinsic functional architecture of the brain and its segregation across these large-scale networks. For example, the strength of RSN connectivity has been found to be correlated with cognitive or behavioural performance measures (Seeley et al., 2007). More recently, the role of resting state fMRI has being increasingly explored as a potential biomarker for neuropsychiatric disorders (Damoiseaux, 2012). Additionally, several local measures of resting state BOLD time series have been associated with functional connectivity and neurobehavioral changes, such as regional homogeneity (ReHo; Zang et al., 2004) and fractional amplitude of low frequency fluctuations (fALFF; Zou et al., 2008), which are described in more detail in Chapter 4.

Most networks observed in specific task-based paradigms have also been observed during resting state scanning. The sensorimotor network was first studied by Biswal et al. (1995) and comprises the primary and higher order motor and sensory areas (Figure 1.6b). The visual network includes most of the occipital cortex (Figure 1.6c) (Beckmann et al., 2005; De Luca et al., 2006; Smith et al., 2009; Power et al., 2011; Yeo et al., 2011). Tomasi and Volkow (2012) reported a language network that includes Broca's and Wernicke's areas extending to prefrontal, temporal, parietal, and subcortical regions (Figure 1.6d).

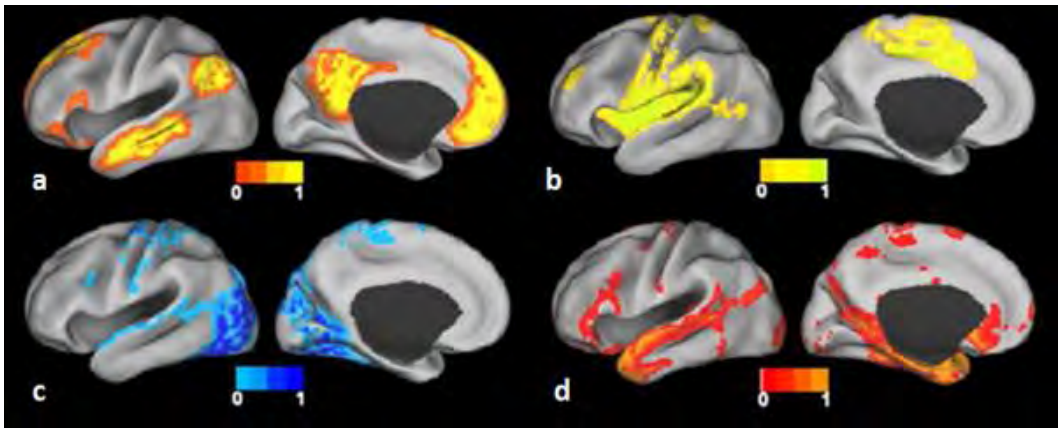

Figure 1.6 Surface plots of RSNs: (a) default mode network, (b) somatosensory network, (c) visual network, and (d) language network. (Figure adapted from Lee et al., 2013)

The salience and executive control networks were first identified by Seeley et al. (2007). The salience network includes dorsal anterior cingulate cortex and orbital frontoinsular cortices, which unites monitoring, goal behavior and cognitive flexibility. The executive control network connects dorsolateral frontal and parietal neocortices and plays a role in working memory and control processes.

Dorsal and ventral attention networks have been identified using both task-based and rs-fMRI studies (Fox et al., 2006; Seeley et al., 2007; Power et al., 2011; Yeo et al., 2011). These networks have been shown to overlap (Fox et al., 2006) (Figure 1.7) in the right middle frontal gyrus, inferior frontal gyrus and inferior parietal cortex. The dorsal attention network, which modulates the saliency of distracter stimuli for action goals (Ptak and Schnider, 2010), is bilateral and includes the intraparietal sulcus, and the precentral and superior frontal sulci in both hemispheres. The ventral attention network comprises the temporal-parietal junction and the ventral-frontal cortex in the right side of the brain only, showing activity upon detection of targets.

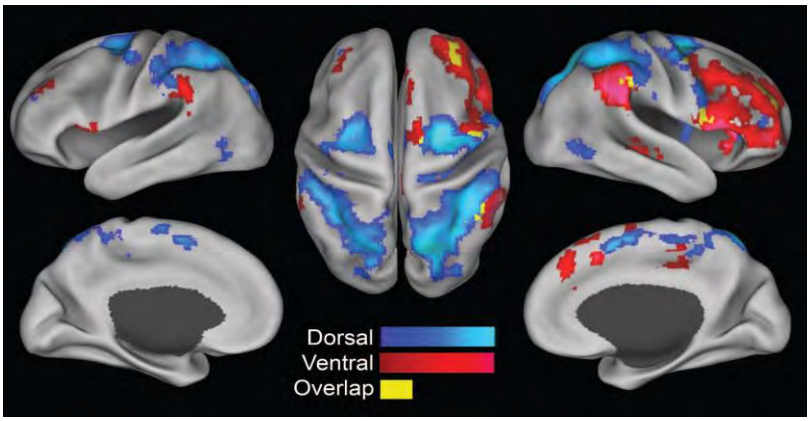

Figure 1.7 Surface plots of dorsal (blue) and ventral (red) attention networks, as well as regions where they overlap (yellow). (Figure from Fox et al., 2006)

The default mode network (DMN) is perhaps the most unique RSN (Figure 1.6a) in that it is not observed during explicit task performance but instead only in the absence of a task, i.e. "at rest" (Shulman et al. 1997; Raichle et al., 2001). It has been studied using both PET (Raichle et

al., 2001) and fMRI (Greicius et al., 2003; Lowe et al., 1998; Xiong et al., 1999). The DMN includes the posterior cingulate cortex (PCC), precuneus, medial prefrontal cortex (MPFC), orbital frontal gyrus (OFG), anterior cingulate gyrus (ACC), inferolateral temporal cortex (ITC), parahippocampal gyrus (PHG), and lateral parietal cortex (LP) (Fransson, 2005; Greicius et al., 2003; Raichle et al., 2001; Shulman et al., 1997).

There are two popular statistical and mathematic methods often applied to quantifying functional connectivity in rs-fMRI data. The first method is the model-driven seed-based analysis, which was used in the first rs-fMRI study by Biswal et al. (1995) and has since been performed in many studies (Raichle et al., 2001; Greicius et al., 2003; Fox et al., 2005, 2006; Margulies et al., 2007; Vincent et al., 2008). This method requires *a priori* selection of a seed based on previous literature, a hypothesis or functional activation maps. The seed can be a voxel, cluster or even an atlas region. The correlation to the BOLD time courses of all other voxels in the brain to this seed provides a map of regions that are most strongly functionally connected with the seed. The map is thresholded to identify the network. Although this method is straightforward, it is limited by the spatial assumption of the seed selection.

The other commonly used method is independent component analysis (ICA) (McKeown et al., 1998; Kiviniemi et al., 2003; Beckmann et al., 2005; Damoiseaux et al., 2006), which decomposes a two-dimensional data matrix into different spatial and temporal components. ICA avoids the drawback of seed selection, however, its results may be ‘split’ into a number of sub-networks depending on the chosen number of components in the decomposition. Despite the differences between the 2 methods, consistent networks have been reported using both seed based analysis and ICA in a group of healthy subjects (Rosazza et al., 2012).

Several sets of RSFC maps, often created using group ICA, have been made publicly available by researchers for use as references in other studies. One particular set was calculated using over one thousand adult subjects from multiple imaging centers as part of the 1000 Functional Connectome Project (Biswal et al., 2010). Other sets using much smaller group sizes have also been made available, such as that of Smith et al. (2009). While pediatric rs-fMRI has been performed, RSNs from De Bie et al. (2012) contained a large group of "small for gestational age"

subjects (these were part of a control group with postnatal "catch-up" growth); additionally, the default mode network was divided into four separate networks. The authors of that study noted that this may have been related to the fact that the rs-fMRI scanning was performed immediately following a 10-minute task-based scan, which might have affected the results. Thomason et al. (2011) have also released a pediatric template, but the networks are provided as masks instead of connectivity maps. Since we prefer a set of connectivity maps with higher regional specificity for matching networks, we used in our study the set of 1000 Functional Connectome Project maps as a reference for determining (by quantitative comparison) the label of a given functional network.

Each processed independent component (IC) map requires thresholding of a statistical quantity (i.e., correlation or some other connectivity measure) in order to determine meaningful networks. Therefore, there are no uniquely-definable, firm boundaries of regions either across studies or even within a single study. In general, the IC maps are transformed to *z*-score maps and thresholded at a *z*-score value > 2.3, a value that was first proposed by Beckmann and Smith in 2004.

1.2.6 Neuroimaging Studies of FASD

The first structural MRI study of FASD was conducted in 1992 (Mattson et al., 1992). Since then, there have been about 50 studies on individuals with PAE using structural MRI. Most of the studies have used T1-weighted MRI on either 1.5 or 3 T scanners. Similar to results of autopsy studies, structural MRI studies show decreased brain volumes in FASD subjects compared to controls. These include 21 studies of total brain volume (e.g. Chen et al., 2012; Rajaprakash et al., 2014; De Guio et al., 2014), 5 studies of cerebral volume (Mattson et al., 1992, 1994, 1996; Archibald et al., 2001; De Zeeuw et al., 2012) and 10 studies of cerebellar volume (e.g. Astley et al., 2009; Spottiswood et al., 2011, De Zeeuw et al., 2012).

A growing body of evidence suggests that WM is a specific target of alcohol teratogenesis. Reductions in white matter volume have been found in individuals with FASD in the whole brain (Archibald et al., 2001; Sowell et al., 2001a; Lebel et al., 2008; Bjorkquist et al., 2010; Nardelli et al., 2011; Roussotte et al., 2012; Yang et al., 2012; De Zeeuw et al. 2012; Treit et al., 2013; De

Guio et al., 2014), frontal lobe (Sowell et al., 2002a; Astley et al., 2009), parietal lobe (Archibald et al., 2001; Sowell et al., 2002b), temporal lobe (Sowell et al., 2002a), and cerebellum (Spottiswoode et al., 2011). However, in most of these studies the differences in WM tissue volume were no longer significant after correcting for reductions in total brain volume.

Several DTI studies have been performed in FASD to examine microstructural WM integrity, many of which have focused on the corpus callosum since it is the largest white matter tract in the human brain and crucial for inter-hemispheric communication. The first DTI study on individuals with FASD in 2005 (Ma et al., 2005) reported that young adults (age 18-25 yrs) with FAS showed lower FA and higher MD in the genu and splenium of the corpus callosum. In the following year Wozniak and colleagues (2006) reported decreased FA and increased MD in the isthmus of the corpus callosum in children (age 10-19 yrs) with FASD, none of whom met criteria for full FAS. In a follow-on study, Wozniak et al. (2009) found lower FA in three posterior tracts of the corpus callosum (posterior mid-body, isthmus, and splenium) in a group of alcohol exposed children (age 10-17 yrs) comprising 8 with FAS and 23 with PFAS. Surprisingly, correlations between measures of facial dysmorphology and FA in the posterior regions of the corpus callosum were, however, not significant.

Using semi-automated DTI tractography, abnormalities were found in 7 of 10 white matter tracts examined (splenium and genu of corpus callosum, inferior and superior longitudinal fasciculus, corticospinal tracts, cingulum, and inferior fronto-occipital fasciculus) in 5-12 year old children with FASD (Lebel et al., 2008). Treit et al. (2013) reported lower FA in the superior fronto-occipital fasciculus and greater MD in the genu of the corpus callosum, as well as atypical developmental trajectories in the superior fronto-occipital, superior longitudinal fasciculus, and inferior fronto-occipital fasciculus in children age 5-15 yrs with FASD. Green et al. (2013) performed a DTI tractography study on 8-13 year old children with FASD by virtually reconstructing white matter pathways. Saccadic reaction times (the time for subjects to move their eyes following the appearance of a target) were negatively related to FA in the cerebellum indicating dysfunction in this region. An enhanced tractography analysis developed by Colby et al. (2012) that examined group differences between children with FASD (n=9, 13.8±2.6 yrs) and

controls (n=11, age=13.2±3.1 yrs) within the inferior longitudinal fasciculus and arcuate fasciculus tracts only found lower FA in the posterior portion of the inferior longitudinal fasciculus.

In 2009, two DTI studies using tract-based spatial statistics (TBSS) (Smith et al., 2006) were published. Youth prenatally exposed to alcohol (age 8-18) showed lower FA in a number of white matter tracts (superior longitudinal fasciculus, uncinate, fronto-occipital fasciculi, coronae radiatae, and body of corpus callosum) (Fryer et al., 2009). Young adults (age 19-27 yrs) with FASD showed lower FA and higher MD in the isthmus of the corpus callosum, changes that were related to increased RD and not to decreased AD (Li et al., 2009).

Using voxel-wise analysis, lower FA values were found in 7 white matter tracts (lateral splenium, bilateral posterior cingulate, right inferior longitudinal fasciculus, right inferior fronto-occipital fasciculus, right internal capsule, and brainstem) in children (age 7-15yrs) with FASD (Sowell et al., 2008). Several regions of altered FA in the left cerebellum, left parietal lobe, left upper parietal lobe and brainstem showed relations to math scores in children (age 5-13 yrs) with FASD (Lebel et al., 2010). Spottiswoode et al. (2011) performed a cerebellar DTI study of a small cross-sectional sample of children with FASD (5 with FAS, 8 with PFAS, and 12 non- or minimally-exposed controls (Ctl), age 9.7-13.7 yrs) and reported lower FA and higher RD in the left middle cerebellar peduncle in children with either FAS or PFAS.

In summary, it is evident from the above that PAE effects on WM are extensive with evidence of microstructural alterations in the corpus callosum, inferior and superior longitudinal fasciculi, corticospinal tract, cingulum, inferior and superior fronto-occipital fasciculi, uncinate fasciculus, corona radiata, and cerebellum.

RSFC has been extensively studied in adults, (Meindl et al., 2010; Shehzad et al., 2009; Van de Ven et al., 2004; Zuo et al., 2010a; Zuo et al., 2010b), though fewer studies of children or adolescents exist, and very few rs-fMRI studies have been conducted in FASD. To date, rs-fMRI studies in FASD have been performed on only one pediatric (Wozniak et al., 2011, 2013; Kim et al., 2014) and one adult (Santhanam et al., 2011) sample. Wozniak et al. (2011) observed decreased interhemispheric functional connectivity in children (age 10-17 years) with FASD,

comparing average time series correlations in specific regions of interest (ROIs) connected by the corpus callosum. Their follow-on study (Wozniak et al., 2013) found decreased global efficiency and increased path length in FASD subjects in a whole brain study. The adult study, which only focused on the default mode network using seed-based analysis, showed that adults (aged 18-24) with either FAS or PFAS have reduced RSFC in the DMN.

The age ranges of FASD subjects in prior studies are often large and span multiple developmental phases. In addition, the numbers of individuals with FAS are few and many of the subjects exhibit relatively mild levels of alcohol exposure. South Africa is the ideal place for conducting studies of FASD to examine the complex relationships between behavior, cognition and brain structure due to the large number of individuals with very high levels of exposure hailing from the same ethnic group and with similar socioeconomic status, making it possible to recruit large numbers of subjects within the same age range with varying levels of exposure and different clinical diagnoses, including a group of nonsyndromal heavily exposed children who do not meet diagnostic criteria for FASD. These features make it possible to study not only PAE effects on brain development by diagnosis, but to also examine dose dependent effects and whether nonsyndromal heavily exposed individuals exhibit brain alterations similar to subjects with FASD, or whether their brain structure and function are relatively spared.

Chapter 2

White Matter Integrity of the Cerebellar Peduncles as a Mediator of Effects of Prenatal Alcohol Exposure on Eyeblink Conditioning

Jia Fan[1,2], Ernesta M. Meintjes[1,2], Christopher D. Molteno[3], Bruce S. Spottiswoode[4], Neil C. Dodge[5], Alkathafi A. Alhamud[1,2], Mark E. Stanton[6], Bradley S. Peterson[7], Joseph L. Jacobson[2-3,5], and Sandra W. Jacobson[2-3,5]

Abstract

Fetal alcohol spectrum disorders (FASD) are characterized by a range of neurodevelopmental deficits that result from prenatal exposure to alcohol. These can include cognitive, behavioural, and neurological impairment, as well as structural and functional brain damage. Eyeblink conditioning (EBC) is among the most sensitive endpoints affected in FASD. The cerebellar peduncles, large bundles of myelinated nerve fibers that connect the cerebellum to the brainstem, constitute the principal white matter element of the EBC circuit. Diffusion tensor imaging (DTI) is used to assess white matter integrity in fibre pathways linking brain regions.

This Article has been accepted for publication in Human Brain Mapping.

[1]MRC/UCT Medical Imaging Research Unit, University of Cape Town, Cape Town, South Africa; [2]Department of Human Biology, University of Cape Town, Cape Town, South Africa; [3]Department of Psychiatry and Mental Health, University of Cape Town, Cape Town, South Africa; [4]Siemens Medical Solutions USA Inc., Chicago, IL, United States; [5]Department of Psychiatry and Behavioral Neurosciences, Wayne State University School of Medicine, Detroit, MI, United States; [6]Department of Psychology, University of Delaware, Delaware, MD, United States; [7]Institute for the Developing Mind, Children's Hospital Los Angeles and the Keck School of Medicine, University of Southern California, Los Angeles, CA, United States

DTI scans of 54 children with FASD and 23 healthy controls, mean age 10.1±1.0 yrs, from the Cape Town Longitudinal Cohort were processed using voxelwise group comparisons. Prenatal alcohol exposure was related to lower fractional anisotropy (FA) bilaterally in the superior cerebellar peduncles and higher mean diffusivity (MD) in the left middle peduncle, effects that remained significant after controlling for potential confounding variables. Lower FA and higher MD in these regions were associated with poorer EBC performance. Moreover, effects of alcohol exposure on EBC decreased significantly after inclusion of these DTI measures in regression models, suggesting that these white matter deficits partially mediate the relation of prenatal alcohol exposure to EBC. The associations of greater alcohol consumption with these DTI measures are largely attributable to greater radial diffusivity, possibly indicating poorer myelination. Thus, these data suggest that fetal alcohol-related deficits in EBC are attributable, in part, to poorer myelination in key regions of the cerebellar peduncles.

Key words: Fetal alcohol spectrum disorders, eyeblink conditioning, diffusion tensor imaging, white matter, cerebellar peduncles

2.1 Introduction

The term fetal alcohol spectrum disorders (FASD) refers to the range of disorders that result from prenatal exposure to alcohol. These can involve cognitive, behavioural, and neurological impairment associated with structural and functional brain damage. Fetal alcohol syndrome (FAS), the most severe form of FASD, is characterised by small head circumference, growth retardation and distinctive facial anomalies: short palpebral fissures, thin upper lip and flat or smooth philtrum (Hoyme et al., 2005). These facial features, which have been shown to reflect brain damage, are caused by alcohol ingestion between the 10^{th} and 20^{th} weeks of pregnancy (Renwick and Asker, 1983). Partial fetal alcohol syndrome (PFAS) is diagnosed when an individual with prenatal alcohol exposure shows two of the three alcohol-related facial anomalies and at least one of the following: small head circumference, growth retardation ($<10^{th}$ percentile), or neurobehavioral impairment. An individual with prenatal alcohol exposure

who exhibits neurobehavioural deficits but lacks the facial features is diagnosed with alcohol-related neurodevelopmental disorder.

We have found that eyeblink conditioning (EBC) is remarkably sensitive to prenatal alcohol exposure (Jacobson et al., 2008, 2011). EBC is a cerebellar-mediated Pavlovian conditioning paradigm that involves contingent temporal pairing of a conditioned stimulus (usually an auditory tone) with an unconditioned stimulus (usually an air puff). In the 5-year follow-up of our Cape Town Longitudinal Cohort study, not a single child with full FAS met criterion for conditioning, compared to 75% of controls; 72.3% of the other children with prenatal alcohol exposure also failed to meet criterion for conditioning (Jacobson et al., 2008). These findings corroborated a report of poorer EBC in a small sample of school-aged, alcohol-exposed children (Coffin et al., 2005) and were replicated in a cross-sectional sample of school-age Cape Town children at 11 years of age (Jacobson et al., 2011). Impairment of EBC has also been documented in laboratory studies of weanling and adult rats heavily exposed to alcohol during the equivalent of the third trimester of pregnancy (Stanton and Goodlett, 1998). Even a single heavy dose produced apoptosis of Purkinje cells and reduced neuronal density in the cerebellar deep nuclei (Dikranian et al., 2005; Green, 2004).

The EBC neural circuit has been extensively studied in animal models (Christian and Thompson, 2003; Lavond and Steinmetz, 1989). The cerebellar peduncles, which are large bundles of myelinated nerve fibers that connect the cerebellum to the brainstem, constitute the principal white matter elements of the EBC circuit. The auditory tone is conveyed from the pontine nucleus in the brainstem to the cerebellum via the middle cerebellar peduncle; information about the air puff is transmitted from the inferior olive via the inferior peduncle. Both inputs reach Purkinje cells in the cerebellar cortex and send signals to the cerebellar deep nuclei. Neural plasticity in these cerebellar regions produced by appropriately timed conditioned and unconditioned stimulus inputs underlies EBC. The essential efferent signal for the conditioned response is transmitted via the superior cerebellar peduncle to the red nucleus, where the conditioned response is projected to motor neurons that generate the conditioned eyeblinks (Cheng et al., 2008, 2014; Woodruff-Pak and Disterhoft, 2008; Tran and Thomas, 2007).

Although effects of prenatal alcohol exposure have not been extensively studied in the cerebellar peduncles, reductions in white matter volume have been found in individuals with FASD in whole brain (Archibald et al., 2001; Sowell et al., 2001a; Lebel et al., 2008; Bjorkquist et al., 2010; Nardelli et al., 2011), frontal lobe (Sowell et al., 2002a; Astley et al., 2009), parietal lobe (Archibald et al., 2001; Sowell et al., 2002b), temporal lobe (Sowell et al., 2002a), and cerebellum (Spottiswoode et al., 2011). Diffusion tensor imaging (DTI) is an advanced neuroimaging technique used to evaluate white matter integrity in tissue. Local diffusivities quantified in mutually orthogonal orientations are commonly separated into axial (AD = e_1) and radial diffusivity (RD = $(e_2 + e_3)/2$) that are parallel and perpendicular to the white matter tracts, respectively. Fractional anisotropy (FA) is the normalized variance of diffusion tensor eigenvalues and represents the degree to which water diffuses preferentially parallel to the axonal axis rather than perpendicular to it. Mean diffusivity (MD) is the average diffusivity of water in a voxel. High FA and low MD values indicate healthy or highly organized white matter. The value of FA in white matter is typically ≥ 0.2 (Mori and van Zijl, 2002).

Several DTI studies have been performed of individuals with FASD, most of which have focused on the corpus callosum. Young adults (age 19-27 years) with fetal alcohol-related dysmorphology showed greater RD but no difference in AD in the isthmus of the corpus callosum (Li et al., 2009). Ma and colleagues (2005) reported decreased FA and increased MD in young adults (age 18-25 years) with FAS in the genu and splenium of the corpus callosum. By contrast, Wozniak et al. (2006) found lower FA and greater MD in children (age 10-13 years) with FASD only in the isthmus of the corpus callosum. A recent whole brain DTI study of children and adolescents with FASD (age 7–15 years) reported reduced FA in several white matter regions, including the lateral splenium, bilateral posterior cingulate white matter, and the right lateral temporal lobe (Sowell et al., 2008). Despite differences in the findings, which may be related to age, ethnicity, genetics, the degree and timing of alcohol exposure, and different analysis strategies, these studies confirm consistent microstructural white matter abnormalities of the corpus callosum and other regions in FASD. Moreover, using a semi-automated, whole brain tractography technique, Lebel et al. (2008) found abnormalities in 7 of 10 white matter tracts considered (superior longitudinal fasciculus, cingulum, splenium corpus

callosum, inferior fronto-occipital fasciculus, genu corpus callosum, corticospinal tracts and inferior longitudinal fasciculus).

We previously examined the degree to which poorer white matter integrity in the cerebellar peduncles may partially mediate the effects of prenatal alcohol exposure on EBC in a small cross-sectional school-age Cape Town sample—5 diagnosed with FAS, 8 with PFAS, and 12 non- or minimally-exposed controls (Spottiswoode et al., 2011). The FAS/PFAS group exhibited lower FA and greater RD in the left middle cerebellar peduncle compared to the controls. Trace EBC was related to higher FA and less diffusivity in that region, and the relation of delay EBC to those endpoints fell just short of statistical significance. Moreover, multiple regression analysis showed that the adverse effect of prenatal alcohol exposure on trace conditioning was partially mediated by lower FA in that region.

The aim of this study was to test the hypothesis that (1) prenatal alcohol exposure is associated with microstructural deficits in the cerebellar peduncles in a larger sample of children whose mothers were recruited prospectively during pregnancy (Jacobson et al., 2008) and for whom detailed exposure histories were obtained during gestation and (2) the effects of prenatal alcohol exposure on EBC are mediated, in part, by these white matter abnormalities in the cerebellar peduncles. This research presents a unique opportunity to study cerebellar white matter abnormalities in relation to degree of alcohol exposure and EBC in a well-characterized cohort of children.

2.2 Materials and Methods

2.2.1 Participants

Pregnant women were recruited to take part in the Cape Town Longitudinal Cohort study on effects of heavy drinking on infant and child development between 1999 and 2002 at an antenatal clinic serving the Cape Coloured (mixed ancestry) community in Cape Town, South Africa (Jacobson et al., 2008), which was selected for its high prevalence of heavy alcohol use (Croxford and Viljoen 1999). This population, which is comprised of descendants of white

European settlers, Malaysian slaves, Khoi-San aboriginals, and black Africans, historically constituted the large majority of workers in the wine-producing region of the Western Cape. The high prevalence of FAS in this community is attributable to very heavy maternal drinking during pregnancy (May et al., 2000), due to poor psychosocial circumstances and residual impact of the now-outlawed *dop* system, in which farm laborers were paid, in part, with wine.

Each mother was interviewed regarding her alcohol consumption using a timeline follow-back approach to determine incidence and amount of drinking on a day-by-day basis during a typical 2-week period both at time of conception and time of recruitment (Jacobson et al., 2002). The mother was then asked whether her drinking had changed since conception; if so, when the change occurred and how much she drank on a day-by-day basis during the last 2 weeks. Volume was recorded for each type of beverage consumed each day and converted to ounces (oz) absolute alcohol (AA). Two groups of women were recruited: (1) heavy drinkers, who consumed 14 or more standard drinks/week (≈1.0 oz AA/day) and/or engaged in binge drinking (5 or more drinks/occasion), and (2) controls, who abstained from drinking or drank no more than minimally during pregnancy. The timeline follow-back interview was repeated in mid-pregnancy and again at 1 month postpartum to provide information about drinking during the latter part of pregnancy. Data from the three alcohol consumption interviews were tabulated to provide three continuous measures of drinking during pregnancy: average oz AA consumed/day (AA/day), AA/drinking day (dose/occasion), and frequency (days/week). AA/day was used as the principal measure of prenatal alcohol exposure in this study. Smoking during pregnancy was reported in terms of cigarettes smoked per day. Mother's age at delivery, socioeconomic status (SES) based on the Hollingshead Scale (Hollingshead, 2011), and years of education were also recorded. During pregnancy, 1 mother in the PFAS group used cocaine, while 5 mothers smoked marijuana (1 FAS, 2 PFAS, 1 HE and 1 Control). Analyses relating oz AA/day to the DTI measures in the regions of interest (ROIs) identified in the present study yielded virtually identical results with and without inclusion of the subjects whose mothers reported using drugs during pregnancy. Maternal exclusionary criteria included age <18 years, diabetes, epilepsy, cardiac problems requiring treatment, and observant Muslims whose religious practice prohibits alcohol consumption. Infant exclusionary criteria were major

chromosomal anomalies, neural tube defects, multiple births, and seizures. Children in the cohort were examined for growth and cognitive function at 6.5, 12, and 13 months of age. At 5 years they were examined for growth and alcohol-related facial dysmorphic features, as detailed below. The children were assessed for IQ and EBC at ages 5 and 9-11 years, and structural MRI and DTI scans were administered at 10 years.

Human subjects approval was obtained from the Wayne State University and University of Cape Town Faculty of Health Sciences ethics committees. Informed consent was obtained from mothers at recruitment and at the child assessment visits; assent was obtained from the child. Children received a small gift and mothers received a photo of their child and compensation consistent with guidelines from the ethics committees.

2.2.2 Procedures

DTI data were obtained from 57 right-handed children with FASD (11 FAS, 17 PFAS and 29 nonsyndromal heavily exposed (HE)) and 24 non- or minimally-exposed controls (Ctl), from the Cape Town Longitudinal Cohort (Jacobson et al., 2008). In 2005 we organized an FAS diagnostic clinic in which all of the children were assessed by two U.S.-based expert FAS dysmorphologists (HE Hoyme, MD, and LK Robison, MD) around the time of the 5-year assessment visit, following the Revised Institute of Medicine Criteria (Hoyme et al., 2005). The dysmorphologists were blind with respect to prenatal alcohol exposure. A third Cape Town-based FAS dysmorphologist (N Khaole, MD) examined seven children who were not able to attend the clinic. Percent agreement between the two U.S. dysmorphologists was 90.5% (thin upper lip/verimillion), 93.3% (philtrum), and 89.5% (palpebral fissures). When the seven children who were examined by Dr. Khaole were subsequently examined in 2009 by the Drs. Hoyme and Robinson, agreement ranged from 80% to 100%, median = 91.7%.

Each of the alcohol-exposed children was assigned to one of the diagnostic groups: FAS, PFAS, and HE, following a case conference conducted by the U.S. dysmorphologists, and SWJ, CDM, and JLJ. Postnatal lead exposure, based on a venous blood sample obtained at age 5 years, was also assessed since lead levels in this population are within the range in which subtle but

meaningful effects on cognitive function have been consistently reported (Chiodo et al., 2004; Lanphear et al., 2000). Child sex and age at DTI scan were also recorded.

2.2.3 Neuropsychological and EBC Assessments

The mother and child were transported to our University of Cape Town (UCT) Child Development Research Laboratory by a staff driver and research nurse for the IQ and EBC assessments at ages 5 and 9-11 years, which were administered by an MA-level neuropsychologist. IQ was assessed using the Junior South African Individual Scales (JSAIS; Madge, 1981) at 5 years and the Wechsler Intelligence Scale for Children, Fourth edition (WISC-IV) at 10 years (see Diwadkar et al., 2013). The JSAIS, which is available in Afrikaans and English and has been normed for South African children, were strongly related with the WISC scores, r=0.77, p<0.001 (Jacobson et al., 2011). The EBC assessments were administered during 2 days no more than 1 week apart, using a commercially available human EBC system (Model #2325-0145-W (San Diego Instruments, San Diego, CA); see Jacobson et al., 2008, 2011). Facing a monitor displaying a video, the child wore a light-weight headgear, which supported a flexible plastic tube that delivered an air puff to the right eye and a photodiode which measured eyelid closure. Two small 7-Ohm speakers emitted an auditory conditioning stimulus, a 1-kHz, 80-dB tone. Each session consisted of five 10-trial blocks. Two 50-trial sessions were administered each day about 2 hours apart. In delay EBC, the air puff was administered during the last 100 ms of the 750 ms tone. The trace conditioning procedure was administered during two additional UCT laboratory assessment visits at age 11 years, which were conducted 1.3 to 1.8 years after the delay task. The procedure was the same as in the delay task except that a 500-ms stimulus-free interval occurred between the offset of the 750-ms tone and the onset of the air puff. Eyeblinks within 350 ms prior to the air puff onset were considered conditioned responses. The principal dependent measure for both the delay and trace tasks was whether the child met the criterion of 40% conditioned responses within the two sessions. All examiners were blind regarding fetal alcohol exposure history and FASD diagnosis.

2.2.4 Scanning Protocol

The children and their mothers were transported to the Cape Universities Brain Imaging Center (CUBIC), a research-dedicated, child-friendly facility where they were familiarized with the scanning procedures by first practicing in a mock scanner. The children were imaged on a 3T Allegra MRI (Siemens, Erlangen, Germany). Diffusion weighting was performed in 30 directions; 36 slices were acquired in an oblique axial orientation that included primarily infra-tentorial structures to provide high-resolution cerebellar data. The first 18 children (3 FAS, 6 PFAS, 3 HE, 6 Controls) were imaged using five DTI acquisitions; the others, using six acquisitions with alternating phase encoding directions (i.e., anterior-posterior and posterior-anterior) to reduce echo planar imaging distortions. Voxelwise analyses repeated without the 18 children for whom the imaging protocol differed, yielded differences between the same groups in regions overlapping with those found for the whole sample. Further, analyses relating oz AA/day to the DTI measures in the regions where group differences were found were virtually unchanged with these 18 children included or excluded. Cerebellar T2-weighted structural images were acquired with a matched spatial resolution and slice position as the DTI in order to improve coregistration between the cerebellar DTI and whole-brain structural data.

2.2.5 Pre-processing

DTI data were first inspected visually for the presence of dropout slices. Any subjects with dropout slices in any of their DTI acquisitions were excluded from all further analyses. After exclusions, we report data for 54 children with FASD (11 FAS, 16 PFAS, 27 HE) and 23 controls, mean age 10.1±1.0 yr. Pre-processing included eddy current correction, which also entails correction for simple head movement in FSL and susceptibility correction in Matlab (Andersson et al., 2003). For each subject, we computed for each DTI volume the resultant displacement relative to the first unweighted (b_0) volume using the three translation parameters from mcflirt in FSL. For each subject we extracted the maximum resultant displacement throughout all DTI acquisitions. The maximum resultant displacements were below 1.7 mm for all subjects included in the analyses. Rotations in any direction were less than 1.1 degree in all subjects. Moreover, the extent of motion did not differ between diagnostic groups. To compute *z*-scores,

we calculated the mean and standard deviation based only on values between the 25 and 75 percentile limits and generated *z*-score maps for each acquisition; any data points more than three standard deviations beyond the mean of the *z*-score map were discarded. The DTI acquisitions were averaged and FA, MD, AD and RD images were generated. Each subject's b_0 images were coregistered to their own T2-weighted structural images using linear and nonlinear coregistration algorithms in FSL with a mutual information cost function and 12 degrees of freedom. The same procedure was used for all registration steps. T2 images of controls were coregistered to the 'most representative' control image and then averaged to create a mean T2. All T2s were coregistered to this mean T2 image. The FA, MD, AD and RD images of each subject were warped using the same transforms to achieve intra- and inter-subject alignment. As a final step, coregistered FA maps of all controls were averaged, whereafter individual FAs were again coregistered to this mean FA. These transformations were then used to again warp MD, AD, and RD images to further improve coregistration.

2.2.6 Statistical Analyses

Masks of the inferior, middle, and superior cerebellar peduncles were created manually from the average FA image of all subjects. In addition, an FA threshold >0.2 was applied to ensure that only white matter was included in the masks. The resulting masks of the cerebellar peduncles were applied to the pre-processed FA, MD, AD and RD images of each subject. Voxelwise comparisons were performed in FSL to identify ROIs where FA and MD differed in the FAS and PFAS groups compared with the controls. To control for Type I error, Monte Carlo simulations (Forman et al., 1995) were performed, which indicated that activation clusters of at least 67 mm^3 voxels were significant at a $p<0.01$ level. Mean FA or MD, as well as AD and RD, were extracted in a 2x2x2 mm^3 ROI around the peak coordinate within each cluster and examined in relation to AA/day using Pearson correlation analysis. The statistical analyses were performed using SPSS (version 21).

The values of absolute alcohol consumed per day were logged due to skewness. Two variables each had a single outlier (>3 standard deviations above the mean)—absolute alcohol consumed per drinking occasion and cigarettes smoked per day during pregnancy. For each of these

variables, the outlier was recoded to 1 point higher than the next highest observed value as recommended by Winer (1971). Missing demographic data were estimated a few cases as detailed in notes to Table 2.1. Eight control variables were considered as potential confounders—four child characteristics (child sex, age at DTI scan, maximum resultant displacement during DTI, and postnatal lead exposure), and four maternal characteristics (maternal age at delivery, cigarettes smoked/day during pregnancy, socioeconomic status (SES), and years of education). Pearson correlations were used to examine the relation of each of the control variables to FA or MD in each of the ROIs in which significant group differences were seen. Based on data from a Monte Carlo simulation, Maldonado and Greenland (1993) concluded that inclusion of all control variables related to the outcome at $p<0.20$ would be optimally protective against potential confounding. Analysis of covariance (ANCOVA) was, therefore, used to determine whether the effects of exposure group on FA or MD in each ROI remained significant after controlling for all control variables related to each of the outcomes at $p<0.20$. Child IQ was not considered a potential confounder since it does not provide an alternative causal explanation for effects of prenatal alcohol exposure on the DTI outcomes. Analyses were re-run omitting the six children whose mothers admitted using marijuana and cocaine to determine if the effects were altered.

Pearson correlation analysis was used to examine the relation of the diffusion measures in each of the ROIs to delay conditioning at 5 and 10 years, which was assessed as a dichotomous variable indicating whether the child reached criterion for conditioning (at least 40% conditioned responses; Jacobson et al., 2008) within three conditioning sessions. The hypothesis that FA or MD in the cerebellar peduncles mediates the effect of prenatal alcohol exposure on eyeblink conditioning was tested using hierarchical multiple regression analysis. Alcohol exposure was entered in the first step of the regression; the mediator (FA or MD in the ROI) was entered in the second step. Mediation was inferred if the addition of the diffusion measure substantially reduced the magnitude of the regression coefficient for prenatal alcohol exposure (Baron and Kenny, 1986). The Difference in Coefficients Test (Clogg et al., 1992) was used to assess whether the reduction in the magnitude of the regression coefficient was statistically significant. The Clogg Test was selected because in a Monte Carlo study comparing

14 methods to test the statistical significance of mediation hypotheses, MacKinnon et al. (2002) found that it was one of two with the greatest power.

2.3 Results

2.3.1 Sample Characteristics

Table 2.1 summarizes the demographic information for the children included in the study. There were no significant between-group differences in child sex, maximum displacement during DTI and lead exposure. The children with PFAS were slightly younger than the children in the other groups at the time of the DTI scan (*p*s<0.05), and the HE children were slightly older (*p*s<0.05). As expected, children with FAS and PFAS had lower IQ scores than the HE and control children (*p*s<0.01). The low IQ scores for the sample as a whole reflect the highly disadvantaged backgrounds of the children in this population. As has been seen in previous studies (May and Gossage, 2011; Jacobson et al., 1996, 2004), mothers of children with FAS were older at delivery than the mothers in the other groups (*p*s<0.01). Mothers of the children with FAS and PFAS were lower in socioeconomic status and less educated compared to the mothers in the other groups. Levels of prenatal alcohol exposure were very high, averaging 10.0 drinks/occasion for the children with FAS, 7.2 for those with PFAS, and 6.8 for the nonsyndromal HE children. Twenty-one of the 23 mothers in the control group (91.3%) abstained from alcohol during pregnancy; the other two drank no more than one drink on four occasions. There were no significant group differences in maternal cigarette use during pregnancy.

Table 2.1 Sample characteristics (*N*=77)

	FAS	PFAS	HE	Control	*F* or χ^2
N	11	16	27	23	
Child characteristics					
Sex (% male)	45.5	56.3	51.9	52.2	0.31
Age at 5-yr delay EBC	5.0 (0.2)	5.0 (0.2)	5.1 (0.1)	5.0 (0.2)	3.81*
Age at 9- to 10-yr delay EBC	9.6 (1.0)	9.2 (0.3)	10.5 (1.0)	9.9 (0.8)	7.34***
Age at 11-yr trace EBC[a]	10.8 (0.6)	11.1 (0.4)	11.3 (0.4)	10.9 (0.4)	5.22**
Age at DTI scan (yr)	9.7 (1.1)	9.4 (0.2)	10.6 (1.1)	10.0 (0.8)	6.68***
Maximum resultant displacement during DTI (mm)	1.0 (0.4)	0.9 (0.3)	0.9 (0.3)	0.9 (0.3)	0.28
Lead exposure[b]	12.5 (4.7)	10.8 (6.6)	9.3 (3.4)	8.6 (3.6)	2.28
WISC-IV IQ	64.4 (12.3)	66.6 (8.1)	76.0 (12.4)	75.2 (10.1)	4.86*
Maternal characteristics					
Maternal age at delivery	32.1 (6.7)	25.5 (5.3)	25.1 (5.0)	25.4 (4.0)	5.69**
Socioeconomic status (SES)	17.2 (9.8)	16.3 (6.7)	22.2 (9.3)	25.4 (7.6)	4.73**
Education (yr)[c]	8.8 (2.8)	7.4 (1.8)	9.1 (2.3)	10.1 (1.3)	5.43**
Absolute alcohol consumed per day across pregnancy (oz)[d]	2.1 (2.0)	0.8 (0.4)	0.5 (0.5)	0.0 (0.0)	16.86***
Absolute alcohol consumed per occasion across pregnancy (oz)[d,e]	5.0 (1.7)	3.6 (1.8)	3.4 (2.3)	0.1 (0.3)	27.62***
Drinking days per week across pregnancy[d]	2.0 (1.2)	1.8 (0.9)	1.2 (0.9)	0.0 (0.0)	20.14***
Cigarettes smoked per day during pregnancy[e]	7.3 (5.7)	6.7 (5.6)	6.2 (6.1)	4.3 (9.2)	0.67

Values are means (standard deviations)
*p<0.05, **p<0.01, ***p<0.001
FAS = fetal alcohol syndrome. PFAS = partial FAS. HE = heavily exposed nonsyndromal group
[a]Missing for 5 children: 2 with FAS, 1 HE, 2 controls
[b]Missing values estimated at group median for 1 child with PFAS, 1 HE, 2 controls
[c]Missing value estimated at group median for 1 child with PFAS
[d]Missing values estimated at group median for 2 children with FAS, 1 PFAS, 2 HE
[e]One outlier 3 standard deviations (SD) beyond the mean recoded to 1 point higher than highest observed value (Winer, 1971)

2.3.2 FA Findings

Voxelwise group comparisons of FA maps revealed significant differences in FA between the FAS and control groups bilaterally in the superior cerebellar peduncle (Figure 2.1). The peak coordinates and size of these clusters are shown in Table 2.2, together with the group averages of the mean FA within a 2x2x2 mm^3 ROI around the peak coordinates of the clusters. *Post-hoc* comparisons revealed that mean FAs in both regions were lower for the children with FAS than for those in each of the other groups (all *p*s<0.05). Table 2.2 also shows the correlation of oz AA consumed per day during pregnancy with mean FA, AD and RD in these two ROIs. The association of greater alcohol consumption with lower FA in both regions is largely attributable to greater radial diffusivity in these regions, with no relation between extent of alcohol exposure and axial diffusivity.

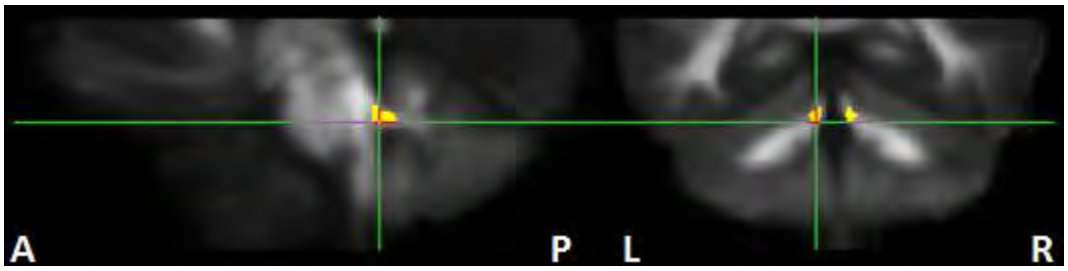

Figure 2.1 Bilateral regions in the superior cerebellar peduncle (native space) where FA in children with FAS is lower than that in healthy controls. Cross-hairs indicate peak coordinates.

Table 2.2 Size and peak coordinates (in MNI pediatric standard space; Fonov et al., 2011) of regions where FA is lower in children with FAS compared to controls, as well as group averages of the mean FA in 8mm^3 ROIs around the peak coordinates, relations of FA, AD, and RD to extent of prenatal alcohol exposure (AA/day)

Region (MNI Peak coordinates)	Size (mm^3)	Mean FA in ROIs					Relation of AA/day to mean FA		
		FAS (*n*=11)	PFAS (*n*=16)	HE (*n*=27)	Control (*n*=23)	*F*	FA	AD	RD
Left superior peduncle (-6, -43, -29)	311	0.37 (0.04)	0.42 (0.06)	0.44 (0.05)	0.44 (0.06)	5.74**	-0.39***	-0.09	0.24*
Right superior peduncle (7, -43, -28)	125	0.36 (0.05)	0.40 (0.06)	0.42 (0.04)	0.42 (0.05)	5.63**	-0.39***	-0.06	0.27*

*p<0.05, **p<0.01, ***p<0.001
Values are means (standard deviations)
FA = fractional anisotropy. AD = axial diffusivity. RD = radial diffusivity. AA/day = absolute alcohol per day during pregnancy
FAS = fetal alcohol syndrome. PFAS = partial FAS. HE = heavy exposure nonsyndromal group

2.3.3 MD Findings

Voxelwise group comparisons of MD revealed two clusters in which the FAS and/or PFAS groups differed from the controls—one within the left middle peduncle (Figure 2.2a), in which children with FAS and PFAS had higher MD than controls, and one within the right inferior peduncle (Figure 2.2b), in which children with PFAS had higher MD than controls. Peak coordinates, cluster size, and group averages of mean MD for a 2x2x2 mm^3 ROI around the peak coordinate are shown in Table 2.3. Greater AA/day was associated with greater radial diffusivity in the left middle peduncle but not in the right inferior peduncle.

The region in the left middle peduncle that emerged from the analysis is very close to the one seen in the Spottiswoode et al. (2011) study (MNI coordinates: -24, -46, -44). In a voxelwise exploratory analysis, in which MD in the cerebellar peduncles was regressed on frequency of maternal drinking during pregnancy, an ROI emerged that overlapped with that seen in the previous study (MNI coordinates: -22, -42,-44).

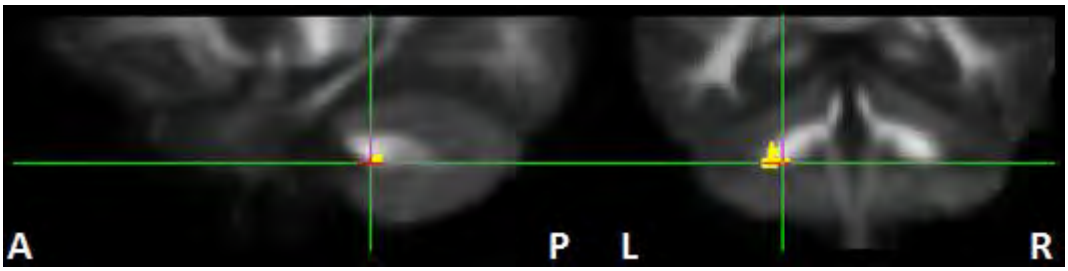

(a)

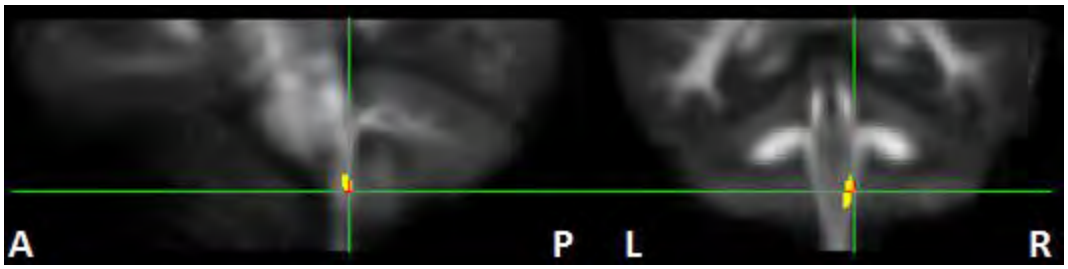

(b)

Figure 2.2 Regions in the (a) left middle cerebellar peduncle (native space) where MD in the children with FAS and PFAS is higher than in healthy controls, and (b) in the right inferior cerebellar peduncle (native space) where MD in children with PFAS is higher than in healthy controls. Cross-hairs indicate peak coordinates.

Table 2.3 Size and peak coordinates (in MNI pediatric standard space; Fonov et al., 2011) of regions where MD is higher in children with FAS and/or PFAS compared to controls, as well as group averages of the mean MD in 8mm^3 ROIs around the peak coordinates, and relations of MD, AD, and RD to extent of prenatal alcohol exposure (AA/day)

Region (MNI Peak coordinates)	Size (mm^3)	Mean MD (10^{-3} mm^2/s)					Relation of AA/day to mean MD		
		FAS (*n*=11)	PFAS (*n*=16)	HE (*n*=27)	Controls (*n*=23)	*F*	MD	AD	RD
Left middle peduncle[a] (-18,-35,-41)	233	1.56 (0.28)	1.60 (0.20)	1.42 (0.26)	1.36 (0.22)	4.30**	0.37***	-0.08	0.24*
Right inferior peduncle[b] (5,-43,-57)	136	1.01 (0.11)	1.07 (0.07)	0.97 (0.08)	1.00 (0.10)	4.84**	0.09	-0.03	0.10

*p<0.05, **p<0.025, ***p<0.01

Values are means (standard deviations)

MD = mean diffusivity. AD = axial diffusivity. RD = radial diffusivity. AA/day = absolute alcohol per day during pregnancy

FAS = fetal alcohol syndrome. PFAS = partial FAS. HE = heavily exposed nonsyndromal group

[a]MD higher in children with FAS than controls (p=0.021), and in children with PFAS than in both HE and control children (p=0.016 and p=0.002, respectively).

[b]MD higher in children with PFAS than children in all the other groups (all ps<0.01)

2.3.4 Control for Confounders

The correlations of the control variables with FA and MD in the four regions in which significant group differences were seen are shown in Table 2.4. When the potential confounders that were related to the DTI measures at p<0.20 were included as covariates in ANCOVAs relating exposure group to FA in both the left and right superior peduncles and to MD in the left middle peduncle, the following effects of exposure remained significant: FA in the left superior peduncle—$F(3,70)=4.10$, p=0.010; FA in right superior peduncle—$F(3,71)=4.26$, p=0.008; MD in the left middle peduncle — $F(3,71)=3.64$, p=0.017. However, the effect of exposure group on MD in the right inferior peduncle was no longer statistically significant after adjustment for child's age at scan—$F(3,72)=2.58$, p=0.060. The effects were essentially unchanged when the analyses were re-run omitting the five children whose mothers admitted using marijuana and the one who reported using cocaine.

Table 2.4 Correlation of eight control variables with FA or MD in the four ROIs

	Child's sex	Child's age at DTI scan	Lead exposure	Maximum resultant displacement	Maternal age	SES[a]	Maternal education	Smoking during pregnancy
FA								
Left superior peduncle	0.16[†]	0.04	0.10	-0.10	-0.24*	0.10	0.08	-0.22[†]
Right superior peduncle	0.20[†]	0.07	0.01	-0.13	-0.15[†]	0.03	0.07	-0.11
MD								
Left middle peduncle	0.15[†]	-0.11	0.04	0.12	0.23[†]	-0.10	-0.06	0.06
Right inferior peduncle	-0.01	-0.37**	-0.02	-0.08	0.07	-0.12	-0.06	0.07

Values are Pearson *r*s
[†]$p<0.20$, *$p<0.05$, **$p<0.001$
[a]SES: Socioeconomic status. FA = fractional anisotropy. MD = mean diffusivity.

2.3.5 Mediation of Effects of Prenatal Alcohol Exposure on Eyeblink Conditioning

Higher FA in the left and right superior peduncles was associated with more optimal EBC performance at 5 years (r=0.39, $p<0.001$, and r=0.32, $p<0.01$). Higher MD in the left middle peduncle was associated with poorer EBC performance at 9-10 years (r=-0.28, $p<0.05$). Mediation of the effect of prenatal alcohol exposure on EBC by the diffusion measures was assessed using multiple regression analysis. Since the ROI in the superior peduncles was generated from a contrast between the children with FAS and the controls, prenatal alcohol exposure was measured in terms of the presence or absence of FAS in the first two regressions; it was measured by AA/day in the third. As shown in Table 2.5, the standardized regression coefficient for exposure increased from -0.34 to -0.23 when FA in the left superior peduncle was entered into the regression, a decrease that was statistically significant. This mediation of the effect of prenatal alcohol exposure on EBC by lower FA in the left superior peduncle is illustrated in Figure 2.3. The regression coefficients for prenatal alcohol exposure also decreased significantly when FA in the right middle peduncle and MD in the left middle peduncle were added to their respective regression analyses. Mediation of the effect on EBC was inferred for all three ROIs based on the significant reduction in the magnitude of the regression coefficients for exposure following the addition of the diffusion measures to the regression analyses.

Table 2.5 Mediation of the effect of prenatal alcohol exposure on eyeblink conditioning by FA or MD in three regions of interest

Mediator	Alcohol exposure		t^a
	β_1	β_2	
Left superior peduncle (FA)[b]	-0.34***	-0.23†	-2.57**
Right superior peduncle (FA)[b]	-0.34***	-0.26*	-1.99*
Left middle peduncle (MD)[c]	-0.25*	-0.17	-2.15*

†p <0.10, *p<0.05, **p<0.025, ***p<0.01.

β_1 = Standardized correlation coefficient for alcohol exposure before controlling for the mediating variable. β_2 = Standardized correlation coefficient for alcohol exposure after controlling for the mediating variable. FA = fractional anisotropy. MD = mean diffusivity. AA/day = absolute alcohol per day during pregnancy.

[a]Significance of the reduction in β following the addition of the mediator to the model, based on the difference in coefficients method (Clogg et al., 1992).

[b]Mediation by FA in the superior peduncle of the effect of alcohol exposure (measured by contrasting the FAS group with the others in the sample) on eyeblink conditioning at 5 years.

[c]Mediation by MD in the left middle peduncle of the effect of alcohol exposure (measured by AA/day) on eyeblink conditioning at 9-10 years.

Figure 2.3 Path model illustrating mediation of the effect of FAS status on eyeblink conditioning by lower FA in the left superior cerebellar peduncle

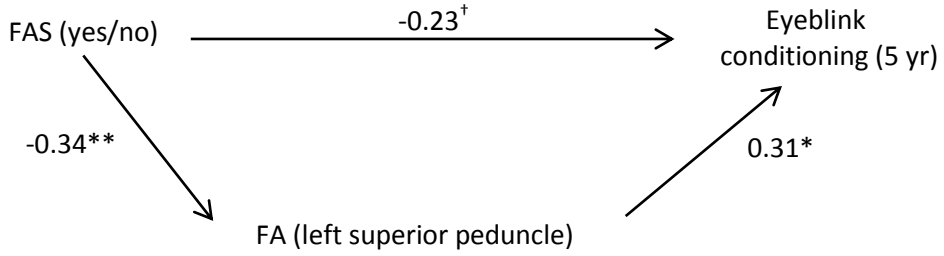

† p<0.10, *p<0.05, **p<0.01

2.4 Discussion

This study used DTI to examine the effects of prenatal alcohol exposure on microstructural integrity in the cerebellar peduncles in a heavily exposed cohort of school-age children. Voxelwise group comparisons showed lower FA bilaterally in the superior cerebellar peduncle only in the most severely affected children, that is, those with full FAS, compared to non- or minimally exposed controls. Group differences in MD were found in regions in the left middle and right inferior peduncles. The continuous measure of prenatal alcohol exposure, oz AA/day,

was also related to lower FA in the left and right superior peduncles and to higher MD in the left middle peduncle, effects that remained significant after control for potential confounders. Further, lower FA in the left and right superior peduncles and higher MD in the left middle peduncle were significantly associated with poorer EBC performance. In all three of these regions, these deficits were found to partially mediate the effect of alcohol on EBC performance.

The larger sample in this study confirmed evidence of a fetal alcohol-related microstructural deficit in the left middle peduncle reported in our previous study on a different sample of Cape Town school-age children with FASD (Spottiswoode et al., 2011). The coordinates of the region showing lower FA in that study are very close to the region where microstructural deficits were observed in the present study. In the only other study to use DTI to examine structural integrity in the cerebellar peduncles in children with FASD, Lebel et al. (2010) found that poorer math performance was associated with lower FA in a region in the left middle peduncle (MNI coordinates: -12, -34, -42) that overlaps with the region we found to be affected in this study (MNI coordinates: -18, -33, -41). Lower FA in similar regions of the left middle peduncle has also been reported in adolescents with attention deficit/hyperactivity disorder (ADHD; MNI coordinates: -21, -49, -27) (Ashtari et al., 2005); decreased FA values in this region were associated with increased severity of inattentive scores on the Conners (1997) ADHD scale. By contrast to the middle peduncle, the group differences seen in the superior peduncles in the FAS group were not detected in our previous study, possibly because there were only five children with full FAS in the smaller sample examined in that study. The finding of this deficit only in the FAS group may explain, in part, the greater vulnerability to EBC impairment in the children with FAS, none of whom met criterion for conditioning at 5 years of age (Jacobson et al., 2008).

It is noteworthy that the group differences in both the bilateral superior and left middle peduncles were seen in radial but not axial diffusivity. This pattern is consistent with the finding in our previous study that prenatal alcohol exposure was associated with an increase only in radial diffusivity (Spottiswoode et al., 2011). Specific effects on radial diffusivity were also seen in the only three other DTI studies to measure patterns of directional diffusivity in relation to

FASD. In their math study, Lebel et al. (2010) found an association between math achievement test scores and higher radial diffusivity in the left anterior cerebellar white matter tracts connected to the middle peduncle but no association with axial diffusivity in children with FASD. Similarly, Li et al. (2009) found increased radial diffusivity (with no difference in axial diffusivity) in the isthmus of the corpus callosum in young adults with fetal alcohol-related dysmorphology. Green et al. (2013) showed that saccadic reaction times are positively correlated to FA and negatively correlated to radial diffusivity in the corpus callosum in children with FASD during an antisaccadic task.

Radial diffusivity indicates the degree to which water diffuses in a direction that is perpendicular to the axonal tract. Data from experimental studies with laboratory animals suggest that higher radial diffusivity may be caused by decreased axonal packing density and/or poor myelination (Beaulieu, 2002). Data from laboratory animal and human studies suggest that maternal alcohol ingestion during pregnancy can alter iron homeostasis in the brain, which may modify the expression of the basic myelin protein, subsequently interfering with normal myelination (Connor and Menziers, 1996; Carter et al., 2007). Moreover, prenatal alcohol exposure can lead to impairment in oligodendrocytes that produce the myelin sheaths (Phillips and Krueger, 1992; Ozer et al., 2000). These findings suggest that poor myelination may play an important role in the increased radial diffusivity associated with lower FA in the superior and higher MD in the middle peduncles in the children with FASD.

The primary aim of this study was to test the hypothesis that microstructural defects in the cerebellar peduncles might be responsible, in part, for the poorer eyeblink conditioning seen in fetal alcohol-exposed children. Prenatal alcohol exposure was associated with microstructural deficits in three ROIs within the cerebellar peduncles after control for confounders—one in the middle peduncle, which mediates transmission of the auditory conditioned stimulus from the pontine nucleus in the brainstem to the cerebellum; the other two in the superior peduncles, which mediate transmission of the efferent signal for the conditioned response from the cerebellar deep nuclei to the red nucleus. Pearson correlation analysis linked the microsctructural deficit in the left middle peduncle to poorer EBC performance at 9-10 years,

confirming our previous finding (Spottiswoode et al., 2011); the deficit in the superior peduncles was associated with poorer EBC performance at 5 years. Moreover, multiple regression analyses provided statistical evidence that the effects of prenatal alcohol exposure on these EBC measures were partially mediated by the microstructural deficits revealed in the DTI analyses. It should be noted that, because the DTI assessment was conducted at 10 years, the inference that prenatal alcohol exposure-related deficits in microstructural integrity in the cerebellar peduncles partially mediated the effects of alcohol exposure on EBC performance depends on the assumption that these white matter deficits were already present from a younger age. A replication of these findings using DTI data obtained earlier in development is, therefore, warranted.

These data suggest that the fetal alcohol-related deficit in EBC can be attributed, in part, to less optimal transmission of information to and from the brainstem via the cerebellar peduncles. Our findings are consistent with evidence from 12 recent DTI studies (e.g. Paolozza et al., 2014, Treit et al., 2013, Green et al., 2013) showing alcohol-related deficits in the structural integrity of white matter tracts in multiple regions throughout the brain. To our knowledge, our two DTI EBC studies are the only ones to date to use a statistical model to evaluate the role of a white matter deficit in mediating the effect of prenatal alcohol exposure on a specific neurobehavioral endpoint.

Given that the peduncles appear to be a homogeneous white matter structure, it seems unlikely that fetal alcohol exposure affects only the particular ROIs in the superior and middle peduncles identified in this study. A tractography-based approach might reveal fetal alcohol-related microstructural deficits in broader regions of the cerebellar peduncles. Moreover, although care was taken to ensure satisfactory coregistration, the potential existence of regional misregistration errors are a limitation of any voxel-based approach. The cerebellar region is also prone to susceptibility and pulsatility artifacts. The susceptibility artifacts may amplify misregistration errors, and the pulsatility artifacts can degrade the data quality in the inferior aspects of the cerebellum as the brainstem/CSF recoils when high velocity blood enters the brain just after systole. These artifacts did not noticeably affect the data quality in this study.

2.5 Conclusions

This study adds to the growing body of evidence linking prenatal alcohol exposure to poorer microstructural white matter integrity in the corpus callosum and throughout the brain. These data replicate our previous finding from a smaller, cross-sectional sample of a fetal alcohol-related increase in radial diffusivity in a region of the left middle cerebellar peduncle and provide evidence confirming our report that the alcohol-related deficits in EBC may be mediated, in part, by microstructural deficits in this region. This study also provides evidence of lower FA in the superior peduncles specifically in the children with full FAS, which may account, in part, for their heightened risk for impairment in EBC performance. Prenatal alcohol exposure was related to increased radial rather than axial diffusivity in both the superior and middle peduncles, suggesting poorer axon packing density and/or myelination. The inference of a myelination deficit is supported by the animal model studies linking prenatal alcohol exposure to impairment in the oligodendrocytes and expression of myelin basic protein involved in producing the myelin sheath. Consistent with what is known from animal models about the neurophysiology of EBC, the microstructural deficits in both regions of the cerebellar peduncles were related to poorer EBC performance. Moreover, data from mediation models provided statistical evidence that poorer microstructural integrity in the cerebellar peduncles may play an important role in the eyeblink conditioning deficit commonly seen in fetal alcohol-exposed children.

Chapter 3

Effects of Prenatal Alcohol Exposure on White Matter Integrity

Jia Fan[1,2], Sandra W. Jacobson[2-4], Paul A. Taylor[1,2,5], Christopher D. Molteno[3], Joseph L. Jacobson[2-4], Ernesta M. Meintjes[1,2]

Abstract

Fetal alcohol spectrum disorders (FASD) describe the spectrum of cognitive, behavioural and neurological impairments caused by prenatal alcohol exposure (PAE). In this study, diffusion tensor imaging (DTI) was performed on 41 children with FASD (26 with either full fetal alcohol syndrome (FAS) or partial FAS (PFAS), 15 nonsyndromal heavily exposed (HE)) and 13 age-matched controls (total group mean age 10.4±0.4 yrs) from the Cape Town Longitudinal Cohort, for whom detailed drinking histories during pregnancy were available. Voxelwise group comparisons were performed between the control group and each of two FASD groups: (1) HE, and (2) a combined FAS and PFAS group (FAS/PFAS). Compared to healthy controls, children with FAS/PFAS showed significantly lower fractional anisotropy (FA) in four regions and higher MD in seven regions. Three regions derived from the FA group differences (left inferior longitudinal fasciculus (ILF), medial splenium, and medial isthmus) overlapped with the MD-derived clusters, and the fourth FA-derived cluster was located in a different location of the same fiber bundle (right ILF) as an MD cluster. The additional MD clusters were in the right superior longitudinal fasciculus and bilaterally in the corticospinal tract. Children with HE showed lower FA and higher MD in a subset of these regions. We also investigated the relation

---

[1]MRC/UCT Medical Imaging Research Unit, University of Cape Town, South Africa, [2]Department of Human Biology, University of Cape Town, South Africa, [3]Department of Psychiatry and Mental Health, University of Cape Town, South Afrca, [4]Department of Psychiatry and Behavioral Neurosciences, Wayne State University School of Medicine, United States, [5]African Institute for Mathematical Sciences, South Africa

between three continuous measures of alcohol exposure during pregancy and DTI parameter values at the cluster peaks. In all the regions, FA and MD were significantly correlated with each of the alcohol measures, effects that for the most part remained significant after controlling for potential confounders, indicating that white matter damage in these regions is dose dependent. This study provides insight into the locations and the gradation of effects of PAE on white matter development in the cerebra of pre-adolescent children.

Key words: Prenatal alcohol exposure, fetal alcohol spectrum disorders, diffusion tensor imaging, white matter alterations

3.1 Introduction

Prenatal alcohol exposure (PAE) has numerous adverse consequences on fetal development, which are often encompassed under an umbrella term, fetal alcohol spectrum disorder (FASD). These include life-long cognitive and behavioural impairments, as well as potential structural damage in the brain (Jacobson and Jacobson, 2002; Burden et al., 2005; Kalberg et al., 2006; Mukherjee et al., 2006; Spadoni et al., 2007). As an example of the prevalence of PAE, the Center for Disease Control and Prevention (2012) reported that, among a sample of 13,880 pregnant women in the USA between 2006 and 2010, 7.6% admitted to consuming alcohol during the prior 30 days and 1.4% to binge drinking. While prenatal alcohol exposure does not always result in FASD for a child, there is no medical guideline for safe levels of alcohol consumption during pregnancy (Barr and Streissguth, 2001; Mattson and Riley, 1998; Spadoni et al., 2007). The prevalence of FASD in the US is estimated to be as high as 2-5% of the total population (May et al., 2009) and has been identified in all racial and ethnic groups (Abel, 1995). In the Cape Coloured community in the Western Cape Province of South Africa, incidence rates 18 to 141 times higher than in the United States have been reported (May et al., 2000). The Cape Coloured population is a mixed ancestry group, originally from Africa, Europe and Malaysia. Heavy maternal drinking is very prevalent in this community (Croxford and Viljoen, 1999) both due to poor psychosocial circumstances and the traditional *dop* system where

labourers were paid in part with wine, making this population ideally suited to studies of the effects of PAE.

The term fetal alcohol syndrome (FAS) was introduced in 1973 as the most severe classification of FASD (Jones and Smith, 1973). FAS is characterized by the observation of three criteria: central nervous system dysfunction, pre- and post-natal growth deficiencies, and the presence of certain craniofacial features (specifically, short palpebral fissures, an indistinct philtrum, and a thin vermillion) (Hoyme et al., 2005; Stratton et al., 1996). Partial FAS (PFAS) is used to describe a case of PAE in which two of the three alcohol-related facial anomalies and at least one of the following are present: small head circumference, growth retardation, or neurobehavioral impairment. Exposed individuals who do not show all of the diagnostic criteria but who still exhibit neurobehavioral deficits are clinically diagnosed as having alcohol-related neurodevelopmental disorder (ARND).

Brain structure abnormalities have been reported in autopsies of children with FASD, including agenesis of the corpus callosum (CC), microcephaly, ventriculomegaly, a small cerebellum, and a variety of other malformations caused by neuronal and glial migration errors (Jones and Smith, 1973; Clarren et al., 1978, Peiffer et al., 1979; Kinney et al., 1980; Wisniewski et al., 1983; Coulter et al., 1993). Fifty structural MRI studies have been published on individuals with prenatal alcohol exposure, typically using a T1-weighted (T1w) protocol, including 21 studies on total brain volume (e.g., Chen et al., 2012; Rajaprakash et al., 2014; De Guio et al., 2014), 5 studies on cerebral volume (Mattson et al., 1992, 1994, 1996; Archibald et al., 2001; De Zeeuw et al., 2012), and 10 studies on cerebellar volume (e.g., Astley et al., 2009; Spottiswood et al., 2011; De Zeeuw et al., 2012). Similar to autopsy studies, MRI has shown decreased brain structural volumes in FASD subjects compared to healthy controls.

A growing body of evidence has suggested that white matter (WM) tissue is a specific target of alcohol teratogenesis. Reductions in the total WM volume have been found in individuals with FASD (Archibald et al., 2001; Sowell et al., 2001b; Lebel et al., 2008; Bjorkquist et al., 2010; Nardelli et al., 2011; Roussotte et al., 2012; Yang et al., 2012; De Zeeuw et al. 2012; Treit et al., 2013; De Guio et al., 2014). Studies have also reported smaller WM volumes in the frontal lobe

(Sowell et al., 2002a; Astley et al., 2009), parietal lobe (Archibald et al., 2001; Sowell et al., 2002b), temporal lobe (Sowell et al., 2002a), and cerebellum (Spottiswoode et al., 2011), though many of these differences were not significant after correcting for whole brain volume. Thus, further investigation of regional WM alterations in individuals with FASD remains necessary to understand the effects of PAE on WM integrity and the complex relationships between behaviour, cognition, and brain structure.

Diffusion tensor imaging (DTI) has been shown to provide useful, quantitative information regarding brain anatomy and particularly WM fiber pathways (Basser et al., 1994). The MRI-based method measures water diffusion in brain tissue, which tends to be highly anisotropic (spatially variant) in WM and strongly isotropic (spatially homogenous) in gray matter and cerebrospinal fluid. The diffusion tensor can be represented geometrically as an ellipsoid surface with semi-axes whose lengths are described, in descending order, by the eigenvalues, e1, e2 and e3; e1 is often called parallel or axial diffusivity (AD), while the average of e2 and e3 is termed perpendicular or radial diffusivity (RD). The average of the three eigenvalues is the mean diffusivity (MD), which quantifies the average random motion within a voxel, and their normalised standard deviation is the fractional anisotropy (FA), which represents the degree to which water diffuses preferentially parallel to the axonal axis rather than perpendicular to it.

To date, 14 DTI studies have been performed on individuals with FASD, often focusing on the CC as a region of interest (ROI), since it is relatively easy to delineate and crucial for inter-hemispheric communication. Several studies, which have employed a variety of techniques, including manual drawing (Ma et al., 2005; Wozniak et al., 2006, 2009), tractography (Lebel et al., 2008; Colby et al., 2012; Treit et al., 2013; Green et al., 2013; Taylor et al., 2015), tract-based spatial statistics (TBSS) (Li et al., 2009; Fryer et al., 2009), and voxelwise analysis (Sowell et al., 2008; Lebel et al., 2010; Spottiswoode et al., 2011, Fan et al., 2015), have confirmed microstructural abnormalities of the CC in FASD in the splenium (SCC) (Ma et al., 2005, Lebel et al., 2008; Sowell et al., 2008; Wozniak et al., 2009), the isthmus (ICC) (Wozniak et al., 2006, 2009; Li et al, 2009), the genu (GCC) (Ma et al., 2005; Lebel et al., 2008; Treit et al., 2013) and the body of the CC (BCC) (Wozniak et al., 2009; Frey et al., 2009). WM deficits have also been

reported in other regions, such as the inferior (Lebel et al., 2008; Sowell et al., 2008; Colby et al., 2012) and superior longitudinal fasciculi (Lebel et al., 2008; Frey et al., 2009; Treit et al., 2013), and in the superior (Fan et al., 2015) and middle cerebellar peduncles in the cerebellum (Spottiswoode et al., 2011; Fan et al., 2015).

In this study, we investigated the effects of PAE on cerebral white matter within a cohort of pre-adolescent Cape Coloured children across several FASD diagnoses. A strength of this study is the fact that the mothers of the children were recruited as part of a longitudinal study during pregnancy, so that detailed information of their drinking during pregnancy is available (Jacobson et al., 2008). This presents a unique opportunity to study white matter abnormalities in relation to the degree of alcohol exposure in a well-characterized cohort of children. We hypothesized that (1) PAE will adversely impact cortical WM and that effects may vary with clinical diagnosis, and (2) that the extent of WM alterations (in terms of volume or numbers of regions) would be related to the degree of alcohol exposure (i.e. the amount or frequency of drinking).

3.2 Materials and Methods

3.2.1 Participants

Pregnant women were recruited from a Cape Coloured community in the Western Cape, South Africa (Croxford and Viljoen, 1999). Exclusionary criteria included: age less than 18 years, diabetes, epilepsy, or cardiac problems requiring treatment. Timeline follow-back interviews were conducted to determine the incidence and amount of drinking on a day-by-day basis during a typical 2-week period, both at time of conception and time of recruitment (Jacobson et al., 2002). The timeline follow-back interview was repeated in mid-pregnancy and again at 1 month postpartum. More details can be found in our previous study of the cerebellum (Fan et al., 2015). Drinking was quantified in units of ounces (oz) of absolute alcohol (AA), and maternal consumption was recorded using three measures: oz AA consumed per day across pregnancy (AA/day), oz AA consumed per occasion across pregnancy (AA/occasion), and drinking days per

week across pregnancy (days/week). Two groups of women were invited to participate in the study: (1) any woman reporting a minimum of 14 drinks per week (1.0 oz AA/day) or at least two incidents of binge drinking (≥ 5 drinks per occasion) per month during the first trimester of pregnancy, and (2) controls who abstained from drinking or drank no more than minimally during pregnancy. Smoking during pregnancy was reported in terms of cigarettes smoked per day. The mother's age at delivery and years of education were also recorded.

3.2.2 Procedures

Whole-brain DTI data were obtained from 56 right handed children from the Cape Town Longitudinal Cohort (Jacobson et al., 2008). These data were collected about a year after the cerebellar DTI data (Fan et al., 2015). IQ was assessed using the Wechsler Intelligence Scale for Children-IV (WISC-IV; see Diwadkar et al., 2013). Postnatal lead exposure, based on a venous blood sample obtained at age 5 years, was also assessed since lead levels in this population are within the range in which effects on cognitive function have been reported (Chiodo et al., 2004; Lanphear et al., 2000). Each child was examined for growth and FAS dysmorphology at around 5 years by three expert dysmorphologists using the Revised Institute of Medicine criteria (Hoyme et al., 2005) at an FAS diagnostic clinic. Each of the alcohol-exposed children was assigned to one of the following diagnostic groups: FAS, PFAS, or nonsyndromal heavily exposed (HE). It should be noted that the children in the HE group did not meet any diagnostic criteria for FASD (as with ARND) but were born to mothers who had been recruited prospectively based on their heavy alcohol consumption during pregnancy. The diagnosis procedures are detailed in our previous study (Fan et al., 2015). The sample comprised 8 children with FAS, 19 PFAS, 15 HE, and 14 controls. Approval for human research was obtained from the Human Investigation Committee at Wayne State University and the Faculty of Health Sciences Human Research Ethics Committee at University of Cape Town. Informed consent was obtained from mothers at recruitment and at the child assessment visits; assent was also obtained from the child. Children received a small gift, and mothers received a photo of their child and compensation consistent with guidelines from the ethics committees.

3.2.3 Scanning Protocol

The children and their mothers were transported to the Cape Universities Brain Imaging Center (CUBIC), where they were familiarized with the scanning procedures. Data were acquired using two DTI acquisitions with alternating phase encoding directions (i.e., anterior-posterior and posterior-anterior (AP-PA)) on a 3T Allegra MRI (Siemens, Erlangen, Germany). For each acquisition, the following parameters were used: 4 reference images with b=0 s/mm^2 and 30 diffusion weighted images (DWIs) with b=1000 s/mm^2; 72 slices; field of view (FOV)=230x230x130 mm^3; slice thickness 1.8 mm, 1.8x1.8 mm^2 in-plane resolution; TR 10000 ms; TE 88 ms. A 3D echo planar imaging (EPI) navigated (Tisdall et al., 2009) multiecho magnetization prepared rapid gradient echo (MEMPRAGE) (Van der Kouwe et al., 2008) structural image (resolution=1.3x1.3x1.0 mm^3, FOV=256x256x167 mm^3, 128 slices, TR 2530 ms, TI 1100ms, TE's 1.53/3.21/4.89/6.57 ms, flip angle 7°) was also acquired for each subject.

3.2.4 Pre-processing

Pre-processing included motion correction using FSL-flirt (Smith et al., 2004) and susceptibility correction in Matlab using the AP-PA acquisitions (Anderson et al., 2003). DTI data were initially inspected visually for the presence of dropout slices. Any subjects with dropout slices in any of their DTI acquisitions were excluded from all further analyses. After exclusions, we report data for 41 children with FASD (7 FAS, 19 PFAS, 15 HE) and 13 non- or minimally-exposed controls (Ctl), mean age 10.1±1.0 yr. For each subject, we computed for each volume the resultant displacement relative to the first unweighted (b_0) volume using the three translation parameters from mcflirt in FSL. The resultant displacements for all volumes were below 2.0 mm for all subjects included in the analyses. Maximum resultant displacement also did not differ between diagnostic groups. Rotations in any direction were less than 1.3 degrees in all subjects. To compute *z*-scores, we calculated the mean and standard deviation based only on values between the 25 and 75 percentile limits and generated *z*-score maps for each acquisition; any data points more than 3 standard deviations (SDs) beyond the mean of the *z*-score map were discarded. The diffusion tensors (DTs) were estimated, and the relevant maps of DTI scalar parameters (FA, MD, etc.) were generated.

A mean standard space and WM mask for this study were created as follows. For each subject, the b_0 volumes were co-registered to his/her own T1w structural image using nonlinear algorithms in FSL. T1w images of controls were coregistered to a single control image and then averaged to create a mean T1w image. Each subject's T1w and DTI parameter images were transformed to this mean T1w space. As a final step, coregistered FA maps of all controls were averaged, after which individual DTI parameter maps were coregistered to this mean FA image. The cerebrum was extracted using an MNI 1x1x1 mm^3 template and thresholded at an average FA > 0.2 to ensure that only white matter was included in the analysis (Mori and van Zijl, 2002). For presentation and reporting of cluster locations, final clusters were mapped to a $1mm^3$ MNI pediatric standard image (Fonov et al., 2011).

3.2.5 Statistical Analyses

Differences in DTI parameters were calculated between the Ctl group and each of two FASD groups: (1) a combined FAS and PFAS group (FAS/PFAS), and (2) an HE group, which comprises heavily exposed children who do not meet criteria for a clinical diagnosis of FASD. Voxelwise group comparisons were performed using FSL-randomise to identify clusters showing significant differences between groups. To control for Type I error, Monte Carlo simulations (Forman et al., 1995) were performed using AFNI-AlphaSim, which indicated that activation clusters of at least 168 mm^3 in the mean template space were significant at $p<0.01$.

In order to examine dose dependence in regions where diagnostic groups revealed white matter differences, we extracted the average FA, MD, AD and RD in a 2x2x2 mm^3 region-of-interest (ROI) around the peak coordinate within each cluster and correlated these separately with the three PAE parameters (AA/day, AA/occasion, and days/week). The statistical analyses were performed using SPSS (version 21). The values of AA/day were logged due to skewness. Days/week, maternal smoking during pregnancy and postnatal lead exposure each had a single outlier (>3 SD above the mean), which was recoded to 1 point higher than the next highest observed value (a standard process known as 'winsorization', Winer (1971)). Missing demographic data were estimated as the median for each diagnostic group (as noted in Table 3.1). When excluding subjects with missing data, results remained essentially unchanged.

Seven control variables were considered as potential confounders: four child characteristics (child's sex, age at scan, maximum resultant displacement during DTI, and postnatal lead exposure), and three maternal characteristics (maternal age at delivery, average cigarettes smoked/day during pregnancy, and years of education). Child IQ was not considered, since it does not provide an alternative causal explanation for effects of PAE on the DTI outcomes. Model selection of meaningful parameters for each peak cluster was determined in the following manner (see, e.g., Fan et al., 2015): each potential predictor that was weakly related (p<0.1) to the average FA or MD in the cluster was included in the final model. Analysis of covariance (ANCOVA) was used to determine whether group differences remained after controlling for potential confounders, and linear regression to examine whether associations with alcohol exposure measures remained significant after controlling for potential confounders. The mothers of three children (1 FAS, 2 PFAS) admitted to using marijuana during pregnancy and the mother of one PFAS child reported using cocaine. To assess whether inclusion of these children introduced any bias into the results, all analyses were re-run excluding these children.

3.3 Results

3.3.1 Sample Characteristics

The sample characteristics are summarized in Table 3.1. There were no significant between-group differences in child sex, child age at scan, maximum displacement during DTI, maternal age at delivery or maternal cigarette consumption during pregnancy. Children with FAS/PFAS had lower IQ than either of the other groups and their mothers had fewer years of education (ps<0.001). Lead exposure was significantly higher in children with FAS/PFAS compared to controls (p<0.05). As expected, there were significant differences in all alcohol parameters (both quantities and frequency of drinking) across groups, with the highest average values in the FAS/PFAS group. Twelve of the mothers in the control group (92.3%) abstained from alcohol during pregnancy, while the other one consumed no more than 1 drink on four separate occasions.

Table 3.1 Sample characteristics (*N*=54)

	FAS/PFAS	HE	Ctl	*F* or χ^2
N	26	15	13	
Child Characteristics				
Sex (% male)	50%	53%	54%	0.03
Age at DTI scan (yr)	10.4(0.5)	10.5(0.3)	10.4(0.4)	0.63
Maximum resultant displacement during scan (mm)	1.0(0.5)	1.1(0.5)	0.9(0.5)	0.39
Lead exposure[a,d]	11.9(5.5)	9.7(3.7)	8.1(3.3)	3.24*
WISC-IV IQ	64.3(9.7)	73.1(8.0)	74.9(9.0)	7.70***
Maternal characteristics				
Maternal age at delivery	28.8(7.5)	25.2(5.0)	26.0(3.3)	2.04
Education (yr)[b]	7.8(2.2)	9.5(2.2)	10.3(1.4)	7.46***
Absolute alcohol consumed per day across pregnancy (AA/day)[c]	1.3(1.4)	0.5(0.5)	0.0(0.0)	7.26**
Absolute alcohol consumed per occasion across pregnancy (AA/ occasion)[c]	4.1(1.8)	2.9(1.4)	0.1(0.3)	31.75***
Drinking days per week across pregnancy (days/week)[c,d]	2.1(1.3)	1.1(0.8)	0.0(0.0)	17.75***
Cigarettes smoked per day during pregnancy[e]	8.2(5.7)	8.0(7.2)	4.2(10.9)	1.32

*p<0.05, **p<0.01, ***p<0.001; Values are: mean (SD);
FAS/PFAS = combined fetal alcohol syndrome (FAS) and partial FAS (PFAS) group; HE = nonsyndromal heavily exposed group; Ctl = control group
[a]Missing values estimated at group median for 2 children with FAS/PFAS, 1 HE
[b]Missing values estimated at group median for 2 children with FAS/PFAS
[c]Missing values estimated at group median for 2 children with FAS/PFAS, 1 HE
[d]One outlier in FAS/PFAS group was winsorized (value >3 SD above the mean recoded to 1 point higher than highest observed non-outlier) (Winer, 1971)
[e]One outliers in Ctl group was winsorized (Winer, 1971)

3.3.2 FA Findings

Voxelwise group comparisons revealed significant differences in FA between children with FAS/PFAS and controls in four (suprathresholded) clusters, located in the left and right inferior longitudinal fasciculi (L- and R-ILF, respectively), the medial SCC (M-SCC), and the medial ICC

(M-ICC) (Figure 3.1). Table 3.2 shows the cluster sizes, peak coordinates, and group averages of the mean FA in ROIs defined around the peak coordinates, as well as the correlations of FA, AD and RD in these ROIs with the three alcohol exposure measures. These relations are shown in the plots in Figure 3.2.

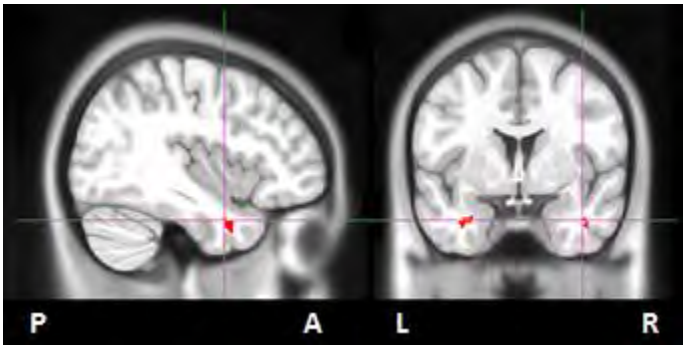

L- and R-inferior longitudinal fasciculi

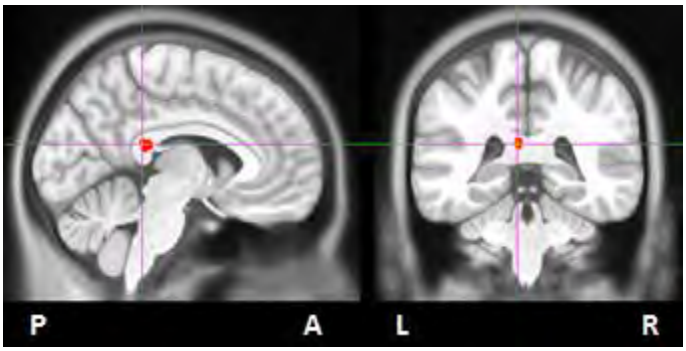

M splenium of corpus callosum

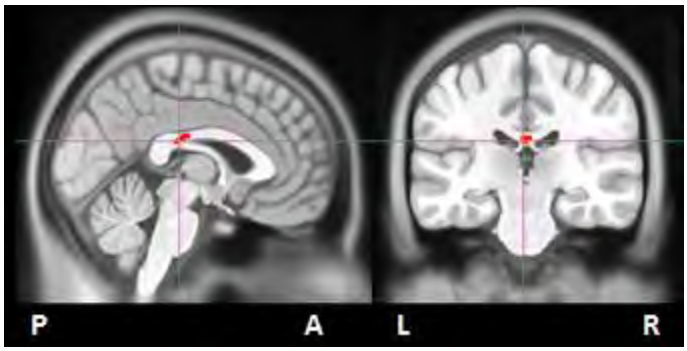

M isthmus of corpus callosum

Figure 3.1 Clusters (MNI pediatric standard space) where the mean FA is lower in children with FAS/PFAS compared to controls. Cross-hairs indicate peak coordinates.

Fewer significant clusters were observed when comparing the HE group with controls. There were 3 clusters where HE children had lower FA than controls, including one in the L-ILF and two in M-SCC. Since each of these clusters overlapped with the clusters derived from the FAS/PFAS versus control comparison, they are not reported separately in Table 3.2.

In each of the ROIs, increasing alcohol exposure was associated with lower FA (all *r*s≤-0.32, *p*s<0.05), effects that appear to be largely attributable to greater RD with increasing alcohol exposure in all regions. By contrast, increased alcohol exposure was only associated with lower AD in the M-ICC.

Table 3.2 Size and peak coordinates (in MNI pediatric standard space) of regions where FA is lower in children with FAS/PFAS compared to controls, as well as group averages of the mean FA in 8mm^3 ROIs centered around the peak coordinate. Columns on the right show relations of continuous alcohol exposure measures to FA, AD and RD in the peak ROIs.

Region MNI coordinates (mm)	Size (mm^3)	Mean FA in ROIs FAS/PFAS (26)	 HE (15)	 Ctl (13)	*F*		Correlations with DTI measures in ROIs AA/day	 AA/occasion	 days/week
L inferior longitudinal fasciculus[a]									
-43,-3,-30	282	0.30 (0.04)	0.30 (0.03)	0.35 (0.04)	8.49***	**FA**	-0.39**	-0.35**	-0.35**
						AD	-0.10	-0.02	-0.12
						RD	0.33*	0.33*	0.28*
R inferior longitudinal fasciculus									
37,2,-30	198	0.30 (0.04)	0.32 (0.04)	0.35 (0.04)	6.36***	**FA**	-0.35**	-0.32*	-0.39**
						AD	0.07	0.03	0.01
						RD	0.48***	0.40**	0.45***
M splenium of corpus callosum[b]									
-8,-39,18	217	0.39 (0.05)	0.42 (0.08)	0.46 (0.05)	5.60***	**FA**	-0.35**	-0.33*	-0.36**
						AD	-0.08	-0.16	-0.11
						RD	0.45***	0.40**	0.43**
M isthmus of corpus callosum									
-4,-25,21	208	0.33 (0.05)	0.35 (0.04)	0.40 (0.04)	7.43***	**FA**	-0.49***	-0.35**	-0.48***
						AD	-0.36**	-0.24	-0.33*
						RD	0.30*	0.23	0.30*

*p<0.05, **p<0.01, ***p<0.001; Values are means (standard deviations); L=left, R=right, M=medial.
FAS/PFAS=combined fetal alcohol syndrome (FAS) and partial FAS (PFAS) group; HE=nonsyndromal heavily exposed group; Ctl=control group.
FA=fractional anisotropy; AD=axial diffusivity (10^{-3} mm^2/s); RD=radial diffusivity (10^{-3} mm^2/s);
AA/day=ounces absolute alcohol consumed per day across pregnancy; AA/occasion=ounces absolute alcohol consumed per occasion; days/week=drinking days per week across pregnancy.
[a]A similar region (342 mm^3) with peak coordinates (-39,-10,-19) survived in the HE<Ctl group comparison.
[b]Two similar regions (247 mm^3 and 243 mm^3) with peak coordinates (-18,-42,9 and -14,-33,23) survived in the HE<Ctl group comparison.

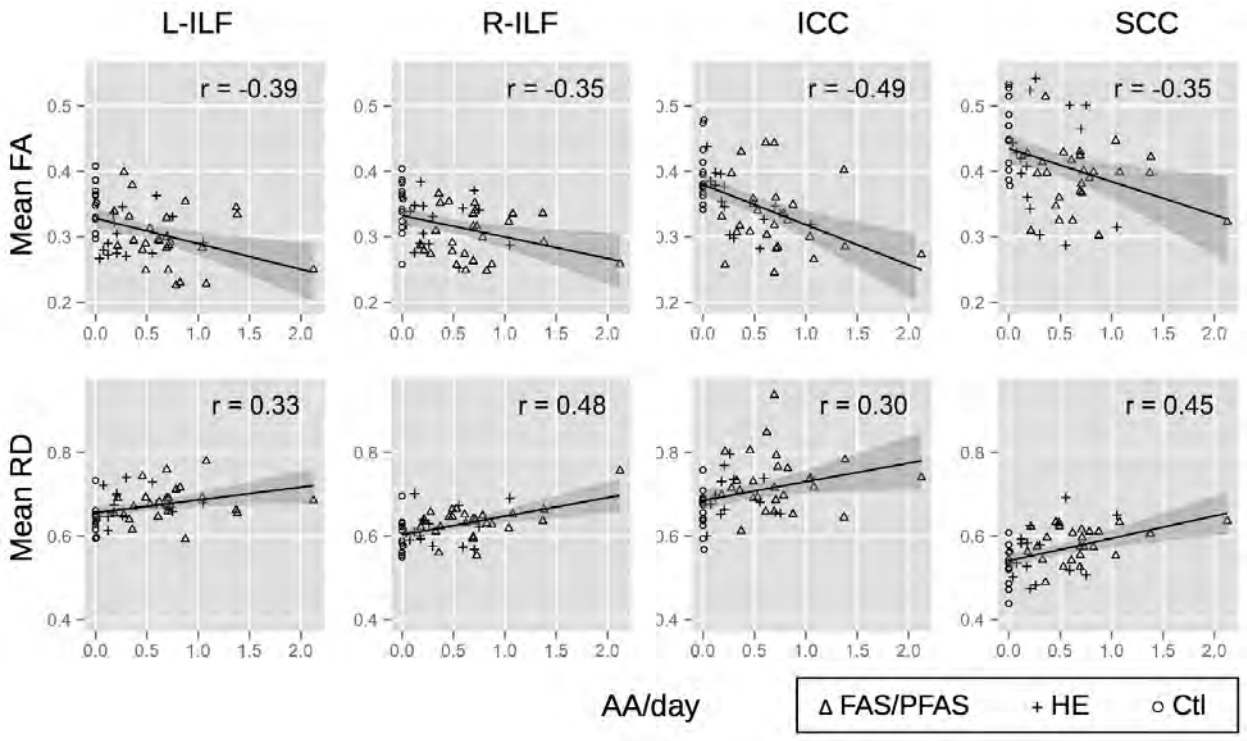

Figure 3.2 Relations of mean FA (top row) and RD (x10^3; bottom row) with the continuous alcohol measure AA/day (absolute alcohol consumed per day across pregnancy, log transformed) for each ROI in Table 2. L- and R-ILF=left and right inferior longitudinal fasciculus; SCC=splenium of corpus callosum; ICC=isthmus of the corpus callosum. FAS/PFAS=combined fetal alcohol syndrome (FAS) and partial FAS (PFAS) group; HE=nonsyndromal heavily exposed group; Ctl=control group.

3.3.3 MD Findings

Voxelwise group comparisons of MD maps produced seven regions (shown in Figure 3.4) where the FAS/PFAS children had significantly higher MD than the control children (descriptive properties and alcohol associations are presented in Table 3.3). Three of these clusters overlapped with those derived in the voxelwise FA analysis described above, namely clusters in the L-ILF, M-SCC and M-ICC (Figure 3.4a). In the R-ILF, an MD-derived cluster (MNI peak coordinate: 42, -29, -12) was found at a different location than the FA-derived one (MNI peak coordinate: 37, 2, -30) (Figure 3.4b). Greater MD was also observed in the FAS/PFAS group compared to controls in the right superior longitudinal fasciculus (R-SLF) and in the left and

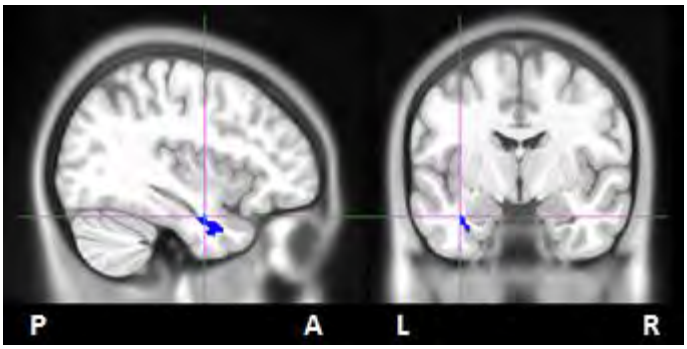

L inferior longitudinal fasciculus

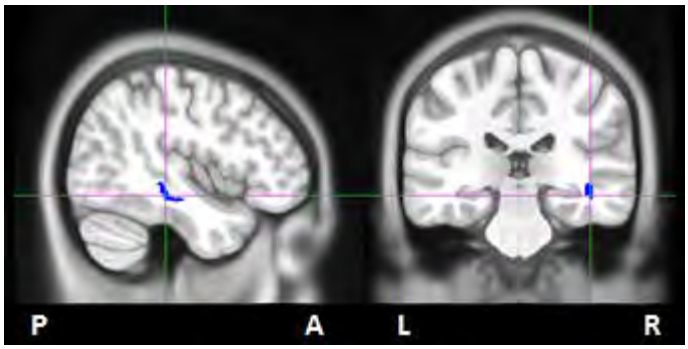

R inferior longitudinal fasciculus

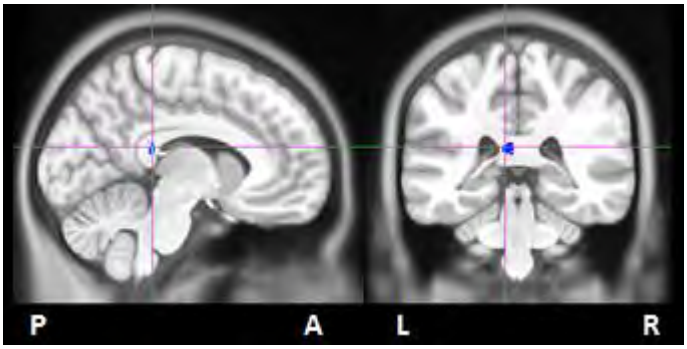

M splenium of corpus callosum

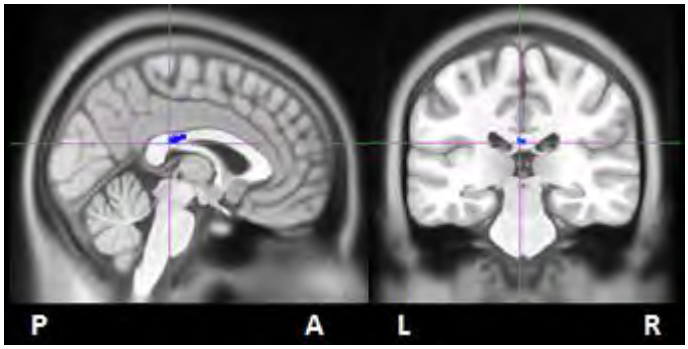

M isthmus of corpus callosum

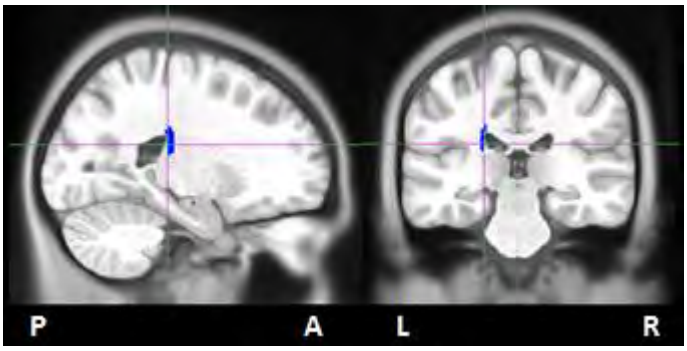

L corticospinal tract

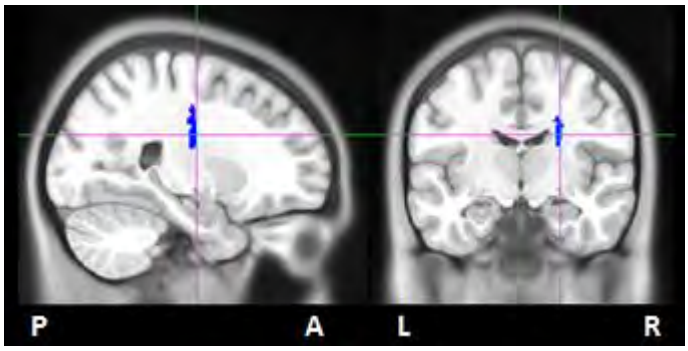

R corticospinal tract

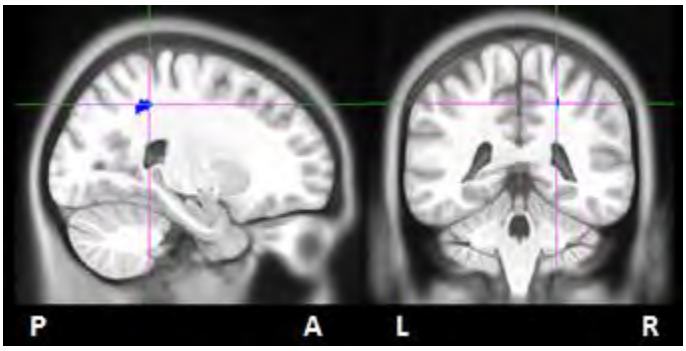

R superior longitudinal fasciculus

Figure 3.3 Clusters (MNI pediatric standard space) where the mean MD is higher in children with FAS/PFAS than in control children. Cross-hairs indicate peak coordinates.

right corticospinal tracts (L- and R-CSTs). All of the regions are well-removed from the ventricles, excepting the latter two, which may be affected by partial voluming. In each of the seven clusters, the mean MD values in the peak ROIs were positively associated with each of the 3 alcohol measures (all *r*s≥0.27, *p*s<0.05).

Table 3.3 Size and peak coordinates (in MNI pediatric standard space) of regions where MD is higher in children with FAS/PFAS compared to controls, as well as group averages of the mean MD in 8mm3 ROIs centered around the peak coordinates. Columns on the right show relations of continuous alcohol exposure measures to MD, AD and RD in the peak ROIs.

Region MNI coordinates (mm)	Size (mm^3)	Mean MD x10^{-3} mm^2/s in ROIs			*F*		Correlations with DTI measures in ROIs		
		FAS/PFAS (26)	HE (15)	Ctl (13)			AA/day	AA/occasion	days/week
L inferior longitudinal fasciculus[a]									
-39, -5,-25	1057	0.80 (0.03)	0.78 (0.04)	0.76 (0.03)	6.92***	**MD**	0.44***	0.58***	0.37**
						AD	0.29*	0.46***	0.25
						RD	0.37**	0.41**	0.30*
R inferior longitudinal fasciculus									
42, -29,-12	434	0.83 (0.04)	0.81 (0.02)	0.77 (0.04)	9.57***	**MD**	0.39**	0.37**	0.39**
						AD	0.31*	0.35**	0.27*
						RD	0.20	0.14	0.23
M splenium of corpus callosum[b]									
-10,-36,18	222	0.82 (0.04)	0.81 (0.05)	0.76 (0.04)	7.29***	**MD**	0.41**	0.31*	0.41**
						AD	0.34*	0.17	0.35**
						RD	0.22	0.24	0.21
M isthmus of corpus callosum[c]									
-4,-30,18	307	0.85 (0.06)	0.85 (0.06)	0.79 (0.04)	6.26***	**MD**	0.53***	0.36**	0.50***
						AD	0.42**	0.25	0.40**
						RD	0.39**	0.30*	0.37**
R superior longitudinal fasciculus									
21,-42,45	234	0.76 (0.02)	0.75 (0.03)	0.73 (0.02)	6.89***	**MD**	0.35**	0.34**	0.35**
						AD	0.20	0.28	0.19
						RD	0.13	0.04	0.14
L corticospinal tract									
-23,-28,20	207	0.76 (0.02)	0.78 (0.04)	0.74 (0.03)	7.67***	**MD**	0.34*	0.35**	0.31*
						AD	0.25	0.21	0.23
						RD	0.26	0.31*	0.23
R corticospinal tract[d]									
22,-11,26	526	0.70 (0.02)	0.70 (0.02)	0.68 (0.02)	6.34***	**MD**	0.29*	0.41**	0.27*
						AD	0.14	0.28*	0.09
						RD	0.18	0.18	0.18

*p<0.05, **p<0.01, ***p<0.001; Values are means (standard deviations); L=left, R=right, M=medial.
FAS/PFAS=combined fetal alcohol syndrome (FAS) and partial FAS (PFAS) group; HE=nonsyndromal heavily exposed group; Ctl=control group. MD=mean diffusivity (10^{-3} mm^2/s); AD=axial diffusivity (10^{-3} mm^2/s); RD=radial diffusivity (10^{-3} mm^2/s); AA/day=ounces absolute alcohol consumed per day across pregnancy; AA/occasion=ounces absolute alcohol consumed per occasion; days/week=drinking days per week across pregnancy.
[a]A similar region (250 mm^3) with peak coordinates (-43,-13,-18) survived in the HE>Ctl group comparison.
[b]A similar region (288 mm^3) with peak coordinates (-13,-36,11) survived in the HE>Ctl group comparison.
[c]Two regions (329 mm^3 and 203 mm^3) with peak coordinates (-11,-32,24 and -6,-32,20) survived in the HE>Ctl group comparison.
[d]A similar region (291 mm^3) with peak coordinates (22,-8,25) survived in the HE>Ctl group comparison.

Comparing the HE group with contorls, higher MD was found in children with HE in 5 clusters within 4 WM pathways, all of which overlapped with MD clusters derived from the FAS/PFAS versus controls comparison. Individual clusters were located in the L-ILF, the M-SCC, and the R-CST, while 2 clusters were in the M-ICC.

The findings were essentially unchanged when the analyses were re-run omitting the three children whose mothers used marijuana and the one who reported using cocaine.

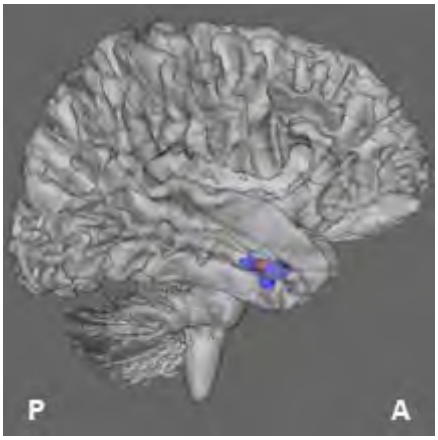

L inferior longitudinal fasciculus

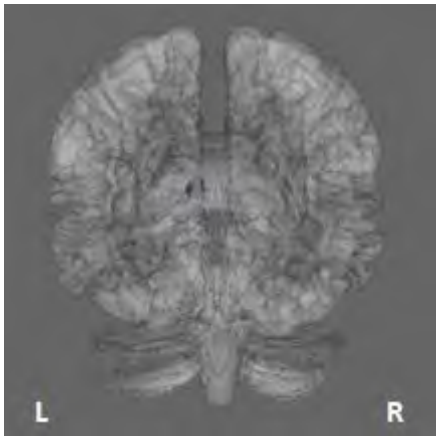

M splenium of corpus callosum

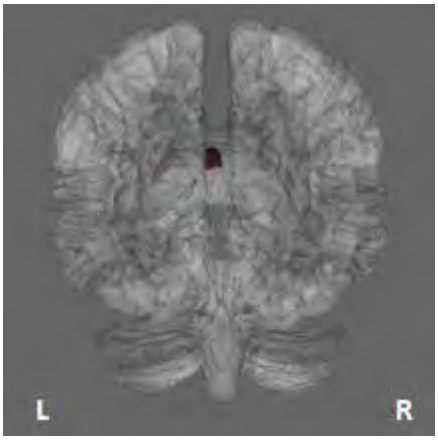

M isthmus of corpus callosum

(a)

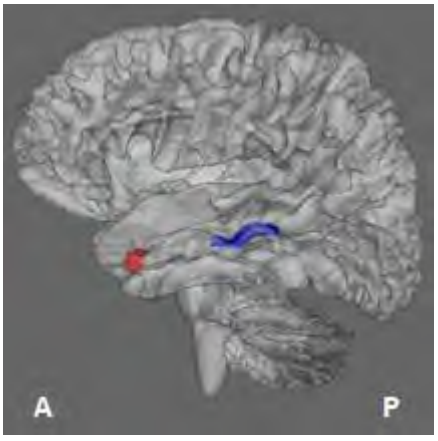

R inferior longitudinal fasciculus

(b)

Figure 3.4 A comparison of locations of FA-derived (red) and MD-derived (blue) clusters. Overlapping pairs are shown in (a), and non-overlapping regions are shown in (b)

3.3.4 Control for Confounders

Table 3.4 shows the relation of the seven control variables with FA and MD in the clusters where FA and MD group differences were found. After controlling for confounders, group differences remained significant in all regions (all *p*s≤0.044). In contrast, AA/day remained significantly associated with FA in L-ILF, M-SCC and M-ICC, and with MD in L- and R-ILF, M-SCC and M-ICC (*p*≤0.05) (Table 3.5).

Table 3.4 Correlation of the seven control variables with FA and MD in the peak ROIs

	Child's gender	Child's age at DTI scan	Maximum displacement	Lead exposure	Maternal age	Maternal education	Smoking during pregnancy
FA							
L inferior longitudinal fasciculus	-0.07	0.11	-0.16	-0.14	-0.03	0.22	-0.21
R inferior longitudinal fasciculus	0.05	0.04	-0.03	-0.25†	-0.22	0.36**	0.01
M splenium of corpus callosum	0.01	-0.13	-0.07	-0.10	-0.22	0.15	-0.11
M isthmus of corpus callosum	-0.02	-0.10	-0.12	-0.27*	-0.13	0.32*	-0.33*
MD							
L inferior longitudinal fasciculus	-0.10	-0.12	-0.09	0.26†	0.35**	-0.26†	0.32*
R inferior longitudinal fasciculus	-0.01	-0.09	0.06	0.23†	0.09	-0.32*	0.25†
M splenium of corpus callosum	-0.11	0.06	0.07	0.18	0.13	-0.10	0.25†
M isthmus of corpus callosum	-0.08	0.09	-0.03	0.15	0.10	-0.06	0.37*
R superior longitudinal fasciculus	0.10	-0.17	0.13	0.16	0.20	-0.24†	0.30*
L corticospinal tract	-0.09	0.00	0.14	0.17	0.12	-0.15	0.43**
R corticospinal tract	0.04	-0.18	0.04	0.17	0.31*	-0.18	0.30*

†*p*<0.10, **p*<0.05, ***p*<0.01; L=left, R=right, M=medial. FA=fractional anisotropy, MD=mean diffusivity.

Table 3.5 Associations of AA/day with FA and MD in the peak ROIs after controlling for potential confounders

	Potential confounders	AA/day	
		r	*β*
FA			
L inferior longitudinal fasciculus	none	-0.39**	-0.39**
R inferior longitudinal fasciculus	lead exposure, maternal education	-0.35**	-0.22
M splenium of corpus callosum	none	-0.35**	-0.35**
M isthmus of corpus callosum	lead exposure, maternal education, smoking	-0.49***	-0.39**
MD			
L inferior longitudinal fasciculus	lead exposure, maternal age, maternal education, smoking	0.44***	0.27*
R inferior longitudinal fasciculus	lead exposure, maternal education, smoking	0.39**	0.29*
M splenium of corpus callosum	smoking	0.41**	0.40**
M isthmus of corpus callosum	smoking	0.53***	0.47***
R superior longitudinal fasciculus	maternal education, smoking	0.35**	0.23†
L corticospinal tract	smoking	0.34*	0.14
R corticospinal tract	maternal age, smoking	0.29*	0.07

†*p* <0.10, **p*<0.05, ***p*<0.01, ****p*<0.001; L=left, R=right, M=medial. FA=fractional anisotropy, MD=mean diffusivity. AA/day=ounces absolute alcohol consumed per day across pregnancy

3.4 Discussion

The primary aim of this study was to examine effects of prenatal alcohol exposure on cortical WM in a cohort of pre-adolescent children with different clinical diagnoses of FASD and different exposure levels. Importantly, and in contrast with many preceding studies, we were able to examine both syndromal and nonsyndromal heavily exposed children, as well as associations with continuous measures of extent of prenatal alcohol exposure derived from prospectively acquired detailed drinking histories. Voxelwise group comparisons showed decreased FA in four WM regions and increased MD in seven regions in children with FAS/PFAS compared to non- or minimally-exposed controls. Three regions derived from the FA group differences (L-ILF, M-SCC and M-ICC) overlapped with the MD-derived clusters, and the fourth FA-derived cluster was located in a different location of the same fiber bundle (R-ILF) as an MD cluster. The additional MD clusters were in the R-SLF and bilaterally in the CSTs. The nonsyndromal alcohol exposed children (HE) showed lower FA only in the L-ILF and M-SCC, as well as higher MD in L-ILF, M-SCC, M-ICC, and R-CST. Interestingly, for each DTI parameter the HE-derived clusters formed a subset of those derived from the group with the more severe FAS/PFAS diagnosis.

Table 3.6 lists previous studies that found WM alterations in regions similar to the FA and MD clusters reported here. Despite some differences, the present study confirmed white matter deficits in these regions. Abnormalities in the corpus callosum in individuals with FASD have been observed previously by autopsy, structural MRI, and DTI (e.g. Jones and Smith, 1973; Coulter et al., 1993; Taylor et al., 2015). The splenium is typically considered the region most vulnerable to PAE, both in terms of severity and the number of studies reporting effects in this region (Riley et al. 1995; Sowell et al., 2001a; Autti-Rämö et al., 2002). Locations of microstructural effects in the SCC in the present study were consistent with regions reported previously. For example, the locations of peak FA and MD differences between the FAS/PFAS and Ctl groups in the M-SCC (MNI coordinates: FA [-8, -39, 18] and MD [-10, -36, 18]) were close to the SCC regions seen in the Sowell et al. (2008) study (MNI coordinates: [-14, -50, 15] and [-4, -43, 18]). Decreased FA in the SCC in FASD have also been reported in one semi-automated DTI

tractography study (Lebel et al., 2008) and two manual DTI-tractography studies (Ma et al., 2005; Wozniak et al., 2009), one of which also found increased MD in this region (Ma et al., 2005).

Table 3.6 Summary of previous DTI studies that have reported white matter alterations in FASD in regions similar to those found in the present study

Region	FAS/PFAS		HE		Previous studies			
	FA	MD	FA	MD	References	Subjects' age	Methods	Results
L -ILF	√	√	√	√	Lebel et al.,2008	5-12 yrs	semi-automated tractography	FA↓
R -ILF	√	√			Lebel et al.,2008	5-12 yrs	semi-automated tractography	FA↓,MD↑
					Sowell et al., 2008[a]	7-15 yrs	voxelwise	FA↓
M-SCC	√	√	√	√	Sowell et al., 2008[b]	7-15 yrs	voxelwise	FA↓
					Lebel et al.,2008	5-12 yrs	semi-automated tractography	FA↓
					Ma et al., 2005	18-25 yrs	manually defined tractography	FA↓,MD↑
					Wozniak et al., 2009	10-17 yrs	manually defined tractography	FA↓
M-ICC	√	√		√	Wozniak et al., 2006	10-19 yrs	manually defined tractography	MD↑
					Wozniak et al., 2009	10-17 yrs	manually defined tractography	FA↓
					Li et al., 2009	8-18 yrs	TBSS	FA↓
					Fryer et al., 2009	19-27 yrs	TBSS	FA↓
R-SLF		√			Lebel et al., 2008	5-12 yrs	semi-automated tractography	FA↓
					Fryer et al., 2009	19-27 yrs	TBSS	FA↓
L-CST		√			Lebel et al., 2010	5-13 yrs	voxelwise	FA↓
R-CST		√		√	Lebel et al.,2008	5-12 yrs	semi-automated tractography	MD↑

FA=fractional anisotropy; MD=mean diffusivity; L=left, R=right, M=medial.
FAS/PFAS=combined fetal alcohol syndrome (FAS) and partial FAS (PFAS) group; HE=nonsyndromal heavily exposed group
ILF=inferior longitudinal fasciculus; SCC=splenium of corpus callosum; ICC=isthmus of corpus callosum; SLF=superior longitudinal fasciculus; CST=corticospinal tract
[a]The coordinate where the maximum MD difference (42,-29,-12) in the R-ILF occurred in the FAS/PFAS vs Ctl comparison overlapped with the maximum FA difference (45,-22,-15) seen in the Sowell et al. (2008) study.
[b]Coordinates where the peak FA (-8,-39,18) and MD (-10,-36,18) differences occurred in the M-SCC in the FAS/PFAS vs Ctl comparison were close to the SCC regions (MNI coordinates: [-14, -50, 15] and [-4, -43, 18]) seen in the Sowell et al. (2008) study.

Similar to PAE effects reported previously in the M-ICC using manually defined tractography (Wozniak et al., 2006, 2009) and voxel-wise TBSS (Li et al., 2009; Fryer et al., 2009), we also found lower FA and greater MD in the M-ICC in children with FAS/PFAS. Although higher MD in the genu of the corpus callosum (GCC) has been reported in children with FASD previously (Ma et al., 2005; Lebel et al., 2008; Treit et al., 2013), this region (peak MNI coordinates: [-11, 27, 6]) did not survive cluster size correction at $p<0.01$ in our study.

Lower FA and higher MD bilaterally in the ILF in children with FASD is consistent with results from a semi-automated DTI tractography study by Lebel et al. (2008). The coordinates where MD differences were maximal in the R-ILF (MNI coordinates: [42,-29,-12]) in our study overlapped with the region where Sowell et al. (2008) found lower FA in children with FASD (MNI coordinates: [45, -23, -15]). Further, lower FA has been reported in children with FASD in the SLF both on the right (Fryer et al., 2009) and bilaterally (Lebel et al., 2008), and higher MD in the R-CST (Lebel et al., 2008). Importantly, Lebel and colleagues (2010) showed that poorer math performance was associated with lower FA in the L-CST in individuals with FASD.

Since detailed maternal drinking histories were collected during pregnancy, a novel aspect of the current study was the ability to quantitatively relate extent of alcohol exposure to WM alterations. All three continuous measures of PAE (AA/day, AA/occasion and days/week) were significantly associated with reduced FA in the L- and R-ILF, M-SCC and M-ICC, and with increased MD in the L- and R-ILF, M-SCC, M-ICC, R-SLF, L- and R-CST. After controlling for potential confounders, the continuous measure, AA/day, remained significantly correlated with both DTI measures *only* in the L-ILF, M-SCC and M-ICC, as well as with MD in the R-ILF, suggesting dose-dependent impairment in these regions. Associations of AA/day with MD were no longer significant in the R-SLF, and L- and R-CST, where MD was strongly related with maternal smoking during pregnancy ($p<0.1$), which may provide additional evidence of neurobehavioral deficits due to maternal smoking in children with PAE (Streissguth et al., 1989; Gusella and Fried, 1984; Martin et al., 1977).

Associations of DTI parameters with measures of continuous alcohol exposure indicate that the degree of microstructural alterations in these regions, and therefore also any associated impairments (such as those observed by Lebel et al., 2010), are dose dependent. In most of the peak ROIs, the mean FA and MD values exhibited stronger associations with AA/day and days/week than with AA/occasion, suggesting that the *frequency* of maternal binge drinking across pregnancy has a stronger impact on the associated WM changes than the exact *number* of drinks per binge drinking occasion. This may be due, in part, to the fact that the minimum threshold for binge drinking (here, 5 drinks per occasion) is already high, and additional

differential amounts may be expected to have less of an effect than the number of such events. It is noteworthy that the majority of the mothers of children in the FAS/PFAS and HE groups in this cohort engaged in weekend binge drinking, with mothers of the most severely affected children with FAS/PFAS drinking roughly two days per week, and the mothers of nonsyndromal HE children drinking on average one day a week.

Decreases in FA with increasing alcohol exposure were largely attributable to increased RD, rather than decreased AD. This pattern is consistent with results of our previous cerebellar DTI studies (Spottiswoode et al., 2011; Fan et al., 2015). Other DTI studies of children within the same age range with FASD have shown similar patterns. For example, in children with FASD, math achievement test scores were associated with higher RD in the left anterior cerebellar white matter tracts connected to the middle peduncle (Lebel et al., 2010), and saccadic reaction times were positively correlated with FA and negatively correlated to RD in the CC during an antisaccadic task (Green et al., 2013). Several studies have shown that alcohol exposure may result in the impairment of oligodendrocytes, which produce the myelin sheaths (Phillips and Krueger, 1992; Ozer et al., 2000). According to animal and human studies, the expression of the basic myelin protein in the brain may be modified by iron homeostasis resulting from PAE (Connor and Menziers, 1996; Carter et al., 2007), with subsequent myelination affected by the modification of this protein.

Several DTI studies have reported correlation between DTI measures and task scores. However, not all regions where white matter deficits were detected in those studies showed significant association with task scores, which may be due to certain white matter tracts not being specifically involved in connecting brain regions recruited during the task. The growing body of evidence of white matter abnormalities in the CC, ILF, SLF and CST in individuals with FASD, suggest that cognitive and behavioural performance may be impaired in tasks involving circuits connected by these tracts. While our findings only showed particular clusters in these tracts, a tractography-based approach might reveal WM deficits in more extensive regions along the tracts. Although care was taken to ensure good co-registration, any voxelwise analysis is limited by potential misregistration errors due to the low resolution of DTI acquisitions.

To control for Type 1 error, Monte Carlo simulations (Forman et al., 1995) were applied to determine the minimum size of clusters for significance. In this study, clusters had to be 168 mm^3 or larger to be deemed significant. This approach makes it difficult to identify small regions with WM abnormalities, which may explain why some regions reported in other studies were not found here. One approach to overcome this limitation in future studies may be to use regions where functional deficits have been detected as seed regions for tractography studies, thus limiting the numbers of voxels being compared to those within particular WM tracts. Furthermore, it is difficult to translate DTI parameters to a single, direct biological phenomenon, making interpretation of results difficult.

3.5 Conclusions

This study examined the effects of PAE on cortical WM in 10-year old children using both FASD diagnosis and continuous measures of extent of PAE. Voxelwise group comparisons revealed seven regions with white matter alterations in children with FAS/PFAS, a subset of which were also found in HE children. The mean FA and MD values in peak ROIs were significantly associated with all three continuous measures of alcohol exposure (AA/day, AA/occasion and days/week). After controlling for confounders, associations of PAE with FA and MD remained significant in the L-ILF, M-SCC and M-ICC, and MD with the R-ILF, suggesting dose-dependent impairments in these regions. FA and MD showed the strongest associations with AA/day and days/week, suggesting that the frequency of binge drinking may be most predictive of long-term WM damage. WM deficits in the ROIs were attributable to increased RD rather than decreased AD, suggesting poorer axon packing density and/or myelination. Further study using both DTI and resting-state fMRI to examine the relationship between brain structural and functional connectivity may provide greater insight into mechanisms underlying PAE-related neurocognitive deficits.

Chapter 4

Changes in Resting-State Functional Connectivity in Children with Prenatal Alcohol Exposure

Jia Fan[1,2], Paul A. Taylor[1,2,3], Christopher D. Molteno[4], Suril Gohel[5], Bharat B. Biswal[5], Sandra W. Jacobson[2,4,6], Joseph L. Jacobson[2,4,6], Ernesta M. Meintjes[1,2]

Abstract

Prenatal alcohol exposure (PAE) can have a range of effects on childhood growth, facial features, and neurocognitive abilities, which are encompassed under the umbrella term fetal alcohol spectrum disorders (FASD). Resting state functional MRI (rs-fMRI) utilizes the low-frequency component of the blood oxygen level dependent (BOLD) signal while a subject performs no explicit task, providing an efficient and powerful mechanism for studying functional brain networks even in low-functioning and young subjects. This study is the first to quantitatively assess PAE effects on multiple resting state networks (RSNs) by using continuous alcohol exposure measures that were obtained throughout pregnancy. Rs-fMRI scans were performed on 38 children with FASD (19 with either full fetal alcohol syndrome (FAS) or partial FAS (PFAS), 19 nonsyndromal heavily exposed (HE)) and 19 controls (Ctl), mean age 11.3±0.9 yrs, from the Cape Town Longitudinal cohort. Voxelwise group comparison between a combined FAS/PFAS group and controls revealed regions of lower resting state functional connectivity (RSFC) in five regions in separate networks, three of which also showed lower RSFC

---

[1]MRC/UCT Medical Imaging Research Unit, University of Cape Town, South Africa, [2]Department of Human Biology, University of Cape Town, South Africa, [3]African Institute for Mathematical Sciences, South Africa, [4]Department of Psychiatry and Mental Health, University of Cape Town, South Africa, [5]New Jersey Institute of Technology, Newark, NJ, [6]Wayne State University School of Medicine, Detroit, MI

in the HE group compared to controls. The regional means of both the fractional amplitude of low-frequency fluctuations (fALFF) and regional homogeneity (ReHo) showed significant correlations with the continuous measures of PAE, with the former showing stronger associations and in more regions.

Key words: Resting-State functional MRI (rs-fMRI); fractional amplitude of low-frequency fluctuation (fALFF); regional homogeneity (ReHo); resting state functional connectivity (RFSC); resting state network (RSN); fetal alcohol spectrum disorder (FASD).

4.1 Introduction

Prenatal alcohol exposure (PAE) has a number of adverse effects on the brain, resulting in a wide range of life-long cognitive, behavioral and neurological impairments, including intelligence, attention, executive functioning, memory, visual-spatial skills, motor ability, processing speed, adaptive functioning, and social skills (e.g. Jacobson and Jacobson, 2002; Burden et al., 2005; Kalberg et al., 2006; Mukherjee et al., 2006; Spadoni et al., 2007). The patterns of disorders typically associated with PAE are quite varied, both in terms of observed effects and severity, and are classified under the umbrella term fetal alcohol spectrum disorder (FASD). Subcategories of FASD are often ascribed using neurocognitive test scores and the presence of a distinctive dysmorphology in either facial, growth or other physical features. Fetal alcohol syndrome (FAS), the most severe category of FASD, was introduced in 1973 (Jones and Smith, 1973) and is characterized by small head circumference, growth retardation and three distinctive facial features, including short palpebral fissures, an indistinct (i.e., flat or smooth) philtrum, and a thin vermillion (Hoyme et al., 2005; Stratton et al., 1996). Partial fetal alcohol syndrome (PFAS) refers to a child who shows at least one of either small head circumference or growth retardation and two of the three alcohol-related facial anomalies. Exposed individuals who do not show all of the diagnostic criteria but who exhibit neurobehavioral deficits are clinically diagnosed as having alcohol-related neurodevelopmental disorder (ARND).

Resting state functional MRI (rs-fMRI) has been widely used to study functionally connected regions of the brain while a subject is not performing any explicit task. It was first proposed by Biswal et al. (1995) and focuses on spontaneous low frequency fluctuations (<0.1 Hz) in the measured blood oxygen level dependent (BOLD) signal. Particularly in pediatric fMRI studies, subject task performance is known to be a significant concern, as well as the potential for task-induced motion, and the task-free nature of rs-fMRI makes it an ideal tool for studying this population (Stevens et al., 2009; Supekar et al., 2009). Resting state functional connectivity (RSFC) has been used to identify and quantify resting state networks (RSNs). About 15 to 20 RSNs have been identified with reliability, reproducibility, and consistency across subjects (Beckmann et al., 2005; Damoiseaux et al., 2006; De Luca et al., 2006; Fox and Raichle, 2007; Smith et al., 2009; Shehzad et al., 2009), stages of cognitive development (Fair et al., 2007; Fransson et al., 2007), degree of consciousness (Boly et al., 2008; Greicius et al., 2008), and even species (Vincent et al., 2007). The networks have been associated with various cognitive features such as motor, language, or visual tasks (Rosazza and Minati, 2011), executive functioning (Seeley et al., 2007), and even the task-negative default mode network (DMN) has been related to attention performance (Raichle et al., 2001; Buckner et al., 2008; Bonnelle et al., 2011). This methodology facilitates an examination of the intrinsic functional architecture of the brain at its highest organizational level across these large-scale networks.

Several methods are available for identifying the extent of networks and for quantifying RSFC. At the network level, two popular statistical and mathematical methods have typically been applied to rs-fMRI data. The first method is seed-based analysis, which has been performed in several studies, including the original rs-fMRI study by Biswal et al. (1995) (Raichle et al., 2001; Greicius et al., 2003; Fox et al., 2005,2006; Margulies et al., 2007; Vincent et al., 2008). This method requires the *a priori* selection of a seed location (either a single voxel or a cluster), for example based on previous literature, functional activation maps, hypotheses, etc. The BOLD time series of the seed is then correlated with all other voxel time series and a functionally connected network is determined by selecting regions with highest correlation (i.e., functional connectivity) values. The other commonly used method is (spatial) independent component analysis (ICA) (McKeown et al., 1998; Kiviniemi et al., 2003; Beckmann et al., 2005; Damoiseaux

et al., 2006), which decomposes a data matrix into distinct spatial maps, i.e., (statistically) independent components (ICs), each with an associated time series; ICs are also thresholded for high connectivity values to define the boundaries of a network.

Several local RSFC parameters have been developed. Regional homogeneity (ReHo) measures the similarity or synchronization between the time series of a given voxel and its nearest neighbors (Zang et al., 2004). Amplitude of low-frequency fluctuation (ALFF) evaluates the strength or intensity of low frequency fluctuations (LFFs) (Zang et al., 2007), while fractional ALFF (fALFF) represents the relative contribution of the LFF band to the whole observed frequency range (Zou et al., 2008). However, it is not certain what quantity is the most appropriate for quantifying the rs-fMRI properties at the voxel level.

Rs-fMRI has previously been applied in only a small number of PAE studies, particularly in a pediatric population. Wozniak et al. (2011) observed decreased interhemispheric functional connectivity in children (age 10-17 yrs) with FASD, comparing average time series correlation in specific regions of interest (ROIs) connected by the corpus callosum. Wozniak et al. (2013) also observed decreased global efficiency and increased path length in FASD children in a whole brain study using graph theory. Finally, Santhanam et al. (2011) examined a group of older subjects (age 18-24 yrs) with either FAS or PFAS using seed-based analysis and reported reduced RSFC in the DMN.

In this study of pediatric brain development, we expand upon previous studies by investigating functional connectivity changes associated with PAE in several functional networks, quantifying RSFC in several ways, and using both FASD diagnosis and measures of extent of alcohol exposure. We first describe the implementation of independent component analysis (ICA) and dual regression for determining functional networks and connectivity in a data-driven manner. These are then utilized for making separate comparisons between alcohol exposed children with different diagnoses (a combined FAS and PFAS group, and a nonsyndromal heavily exposed (HE) group) and matched controls. Additionally, we examine the relation of RSFC in each network with extent of alcohol exposure, obtained from detailed drinking histories of the subjects' mothers, who had been recruited during pregnancy as part of the Cape Town

Longitudinal Study. Finally, we investigate the relation between the alcohol measures and the local RSFC parameters, fALFF and ReHo, in order to determine which characterize the alcohol exposure-connectivity association most strongly.

4.2 Materials and Methods

4.2.1 Participants

Pregnant women were recruited from the Cape Coloured community in the Western Cape Province of South Africa (Croxford and Viljoen, 1999). Women were older than 18 yrs and without diabetes, epilepsy, or cardiac problems requiring treatment. The incidence and amount of drinking on a day-by-day basis during a typical 2-week period both at time of conception and at time of recruitment were determined using a timeline follow-back interview (Jacobson et al., 2002). More details relating to recruitment can be found in our previous DTI study (Fan et al., 2015). Drinking was quantified in units of ounces (oz) of absolute alcohol (AA), and maternal consumption was recorded using three measures: oz AA consumed per day across pregnancy (AA/day), oz AA consumed per occasion (AA/occasion), and drinking days per week across pregnancy (days/week). Any woman reporting a minimum of 14 drinks per week (1.0 oz AA/day) or at least two incidents of binge drinking (≥ 5 drinks) per month during the first trimester of pregnancy was invited to participate in the study. Additionally, women who abstained from drinking or drank minimally during pregnancy were recruited as controls. Smoking during pregnancy was reported in terms of cigarettes smoked per day. The mother's age at delivery and years of education were also recorded. At an FAS diagnostic clinic conducted in 2005, each of the alcohol-exposed children was assigned to one of the diagnostic groups: FAS, PFAS, or HE. During pregnancy, a mother of FAS children used methaqualone, mothers of 2 PFAS children used either marijuana or methaqualone, and mothers of 2 HE children used both marijuana and methaqualone.

4.2.2 Procedures

Rs-fMRI data were acquired in 57 right-handed children (mean age±sd: 11.3±0.9 yrs) from the Cape Town Longitudinal Study (Jacobson et al., 2008): 19 with FAS or PFAS; 19 HE; and 19 non- or minimally-exposed controls (Ctl). Child sex, age at scan, IQ, and postnatal lead exposure were also recorded. Approval for human research was obtained from the Human Investigation Committee at Wayne State University and the Faculty of Health Sciences Human Research Ethics Committee at University of Cape Town. Informed consent was obtained from mothers at recruitment and at the child assessment visits; assent was obtained from the child. Children received a small gift and mothers received a photo of their child and compensation consistent with guidelines from the ethics committees.

4.2.3 Scanning Protocol

The children were scanned using a 3T Allegra MRI (Siemens, Erlangen, Germany), located at the Cape Universities Brain Imaging Center (CUBIC) in Cape Town, South Africa. Rs-fMRI were performed using a gradient echo planar imaging (EPI) sequence (resolution=3.1 x 3.1 x 3.0 mm^3, FOV=200x200x152 mm^3, 34 slices, 180 volumes, TR = 2000 ms, TE = 30 ms, flip angle of 90°). T1-weighted structural images were acquired in the sagittal orientation using a 3D EPI-navigated multi-echo MPRAGE sequence (resolution=1.3x1.3x1.0 mm^3, FOV=256x256x167 mm^3, 128 slices, TR 2530 ms, TI 1100ms, TE's 1.53/3.21/4.89/6.57 ms, flip angle 7°) (Van der Kouwe et al., 2008; Tisdall et al., 2009). All the rs-fMRI scans were acquired with eyes shut.

4.2.4 Pre-processing and Statistical Analysis

A schematic diagram of the processing and analysis steps is illustrated in Figure 4.1. First, all rs-fMRI data were pre-processed using a pipeline of standard procedures, which were constructed and implemented using afni_proc.py in AFNI (Cox, 1996), as follows. The first 4 volumes were discarded to allow for signal stabilization. Remaining time points were despiked and motion corrected by rigid body volume registration. The maximum resultant displacement for each subject was below 0.9 mm and the maximum rotation in any direction was below 1.0 degree. Both linear and non-linear co-registrations were applied to align each EPI set first to that

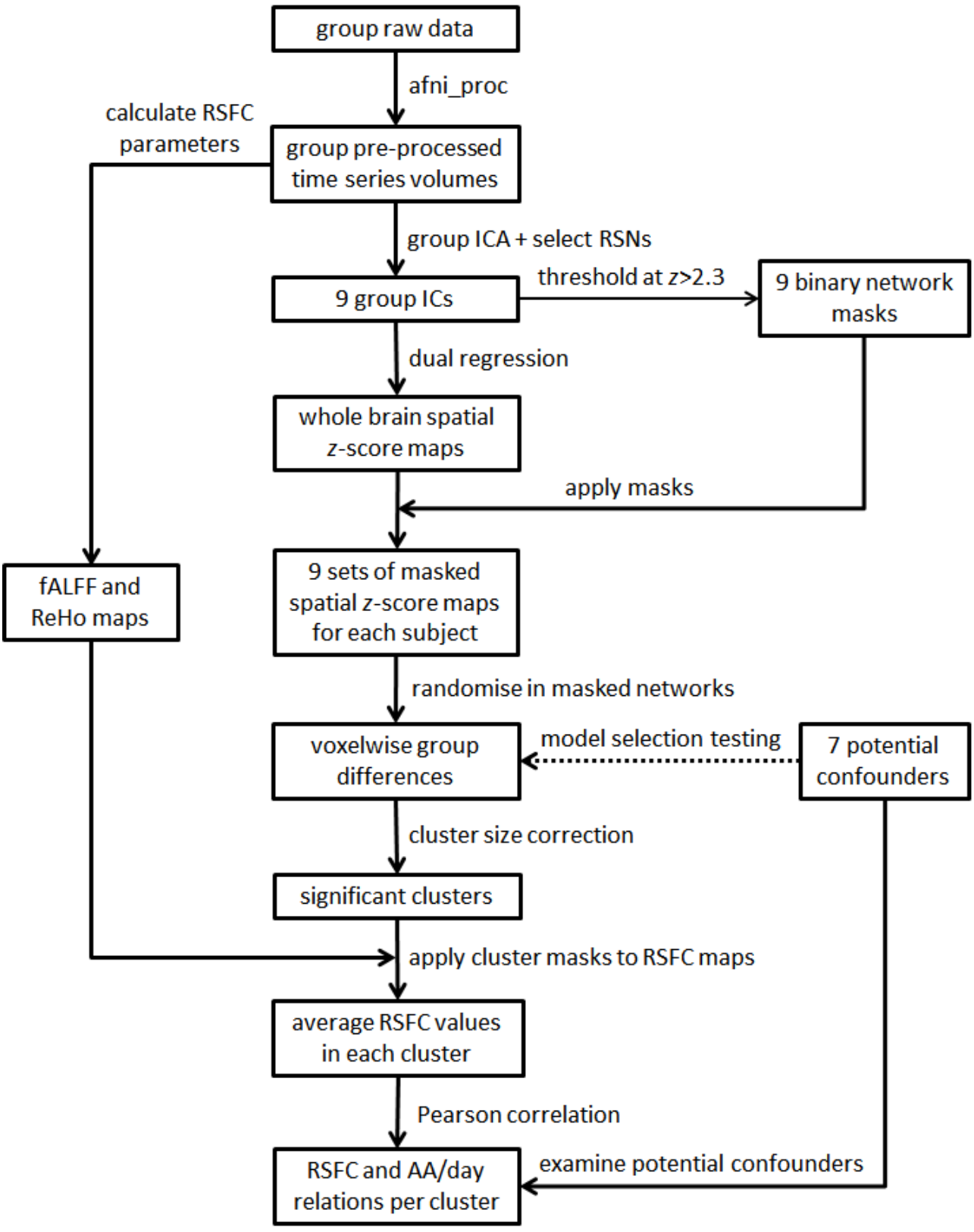

Figure 4.1 Processing and analysis pipeline for this study.

subject's anatomical T1-weighted structural image and then to the 3x3x3 mm^3 Talairach-Tournoux (TT) standard space. Each volume was spatially blurred at a full width at half maximum (FWHM) of 6.0 mm. White matter (WM) and cerebrospinal fluid (CSF) signals were regressed out, and time series were band-passed between 0.01 and 0.1 Hz to reduce physiological contributions of respiratory and cardiovascular components. In the final pre-processing stage, the RSFC parameters, fALFF and ReHo, were calculated for each subject using FATCAT (Taylor and Saad, 2013; See Taylor et al., 2012 for the calculation of fALFF; See He et al., 2007 and Zang et al., 2004 for calculation of ReHo)

Group ICA was performed using MELODIC in FSL (Smith et al., 2004), reducing the group data to 20 independent components (ICs), a commonly selected model order in resting-state analyses. From these ICs, nine standard RSNs were identified by comparison with a standard set of 20 RSNs that had been calculated as part of the Functional Connectome Project (FCP) (Biswal et al., 2010). The remaining ICs, which largely represent noise, alignment features, non-gray matter (GM) tissue, and physiological signals, were not utilized in further analyses. The spatial extent of each network was defined by thresholding each group IC at a *z*-score>2.3 (Beckmann and Smith, 2004) and creating a binary mask. Dual regression (Beckmann et al., 2004) was performed on the whole brain maps in order to backproject the group ICs onto the individual resting data, producing single subject connectivity maps for each RSN.

For each network, the set of subject connectivity maps was entered into FSL-randomise for voxelwise comparisons to determine clusters of significant connectivity differences between each of the two FASD groups, FAS/PFAS and HE, with the Ctl group. Randomise was performed only for voxels within each network mask. AFNI-AlphaSim was used to calculate the minimum volume of a cluster within each network mask at a statistical significance of $p<0.01$ (corrected for the 9 RSNs analyzed in this study) (see Appendix 1 for the significant size of each cluster).

We also investigated whether the inclusion of control variables in the comparison model had an effect on the cluster results. The set of examined control variables included: child sex, age at scan, and postnatal lead exposure, as well as maternal age at delivery, cigarettes smoked per day during pregnancy, and years of education. Missing demographic data were estimated as

the median for the group (as noted in Table 4.1). Additionally, given the sensitivity of rs-fMRI data to head motion, the maximum resultant motion was also added as a control variable. Each of the seven control variables was included separately in the randomise model. The results of the voxelwise group comparison with each predictor added separately showed no significant differences to the original model (see Appendix 2). Although the sizes of the clusters obtained from the voxelwise analyses varied with the inclusion of individual confounders, the peak coordinates remained the same, and no new clusters were revealed. Therefore, these results were not utilized in further analyses.

To investigate dose dependent effects in the clusters where groups differed, we extracted the mean RSFC parameters, fALFF and ReHo, in each cluster and examined associations with the overall measure of extent of alcohol exposure averaged across pregnancy, AA/day. The same seven control variables specified above were considered as potential confounders. Any control variable that was weakly associated (p<0.1) with the mean fALFF in an ROI was considered as a potential confounder and subsequently included in a separate linear regression of the relation between fALFF and AA/day in that ROI. The statistical analyses were performed using SPSS (version 22). Analyses were re-run omitting the 5 children whose mothers admitted using cocaine, marijuana, or methaqualone to determine if the effects were altered.

4.3 Results

4.3.1 Sample Characteristics

The demographic information is summarized in Table 4.1. There were no significant between-group differences in age at scanning, lead exposure, maternal age, cigarette smoking during pregnancy, mother's education, or maximum resultant motion during scan. Significant between-group differences were only found in child's IQ. The children in the FAS/PFAS group had lower IQ scores than the children in the other groups (ps<0.05). As expected, maternal drinking rates and overall alcohol consumption were higher in the most severely affected

children with FAS/PFAS. Only one mother in the Ctl group reported consuming 1 drink on four separate occasions, while others reported abstaining from alcohol during pregnancy.

Table 4.1 Sample characteristics (*N*=57)

	FAS/PFAS	HE	Control	*F* or χ^2
N	19	19	19	
Child characteristics				
Sex (% male)	47%	42%	26%	1.93
Age at rs-fMRI scan (yr)	11.0(1.0)	11.4(0.7)	11.6(1.0)	2.03
Lead exposure[a]	9.9(4.4)	8.0(2.7)	7.5(2.7)	2.91†
WISC-IV IQ	66.2(9.5)	76.6(15.1)	76.9(13.1)	4.31*
Maximum displacement during scan (mm)	0.3(0.1)	0.3(0.1)	0.4(0.1)	1.94
Maternal characteristics				
Maternal age at delivery	29.1(7.6)	24.8(4.7)	26.2(4.6)	2.72†
Cigarettes smoked per day during pregnancy[b]	6.9(6.1)	5.4(3.7)	3.8(9.9)	0.91
Education (yr)[c]	8.6(1.8)	9.0(2.1)	10.1(1.7)	2.89†
Socioeconomic status (SES)	15.8(7.2)	20.4(6.3)	26.0(5.9)	12.21***
Absolute alcohol consumed per day across pregnancy (oz)[d,e]	0.9(0.8)	0.8(0.9)	0.0(0.0)	8.94***
Absolute alcohol consumed per occasion (oz)[d]	3.7(1.8)	3.7(3.2)	0.1(0.3)	17.74***
Drinking days per week across pregnancy[d]	1.5(1.0)	1.3(0.8)	0.0(0.2)	21.99***

†p<0.10,*p<0.05, **p<0.01, ***p<0.001. Values are shown as: mean (SD).
FAS/PFAS = combined group of full fetal alcohol syndrome (FAS) or partial FAS (PFAS). HE = heavily exposed (nonsyndromal) group
[a]Missing values estimated at group median for 1 child with FAS/PFAS
[b]One (Ctl group) outlier (3 SD beyond the mean) recoded to 1 point higher than the highest observed non-outlier group value (Winer, 1971).
[c]Missing values estimated at group median for 2 children with FAS/PFAS
[d]Missing values estimated at group median for 2 children with FAS/PFAS, 3 HE
[e]Two (1 child with FAS/PFAS, 1 HE) outliers recoded to 1 point higher than the highest observed non-outlier group value (Winer, 1971)

4.3.2 RSFC Group Comparisons

Voxelwise group comparisons of the RSFC maps revealed significant reductions (p<0.001) of RSFC in the children with FAS/PFAS compared to the controls in five regions within separate

networks (Figure 4.2). Clusters were located within: the right (R-) postcentral gyrus (POG) in the DMN, the R-medial frontal gyrus (MFG) in the salience (Sal) network, the R-precentral gyrus (PRG) in the ventral attention (V-Att) network, the left (L-) PRG in the dorsal attention (D-Att) network, and the L-crus II (CrII) in the R-executive control (R-Exe) network. The peak coordinates and sizes of these clusters are shown in Table 4.2, as well as the relations of the means of the RSFC parameters (fALFF and ReHo) within these ROIs to extent of PAE (AA/day). Increasing alcohol exposure was associated with reduced fALFF in the default mode (DM), Sal, V-Att, and D-Att networks, and with reduced ReHo in the DM and Sal networks.

The HE group showed lower RSFC in 3 regions within 3 networks compared to controls. Notably, each of these regions overlapped with an individual FAS/PFAS-derived cluster within the same network. These clusters were located in the R-POG within the DMN, the R-MFG within Sal, and the R-PRG within V-Att. Due to the fact that they overlapped with the previously derived clusters, they were not separately investigated further.

Since fALFF showed stronger associations with alcohol exposure than ReHo, only the former was analyzed for the effects of potential confounders. Table 4.3 presents the correlations between each of the control variables and the mean fALFF in the clusters of significant group differences. When the potential confounders were included in the linear regression analysis (Table 4.4), the association of fALFF with extent of alcohol exposure in the DM and Sal networks remained largely unchanged. In contrast, associations of AA/day with fALFF in the R-PRG ROI in the V-Att was no longer significant, while associations of alcohol with fALFF in the L-PRG ROI within the D-Att network became stronger after controlling for lead exposure. Effects were essentially unchanged when the analyses were re-run omitting the 3 FAS/PFAS children whose mothers admitted using cocaine, or marijuana, or methaqualone and the 2 HE children whose mother reported using both marijuana and methaqualone.

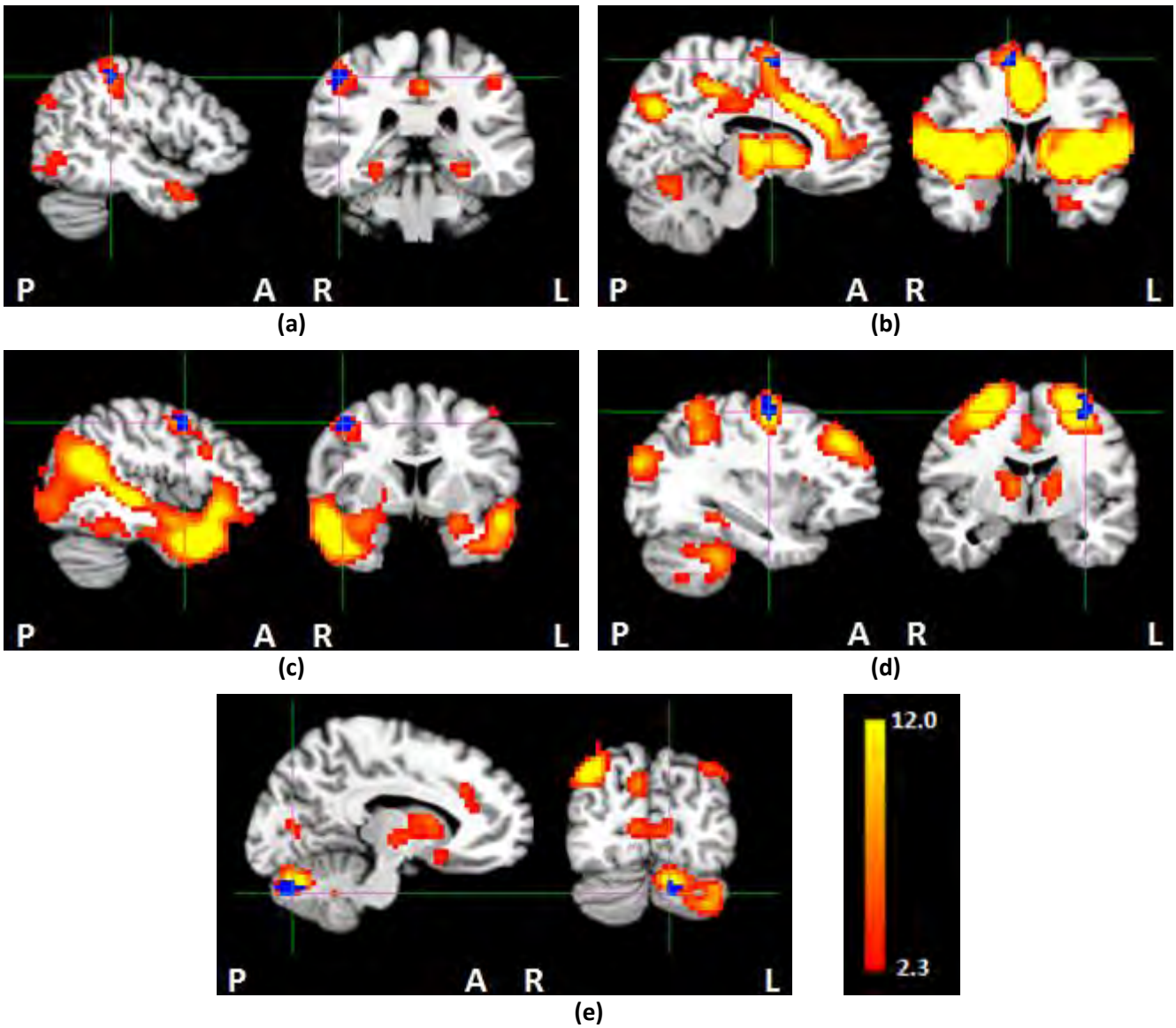

Figure 4.2 **Each panel shows the group ICA map of a resting state network thresholded at *z*>2.3 (hot colors) and clusters of significant RSFC differences (in blue; cross-hairs indicate the peak coordinates). In each case, the RSFC differences were FAS/PFAS<Ctl: (a) R-postcentral gyrus within the DMN, (b) R-middle frontal gyrus within the salience network, (c) R-precentral gyrus within the ventral attention network, (d) L-precentral gyrus within the dorsal attention network, and (e) L-crus II within the R-executive control network. Cross-hairs indicate peak coordinates.**

Table 4.2 Size and peak coordinates (in TT standard space) of regions in different resting state networks where connectivity differs between the FAS/PFAS and Ctl groups; also shown are relations of levels of prenatal alcohol exposure to mean RSFC parameters in each ROI

Network ROI coordinates (mm)	ROI size (mm^3)	RSFC parameter	ROI mean (SD) of each RSFC parameter FAS/PFAS	 HE	 Ctl	RSFC correlation with AA/day
DMN[a]						
46.5, -31.5, 44.5	540	fALFF	0.40(0.02)	0.41(0.02)	0.43(0.02)	-0.46***
		ReHo	0.51(0.04)	0.52(0.07)	0.58(0.05)	-0.35**
Salience[b]						
10.5, -1.5, 59.5	351	fALFF	0.39(0.03)	0.40(0.03)	0.44(0.02)	-0.54***
		ReHo	0.48(0.06)	0.49(0.08)	0.58(0.06)	-0.41**
Ventral attention[c]						
43.5, -7.5, 44.5	729	fALFF	0.40(0.04)	0.41(0.03)	0.41(0.04)	-0.27*
		ReHo	0.56(0.07)	0.55(0.08)	0.56(0.06)	-0.10
Dorsal attention						
-31.5, -7.5, 53.5	486	fALFF	0.46(0.04)	0.46(0.03)	0.48(0.04)	-0.29*
		ReHo	0.63(0.08)	0.60(0.07)	0.66(0.07)	-0.11
R- executive control						
-10.5, -73.5, -30.5	675	fALFF	0.41(0.03)	0.40(0.03)	0.41(0.03)	-0.23†
		ReHo	0.51(0.06)	0.53(0.09)	0.54(0.07)	-0.07

†p<0.10,*p<0.05, **p<0.01, ***p<0.001. Values are shown as: mean (SD).
FAS/PFAS ither fetal alcohol syndrome (FAS) or partial FAS (PFAS). HE=heavy exposure nonsyndromal group. Ctl=Controls.
fALFF=fractional amplitude of low frequency fluctuations
AA/day=ounce absolute alcohol consumed per day across pregnancy
AA/occasion=ounce absolute alcohol consumed per occasion
days/week=drinking days per week across pregnancy
[a]One significant cluster (405 mm^3) with peak coordinates (52.5, -28.5, 38.5) and HE<Ctl RSFC
[b]One significant cluster (891 mm^3) with peak coordinates (7.5 ,1.5, 53.5) and HE<Ctl RSFC
[c]One significant cluster (513 mm^3) with peak coordinates (40.5, -7.5, 44.5) and HE<Ctl RSFC

Table 4.3 Correlation of the seven individual control variables with the mean fALFF in the affected ROIs

Network	Child sex	Child age at scan	Lead exposure	Maximum displacement	Maternal age	Maternal education	Smoking during pregnancy
DMN	0.23†	0.18	-0.23†	-0.11	0.12	0.22	-0.19
Salience	0.25†	0.10	-0.22	-0.18	-0.11	0.23†	-0.22
Ventral attention	0.07	0.11	-0.44***	-0.09	-0.16	0.04	-0.15
Dorsal attention	-0.02	0.16	0.31*	-0.17	-0.02	0.04	-0.12
R executive control	0.19	0.11	-0.07	-0.04	-0.07	0.09	-0.10

Values are Pearson *rs*; †p<0.10, *p<0.05, **p<0.01, ***p<0.001.
fALFF=fractional amplitude of low frequency fluctuations

Table 4.4 Results of separate regression analyses on the correlations of the ROI mean fALFF value with AA/day while controlling for potential confounders

	Potential confounders	AA/day	
		r	β
DMN	child sex, lead exposure	-0.46***	-0.47***
Salience	child sex, maternal education	-0.54***	-0.55***
Ventral attention	lead exposure	-0.27*	-0.14
Dorsal attention	lead exposure	-0.29*	-0.44***
R-executive control	none	-0.23	-0.23

$^{\dagger}p$ <0.10, *p<0.05, **p<0.01, ***p<0.001.
fALFF=fractional amplitude of low frequency fluctuations
AA/day= ounce absolute alcohol consumed per day across pregnancy

4.4 Discussion

This is the first rs-fMRI study to use group ICA and dual regression to quantitatively assess the effects of prenatal alcohol exposure on multiple RSNs in separate groups of syndromal and nonsyndromal children with FASD. Voxelwise group comparison showed lower RSFC in 5 regions within 5 networks in children with FAS/PFAS compared to non- or minimally exposed controls. The regions and networks were the following: R-POG in DMN, R-MFG in Sal, R-PRG in V-Att, L-PRG within D-Att and L-Cr II in R-Exe. HE children also showed lower RSFC in 3 ROIs, which directly overlapped those of the FAS/PFAS group in the DM, Sal and V-Att networks. The smaller number of regions showing reduced connectivity compared to controls in the HE group is consistent with the lower levels of alcohol exposure in this group.

The reduced connectivity found in the DMN in our study is consistent with the results of a previous study (Santhanam et al., 2011) where adults with FASD revealed less DMN deactivation compared to controls. Although few FASD investigations have used rs-fMRI, several studies have reported effects of PAE on brain structure and altered activation during task-based fMRI in the same cortical regions where lower RSFC was found in this study. Reduced cortical GM thickness has been reported in R-POG, R-MFG, R-PRG and L-PRG in children with FASD aged between 6 and 30 years (Zhou et al., 2011). FASD individuals (age 8-18 yrs) were also found to have greater BOLD response in the R-MFG during a response inhibition (go/no-go) task (Fryer et al., 2007). Another fMRI investigation of children in the Cape Town Longitudinal Cohort with similar ages to those of the present study (mean age: 10.7 ± 0.6 yrs)

(Du Plessis et al., 2014) reported less BOLD activation in R- Crus I (Cr I) in FASD children during a rhythmic finger tapping task. The neighboring Cr I and Cr II regions are both standard parts of the executive control network (Habas et al., 2009; Bernard and Mittal, 2014) and deficits in executive function and attention have consistently been reported in FASD (Mattson et al., 1999, 2011).

The DMN has been found to be activated during rest and deactivated when individuals perform a task (Shulman et al. 1997; Raichle et al., 2001). Reduced activation of the DMN during attention-demanding tasks has been reported previously (Raichle et al., 2001; Buckner et al., 2008; Bonnelle et al., 2011), and attentional lapses have been related to failure of DMN deactivation in either healthy human subjects (Weissman et al., 2006) or macaque monkeys (Hayden et al., 2009). In their previous rs-fMRI study, Santhanam et al. (2011) reported that less DMN deactivation during a task was associated with poorer attentional modulation in FASD adults compared to controls.

Alterations in the DMN were also reported in patients with brain injury damage in the WM tracts of the salience network (Bonnelle et al., 2011). It has been proposed that the salience network regulates dynamic changes in other networks (Seeley et al., 2007; Bonnelle et al., 2011). Seeley and colleagues (2007) reported that the Sal and Exe networks were two dissociable networks, which were associated with anxiety and executive functioning, respectively. Therefore, alterations in the DMN may be related to disruptions in the Sal network, while deficits in attention networks may be related to DMN and/or Sal networks. The inter-network connectivity should be considered in further rs-fMRI studies.

In our study, fALFF and ReHo were used to quantify the local RSFC properties. After controlling for potential confounders, increasing alcohol exposure was associated with reduced fALFF and ReHo in the ROIs where children with FAS/PFAS children had reduced connectivity within the DM and Sal networks, and with reduced fALFF in the D-Att network. The relations between altered connectivity and the continuous exposure measures suggest dose-dependent impairments in these regions. The fALFF typically showed stronger associations with the degree of alcohol exposure, than ReHo in the affected regions (R-POG in DMN, R-MFG in Sal, R-PRG in

V-Att, and L-PRG in D-Att). The greater sensitivity of fALFF to resting state patterns has been observed previously in a study of healthy subjects which investigated functional covariance across groups (Taylor et al., 2012).

Of the control variables investigated in this study in addition to alcohol, the strongest associations with RSFC were observed with lead exposure. Lead was significantly correlated with fALFF in the ROIs in the V- and D-Att networks. Combined effects of lead and alcohol exposure in children have been reported previously (Chiodo et al., 2004). Here, lead exposure appeared to suppress the effect of alcohol on the connectivity in the D-Att network (Table 4.4), as its inclusion in the linear regression showed a stronger association between fALFF and AA/day (r=0.27, p<0.05; β=-0.44, p<0.01). In the V-Att network, the association of fALFF and AA/day was no longer significant after the inclusion of lead exposure, which itself had a significant association with connectivity. However, when lead exposure was controlled for in the voxelwise group comparison of RSNs between children with FAS/PFAS and controls, a cluster with the same peak coordinate in the V-Att network emerged from the analysis and no new clusters were revealed (Appendices 2a and 2b), suggesting that the reduced connectivity in this region within the V-Att network is due to PAE rather than postnatal lead exposure. Interestingly, no significant associations were observed between maternal smoking during pregnancy and fALFF in this study, even though several previous studies have reported associations between maternal smoking and neurobehavioral deficits in children with PAE (Streissguth et al., 1989; Gusella and Fried, 1984; Martin et al., 1977).

Pediatric studies are quite sensitive to subject motion and related imaging artefacts. Here, all rs-fMRI data were visually checked during processing and were aligned to standard space. Registration parameters were screened as well to exclude subjects with excessive motion. Despite these precautions, factors such as acquisition artefacts, scanner noise, and minor differences in warping could still affect the results. Future studies will aim to extend the current findings by using a seed-based approach, informed by regions of interest found here, to examine both whole brain and inter-network connectivity in children with FASD.

4.5 Conclusions

This is the first study to use group ICA to evaluate the effect of prenatal alcohol exposure on multiple RSNs in children with FASD. The voxelwise group comparisons showed lower RSFC in 5 regions within 5 networks in children with FAS/PFAS compared to non- or minimally-exposed controls, 3 of which were also observed in HE children. Thus, alterations in connectivity were more extensive in the more severely affected children. This study adds evidence linking prenatal alcohol exposure to poorer functional connectivity in the DM, Sal, Att and executive function networks in FASD individuals. Reduced connectivity was dose dependent in the DM, Sal, and D-Att networks.

Chapter 5

Discussion

The main aims of this study were to assess the effects of PAE on structural and functional connectivity using DTI and rs-fMRI, respectively. We examined these complementary neurophysiological effects within a cohort of Cape Coloured children all of whom are enrolled in the Cape Town Longitudinal Study (CTLS).

Voxelwise group comparisons revealed lower FA bilaterally in the superior peduncles only in children with full FAS compared to non- or minimally-exposed controls. Higher MD in R-inferior peduncle was found in children with PFAS. Children with FAS or PFAS groups revealed higher MD in the L-middle peduncle, as well as lower FA in four regions and higher MD in seven regions within cortical WM. Three FA-derived clusters in cortical WM (in L-ILF, M-SCC and M-ICC) overlapped with MD-derived clusters, while the fourth FA-derived cluster was located in a different location but within the same fibre bundle (R-ILF) as the MD-derived cluster. The other three MD-derived clusters were in the R-SLF and bilaterally in the CSTs. The nonsyndromal alcohol exposed group (HE) revealed lower FA only in the L-ILF and M-SCC, as well as higher MD in L-ILF, M-SCC, M-ICC, and R-CST, which overlapped with the FAS/PFAS-derived clusters. Lower RSFC in 5 regions within 5 networks was also seen in children with FAS or PFAS, including R-POG in DMN, R-MFG in Sal, R-PRG in V-Att, L-PRG within D-Att and L-Cr II in R-Exe. Three of these 5 regions were also found to have lower RSFC in HE children within the DMN, Sal and V-Att networks.

To date, 14 DTI studies (e.g., Ma et al., 2005; Sowell et al., 2008; Lebel et al., 2010) have investigated cortical WM deficits in individuals with FASD. However, most of these studies grouped all the alcohol exposed subjects together and were not able to consider the differences between different diagnoses or dose dependence of effects. One aim of this study was to the test the hypothesis that the adverse impacts of PAE on cortical WM varies with the

clinical diagnoses of FASD and also that they are related to either the amount or frequency of (binge) drinking.

In all cases, we found that the alterations were most extensive in the most affected syndromal children, with nonsyndromal children revealing deficits in only a subset of the regions. Notably, deficits in the superior peduncles were only evident in the children with full FAS, suggesting a threshold effect, with only the most severely affected children showing impairment in this region. Since the superior peduncles mediate transmission of the efferent signal for the conditioned response from the cerebellar deep nuclei to the red nucleus during EBC, this result may explain, in part, the greater vulnerability to EBC impairment observed in children with full FAS (Jacobson et al., 2008), none of whom met criterion for conditioning at 5 years of age. The significant reduction in the magnitude of the regression coefficients for exposure on EBC performance following the addition of the diffusion measures to the regression analyses, provides statistical evidence that the effects of PAE on these EBC measures were partially mediated by the microstructural deficits revealed in the DTI analyses, resulting in less optimal transmission of information to and from the brainstem via the cerebellar peduncles.

Because the mothers of the children in this study had been recruited during pregnancy and interviewed regularly regarding their amount and frequency of drinking on a day-by-day basis both during and after pregnancy, detailed information was available about the levels and frequency of alcohol exposure. This presented a unique opportunity to study abnormalities in brain development in relation to the specific degree of alcohol exposure in this heavily exposed cohort of school-age children with varying degrees of FASD severity (FAS, PFAS, and HE).

Alterations in DTI parameters (FA and MD) were dose dependent in many, but not all, of the regions where group differences were detected, specifically in the L- and R-superior peduncles, L-middle peduncle, L-ILF, M-SCC, and M-ICC. Similar to the DTI findings, reduced connectivity was dose dependent in the DM, Sal, and D-Att networks.

Typically, stronger relations were observed of the measures AA/day and drinking days/week with deficits in cerebral WM, suggesting that the frequency of maternal drinking across pregnancy has a larger impact than the exact number of drinks per binge drinking occasion. This

may be due to the fact that most of the mothers in this study engaged in binge drinking during pregnancy with their drinking concentrated on 1-3 days per week. The minimum threshold for binge drinking (here, 5 drinks per occasion) is already a large amount of alcohol, so that the relatively small differences between such high levels of exposure may matter less than the number of times such events occur.

Decreases in FA with increasing alcohol exposure were largely attributable to increased RD, rather than decreased AD. Only in the M-ICC did we find decreased AD with increasing alcohol exposure. This pattern is consistent with the results of previous pediatric (Spottiswoode et al., 2011; Lebel et al., 2010; Green et al., 2013) and adult (Li et al., 2009) studies. The RD indicates the degree to which water diffuses in a direction that is perpendicular to the axonal tract. Several studies have reported that PAE may cause poor myelination (Connor and Menziers, 1996; Carter et al., 2007; Phillips and Krueger, 1992; Ozer et al., 2000). Beaulieu (2002) suggested that decreased axonal packing density and/or poor myelination may play a role.

In the RSNs where alterations were dose dependent, fALFF showed stronger relations to AA/day than ReHo. This result is consistent with the greater sensitivity of fALFF to resting state patterns observed previously in a study of healthy subjects that investigated functional covariance across groups (Taylor et al., 2012). These findings suggest that fALFF may be more suitable for investigating the properties within RSNs.

Notably, the regions where we did *not* observe dose dependent effects included the R-inferior peduncle, the R-ILF, R-SLF, and L- and R- CSTs, as well as the V-Att and R-Exe networks. Except for the R-CST and the V-Att network, these are all regions where HE children did not differ from controls, indicating that these regions are only affected in the most severely affected syndromal children, but may be relatively spared in children who do not exhibit the FAS facial phenotype.

In the superior and L-middle peduncles, sex and maternal age were the control variables most strongly related to the outcomes, but controlling for these did not alter the effect of exposure group on the outcomes. By contrast, the effect of exposure group on MD in the R-inferior peduncle was no longer significant after adjusting for child's age.

Surprisingly, MD was associated with smoking in all seven clusters in the cerebrum where children with FAS/PFAS revealed higher MD than control children, and in three of those clusters (R-SLF, R-CST, L-CST) associations with alcohol were no longer significant after controlling for smoking. These results provide additional evidence of the damaging effects of maternal smoking during pregnancy in children with PAE (Streissguth et al., 1989; Gusella and Fried, 1984; Martin et al., 1977).

Clusters revealing connectivity differences in the DM, V-Att, and D-Att networks showed associations with lead exposure. In the V-Att network where the association with lead exposure was strongest, the association with alcohol was no longer significant after controlling for lead exposure. Oddly, in the D-Att network, increased lead exposure was associated with greater fALFF, so that controlling for lead exposure increased the effect of alcohol on connectivity in this region.

The fact that fALFF was not associated with maternal smoking during pregnancy suggests that smoking may have a greater impact on WM than GM. In contrast, lead exposure appears to affect GM more than WM.

By combining the results from our rs-fMRI and DTI studies, we are able to examine whether the observed functional connectivity deficits are attributable largely to GM alterations or to microstructural deficits in the WM tracts connecting affected GM regions. We hypothesized that the alterations in RSFC found in the RSNs would be related to WM deficits. The regions in the R-SLF and L-middle cerebellar peduncle where children with FAS/PFAS revealed increased MD are adjacent to the GM clusters showing reduced connectivity in the DM (Figure 5.1a) and R-Exe (Figure 5.1c) networks, respectively, indicating that compromised connectivity in these networks may be due to deficits in the WM tracts connecting regions of the network.

Since the regions where our DTI studies revealed alterations are, however, only isolated clusters within WM tracts, we used the JHU DTI-based WM atlas in FSL to view the tracts connecting regions within the RSNs that showed group differences, enabling us to assess whether any of the regions where WM alterations were observed fall within any of these tracts. The region in the R-CST where increased MD was observed in both children with FAS/PFAS and

HE children compared to controls forms part of the R-superior corona radiata that connects regions within the Sal network. Specifically, this tract appears to form a connection to a region within which the cluster where we found functional connectivity differences in the Sal network is located (Figure 5.1b).

The above results suggest that the deficits in GM connectivity within the DM, Sal and R-Exe networks could be related to WM deficits in specific tracts that provide intra-RSN connections.

Interestingly, DM and Sal networks showed dose dependent effects, while the R-Exe network did not. By contrast, increases in MD were not dose dependent in the WM tracts posited to be the cause of the reduced connectivity in the DM and Sal networks, namely the R-SLF and R-CST, while it was in the L-middle peduncle, indicating that the interaction between WM alterations and functional connectivity may be more complex.

A tractography-based approach using GM regions with reduced connectivity as seeds could reveal fetal alcohol-related microstructural deficits in specific white matter tracts connecting affected regions on a subject-by-subject level. We plan to further examine GM-WM associations by combining DTI-based tractography with our rs-fMRI analyses and to perform a seed-based correlation study, informed by regions of interest found here, of whole brain and inter-network connectivity in children with FASD.

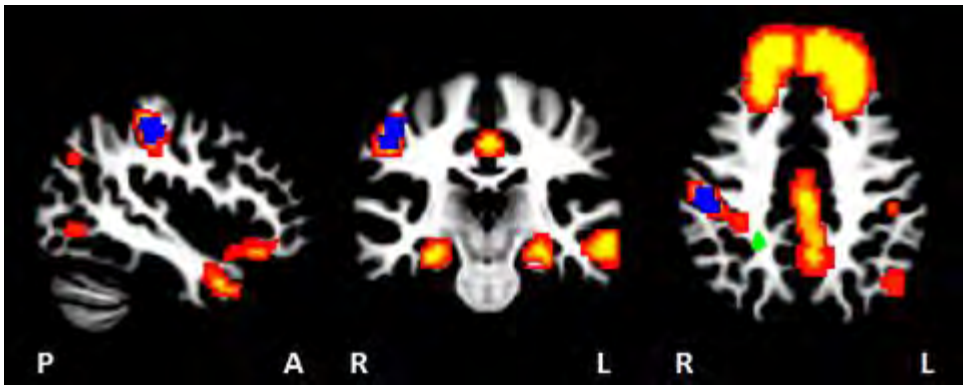

(a)

(b)

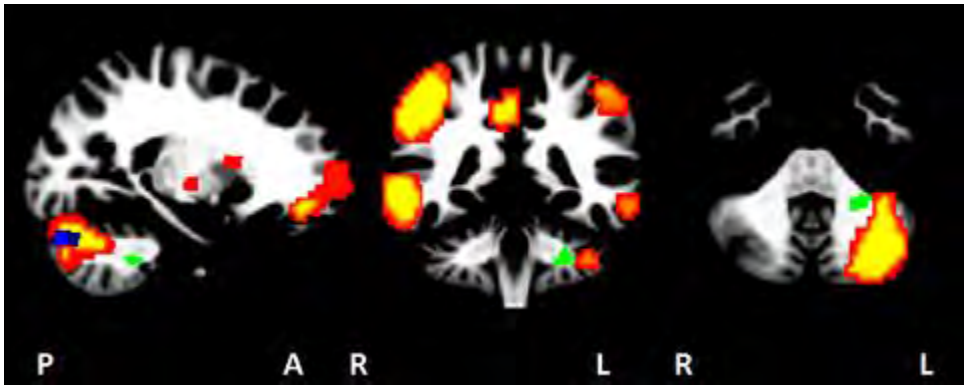

(c)

Figure 5.1 **Regions of functional connectivity and DTI differences, overlayed on thresholded rs-fMRI networks (hot colors). Clusters of RSFC differences are shown in blue and regions in intra-network tracts with WM alterations are shown in green: (a) the R-superior longitudinal fasciculus connects regions of the DMN; (b) the R-corticospinal tract, part of R-superior corona radiata (purple, JHU WM template from FSL), connects regions of the salience network; (c) the R-middle cerebellar peduncle connects regions of the R-executive control network.**

Chapter 6

Conclusions

In summary, this study adds to the growing body of evidence linking prenatal alcohol exposure to poorer microstructural white matter integrity and functional connectivity alterations in the brain. It is also the first study to evaluate the effects of prenatal alcohol exposure on multiple RSNs in children with FASD. Moreover, we were able to examine the effects of PAE both as a function of severity of clinical diagnosis and the degree of prenatal alcohol exposure. Several potential confounding factors were also controlled for, including child age, sex, and lead exposure, maternal age and education, and maternal smoking during pregnancy.

Reduced FA was observed bilaterally in the superior peduncles in children with FAS, and increased MD in the left middle peduncle of a combined FAS/PFAS group. The reduction of PAE effects on EBC performance following the addition of the diffusion measures to the regression analyses provided statistical evidence that poorer microstructural integrity in these three cerebellar peduncles may play an important role in the EBC deficit commonly seen in fetal alcohol-exposed children.

Comparisons of both structural cortical properties and functional connectivity revealed an increasing number of affected regions with increasing severity of FASD diagnosis. There were seven WM regions where DTI parameters differed compared to controls in the combined FAS/PFAS group, of which only four were observed in HE children. Decreases in RSFC were observed in five regions in distinct networks in the FAS/PFAS group, of which three were observed in the HE group. Together, these results strongly suggest that brain abnormalities are more extensive in syndromal children while some regions appear to be relatively less affected in nonsyndromal children, despite very high levels of alcohol exposure. In contrast, regions revealing dose dependent effects appear to be more sensitive to alcohol exposure and demonstrate alterations even in the absence of other diagnostic features.

The observed WM deficits were attributable to increased RD rather than decreased AD, suggesting poorer axon packing density and/or myelination.

Finally, examining the relative locations of regions revealing decreased functional connectivity and regions with decreased FA and/or increased MD, suggest that decreased RSFC in the default mode, salience, and right executive control networks may be attributable to WM deficits in tracts that provide intra-RSN connections. Tractography will be employed in future studies to examine more directly the link between structural and functional connectivity deficits arising from PAE.

References

Abel, E.L. (1995): An update on incidence of FAS: FAS is not an equal opportunity birth defect. Neurotoxicology and teratology, 17:437-443.

Andersson, J.L., Skare, S., Ashburner, J. (2003): How to correct susceptibility distortions in spin-echo echo-planar images: application to diffusion tensor imaging. Neuroimage, 20:870-888.

Archibald, S.L., Fennema-Notestine, C., Gamst, A., Riley, E.P., Mattson, S.N., Jernigan, T.L. (2001): Brain dysmorphology in individuals with severe prenatal alcohol exposure. Developmental Medicine & Child Neurology, 43:148-154.

Ashtari, M., Kumra, S., Bhaskar, S.L., Clarke, T., Thaden, E., Cervellione, K.L., Rhinewine, J., Kane, J.M., Adesman, A., Milanaik, R. (2005): Attention-deficit/hyperactivity disorder: a preliminary diffusion tensor imaging study. Biological psychiatry, 57:448-455.

Astley, S.J., Clarren, S.K. (2000): Diagnosing the full spectrum of fetal alcohol-exposed individuals: introducing the 4-digit diagnostic code. Alcohol and alcoholism, 35:400-410.

Astley, S.J., Olson, H.C., Kerns, K., Brooks, A., Aylward, E.H., Coggins, T.E., Davies, J., Dorn, S., Gendler, B., Jirikowic, T. (2009): Neuropsychological and behavioral outcomes from a comprehensive magnetic resonance study of children with fetal alcohol spectrum disorders. The Canadian journal of clinical pharmacology, 16:178-201.

Autti-Rämö, I., Autti, T., Korkman, M., Kettunen, S., Salonen, O., Valanne, L. (2002): MRI findings in children with school problems who had been exposed prenatally to alcohol. Developmental Medicine & Child Neurology, 44:98-106.

Baron, R.M., Kenny, D.A. (1986): The moderator–mediator variable distinction in social psychological research: Conceptual, strategic, and statistical considerations. Journal of personality and social psychology, 51:1173.

Barr, H.M., Streissguth, A.P. (2001): Identifying maternal self-reported alcohol use associated with fetal alcohol spectrum disorders. Alcoholism: Clinical and Experimental Research, 25, 283-287.

Basser, P.J., Mattiello, J., LeBihan, D. (1994): MR diffusion tensor spectroscopy and imaging. Biophysical journal, 66:259.

Beaulieu, C. (2002): The basis of anisotropic water diffusion in the nervous system–a technical review. NMR in Biomedicine, 15:435-455.

Beckmann, C.F., DeLuca, M., Devlin, J.T., Smith, S.M. (2005): Investigations into resting-state connectivity using independent component analysis. Philosophical Transactions of the Royal Society of London B: Biological Sciences, 360:1001-1013.

Beckmann, C.F., Smith, S.M. (2004): Probabilistic independent component analysis for functional magnetic resonance imaging. Medical Imaging, IEEE Transactions on, 23:137-152.

Bernard, J.A., Mittal, V.A. (2014): Dysfunctional Activation of the Cerebellum in Schizophrenia A Functional Neuroimaging Meta-Analysis. Clinical Psychological Science, 1-22.

Biswal, B., Zerrin Yetkin, F., Haughton, V.M., Hyde, J.S. (1995): Functional connectivity in the motor cortex of resting human brain using echo-planar mri. Magnetic resonance in medicine, 34:537-541.

Biswal, B.B., Mennes, M., Zuo, X., Gohel, S., Kelly, C., Smith, S.M., Beckmann, C.F., Adelstein, J.S., Buckner, R.L., Colcombe, S. (2010): Toward discovery science of human brain function. Proceedings of the National Academy of Sciences, 107:4734-4739.

Bjorkquist, O.A., Fryer, S.L., Reiss, A.L., Mattson, S.N., Riley, E.P. (2010): Cingulate gyrus morphology in children and adolescents with fetal alcohol spectrum disorders. Psychiatry Research: Neuroimaging, 181:101-107.

Boly, M., Phillips, C., Tshibanda, L., Vanhaudenhuyse, A., Schabus, M., Dang-Vu, T.T., Moonen, G., Hustinx, R., Maquet, P., Laureys, S. (2008): Intrinsic brain activity in altered states of consciousness. Annals of the New York Academy of Sciences, 1129:119-129.

Bonnelle, V., Leech, R., Kinnunen, K.M., Ham, T.E., Beckmann, C.F., De Boissezon, X., Greenwood, R.J., Sharp, D.J. (2011): Default mode network connectivity predicts sustained attention deficits after traumatic brain injury. The Journal of Neuroscience, 31:13442-13451.

Buckner, R.L., Andrews-Hanna, J.R., Schacter, D.L. (2008): The brain's default network. Annals of the New York Academy of Sciences, 1124:1-38.

Burden, M.J., Jacobson, S.W., Jacobson, J.L. (2005): Relation of prenatal alcohol exposure to cognitive processing speed and efficiency in childhood. Alcoholism: Clinical and Experimental Research, 29:1473-1483.

Carter, R.C., Jacobson, S.W., Molteno, C.D., Jacobson, J.L. (2007): Fetal alcohol exposure, iron-deficiency anemia, and infant growth. Pediatrics, 120:559-567.

Center for Disease Control and Prevention (2012): Alcohol use and binge drinking among women of childbearing age--United States, 2006-2010. MMWR. Morbidity and mortality weekly report, 61:534.

Chen, X., Coles, C.D., Lynch, M.E., Hu, X. (2012): Understanding specific effects of prenatal alcohol exposure on brain structure in young adults. Human brain mapping, 33:1663-1676.

Cheng, D.T., Disterhoft, J.F., Power, J.M., Ellis, D.A., Desmond, J.E. (2008): Neural substrates underlying human delay and trace eyeblink conditioning. Proceedings of the National Academy of Sciences, 105:8108-8113.

Cheng, D.T., Meintjes, E.M., Stanton, M.E., Desmond, J.E., Pienaar, M., Dodge, N.C., Power, J.M., Molteno, C.D., Disterhoft, J.F., Jacobson, J.L. (2014): Functional MRI of cerebellar activity during eyeblink classical conditioning in children and adults. Human brain mapping, 35:1390-1403.

Chiodo, L.M., Jacobson, S.W., Jacobson, J.L. (2004): Neurodevelopmental effects of postnatal lead exposure at very low levels. Neurotoxicology and teratology, 26:359-371.

Christian, K.M., Thompson, R.F. (2003): Neural substrates of eyeblink conditioning: acquisition and retention. Learning & memory, 10:427-455.

Clarren, S.K., Alvord, E.C., Sumi, S.M., Streissguth, A.P., Smith, D.W. (1978): Brain malformations related to prenatal exposure to ethanol. The Journal of pediatrics, 92:64-67.

Cox, R.W. (1996): AFNI: software for analysis and visualization of functional magnetic resonance neuroimages. Computers and Biomedical research, 29:162-173.

Clogg, C.C., Petkova, E., Shihadeh, E.S. (1992): Statistical methods for analyzing collapsibility in regression models. Journal of Educational and Behavioral Statistics, 17:51-74.

Coffin, J.M., Baroody, S., Schneider, K., O'Neill, J. (2005): Impaired cerebellar learning in children with prenatal alcohol exposure: a comparative study of eyeblink conditioning in children with ADHD and dyslexia. Cortex, 41:389-398.

Colby, J.B., Smith, L., O'Connor, M.J., Bookheimer, S.Y., Van Horn, J.D., Sowell, E.R. (2012): White matter microstructural alterations in children with prenatal methamphetamine /polydrug exposure. Psychiatry Research: Neuroimaging, 204:140-148.

Cole, D.M., Smith, S.M., Beckmann, C.F. (2010): Advances and pitfalls in the analysis and interpretation of resting-state FMRI data. Frontiers in systems neuroscience, 4:1-15.

Coles, C.D., Platzman, K.A., Lynch, M.E., Freides, D. (2002): Auditory and visual sustained attention in adolescents prenatally exposed to alcohol. Alcoholism: Clinical and Experimental Research, 26:263-271.

Coles, C.D., Platzman, K.A., Raskind-Hood, C.L., Brown, R.T., Falek, A., Smith, I.E. (1997): A comparison of children affected by prenatal alcohol exposure and attention deficit, hyperactivity disorder. Alcoholism: Clinical and Experimental Research, 21:150-161.

Conners, C.K. (1997): Conners' Rating Scales-Revised technical Manual. North Tonawanda, New York: Multi-Health Systems Inc., 212.

Connor, J.R., Menzies, S.L. (1996): Relationship of iron to oligondendrocytes and myelination. Glia, 17:83-93.

Coulter, C.L., Leech, R.W., Schaefer, G.B., Scheithauer, B.W., Brumback, R.A. (1993): Midline cerebral dysgenesis, dysfunction of the hypothalamic-pituitary axis, and fetal alcohol effects. Archives of Neurology, 50:771-775.

Croxford, J., Viljoen, D. (1999): Alcohol consumption by pregnant women in the Western Cape. S Afr Med J, 89:962-965.

Damoiseaux, J., Rombouts, S., Barkhof, F., Scheltens, P., Stam, C., Smith, S.M., Beckmann, C. (2006): Consistent resting-state networks across healthy subjects. Proceedings of the national academy of sciences, 103:13848-13853.

Damoiseaux, J.S. (2012): Resting-state fMRI as a biomarker for Alzheimer's disease. Alzheimers Res Ther, 4:8-9.

De Bie, H., Boersma, M., Adriaanse, S., Veltman, D.J., Wink, A.M., Roosendaal, S.D., Barkhof, F., Stam, C.J., Oostrom, K.J., Delemarre-Van de Waal, H.A. (2012): Resting-state networks in awake five-to eight-year old children. Human brain mapping, 33:1189-1201.

De Guio, F., Mangin, J.F., Riviere, D., Perrot, M., Molteno, C.D., Jacobson, S.W., Meintjes, E.M., Jacobson, J.L. (2014): A study of cortical morphology in children with fetal alcohol spectrum disorders. Human brain mapping, 35:2285-2296.

De Luca, M., Beckmann, C., De Stefano, N., Matthews, P., Smith, S.M. (2006): fMRI resting state networks define distinct modes of long-distance interactions in the human brain. Neuroimage, 29:1359-1367.

De Zeeuw, P., Zwart, F., Schrama, R., Van Engeland, H., Durston, S. (2012): Prenatal exposure to cigarette smoke or alcohol and cerebellum volume in attention-deficit/hyperactivity disorder and typical development. Translational psychiatry, 2:1-9.

Dikranian, K., Qin, Y.-Q., Labruyere, J., Nemmers, B., Olney, J.W. (2005): Ethanol-induced neuroapoptosis in the developing rodent cerebellum and related brain stem structures. Developmental Brain Research, 155:1-13.

Diwadkar, V.A., Meintjes, E.M., Goradia, D., Dodge, N.C., Warton, C., Molteno, C.D., Jacobson, S.W., Jacobson, J.L. (2013): Differences in cortico-striatal-cerebellar activation during working memory in syndromal and nonsyndromal children with prenatal alcohol exposure. Human brain mapping, 34:1931-1945.

Du Plessis, L., Jacobson, J.L., Jacobson, S.W., Hess, A.T., Kouwe, A., Avison, M.J., Molteno, C.D., Stanton, M.E., Stanley, J.A., Peterson, B.S. (2014): An In Vivo 1H Magnetic Resonance Spectroscopy Study of the Deep Cerebellar Nuclei in Children with Fetal Alcohol Spectrum Disorders. Alcoholism: Clinical and Experimental Research, 38:1330-1338.

Fair, D.A., Dosenbach, N.U., Church, J.A., Cohen, A.L., Brahmbhatt, S., Miezin, F.M., Barch, D.M., Raichle, M.E., Petersen, S.E., Schlaggar, B.L. (2007): Development of distinct control networks through segregation and integration. Proceedings of the National Academy of Sciences, 104:13507-13512.

Fan, J., Meintjes, E.M., Molteno, C.D., Spottiswoode, B.S., Dodge, N.C., Alhamud A.A., Stanton, M.E., Peterson, B.S., Jacobson, J.L., Jacobson, S.W. (2015): White matter integrity of the cerebellar peduncles as a mediator of effects of prenatal alcohol exposure on eyeblink conditioning. Human Brain Mapping, 36(7):2470-2482.

Fonov, V., Evans, A.C., Botteron, K., Almli, C.R., McKinstry, R.C., Collins, D.L., Group, B.D.C. (2011): Unbiased average age-appropriate atlases for pediatric studies. NeuroImage, 54:313-327.

Forman, S.D., Cohen, J.D., Fitzgerald, M., Eddy, W.F., Mintun, M.A., Noll, D.C. (1995): Improved assessment of significant activation in functional magnetic resonance imaging (fMRI): use of a cluster-size threshold. Magnetic Resonance in medicine, 33:636-647.

Fox, M.D., Corbetta, M., Snyder, A.Z., Vincent, J.L., Raichle, M.E. (2006): Spontaneous neuronal activity distinguishes human dorsal and ventral attention systems. Proceedings of the National Academy of Sciences, 103:10046-10051.

Fox, M.D., Raichle, M.E. (2007): Spontaneous fluctuations in brain activity observed with functional magnetic resonance imaging. Nature Reviews Neuroscience, 8:700-711.

Fox, M.D., Snyder, A.Z., Vincent, J.L., Corbetta, M., Van Essen, D.C., Raichle, M.E. (2005): The human brain is intrinsically organized into dynamic, anticorrelated functional networks. Proceedings of the National Academy of Sciences of the United States of America, 102:9673-9678.

Fransson, P. (2005): Spontaneous low-frequency BOLD signal fluctuations: An fMRI investigation of the resting-state default mode of brain function hypothesis. Human brain mapping, 26:15-29.

Fransson, P., Skiöld, B., Horsch, S., Nordell, A., Blennow, M., Lagercrantz, H., Åden, U. (2007): Resting-state networks in the infant brain. Proceedings of the National Academy of Sciences, 104:15531-15536.

Fryer, S.L., Schweinsburg, B.C., Bjorkquist, O.A., Frank, L.R., Mattson, S.N., Spadoni, A.D., Riley, E.P. (2009): Characterization of white matter microstructure in fetal alcohol spectrum disorders. Alcoholism: Clinical and Experimental Research, 33:514-521.

Fryer, S.L., Tapert, S.F., Mattson, S.N., Paulus, M.P., Spadoni, A.D., Riley, E.P. (2007): Prenatal alcohol exposure affects frontal–striatal BOLD response during inhibitory control. Alcoholism: clinical and experimental research, 31:1415-1424.

Green, C.R., Lebel, C., Rasmussen, C., Beaulieu, C., Reynolds, J.N. (2013): Diffusion tensor imaging correlates of saccadic reaction time in children with fetal alcohol spectrum disorder. Alcoholism: Clinical and Experimental Research, 37:1499-1507.

Green, J.T. (2004): The effects of ethanol on the developing cerebellum and eyeblink classical conditioning. The Cerebellum, 3:178-187.

Greicius, M.D., Kiviniemi, V., Tervonen, O., Vainionpää, V., Alahuhta, S., Reiss, A.L., Menon, V. (2008): Persistent default-mode network connectivity during light sedation. Human brain mapping, 29:839-847.

Greicius, M.D., Krasnow, B., Reiss, A.L., Menon, V. (2003): Functional connectivity in the resting brain: a network analysis of the default mode hypothesis. Proceedings of the National Academy of Sciences, 100:253-258.

Gusella, J., Fried, P. (1984): Effects of maternal social drinking and smoking on offspring at 13 months. Neurobehavioral toxicology and teratology, 6:13-17.

Habas, C., Kamdar, N., Nguyen, D., Prater, K., Beckmann, C.F., Menon, V., Greicius, M.D. (2009): Distinct cerebellar contributions to intrinsic connectivity networks. The Journal of Neuroscience, 29:8586-8594.

Hayden, B.Y., Smith, D.V., Platt, M.L. (2009): Electrophysiological correlates of default-mode processing in macaque posterior cingulate cortex. Proceedings of the National Academy of Sciences, 106:5948-5953.

He Y., Wang L., Zang Y., Tian L., Zhang X., Li K., Jiang T. (2007): Regional coherence changes in the early stages of Alzheimer's disease: a combined structural and resting-state functional MRI study. Neuroimage 35:488–500.

Hollingshead, A.B. (2011): Four Factor Index of Social Status. Yale Journal of Sociology 8:21-51.

Hoyme, H.E., May, P.A., Kalberg, W.O., Kodituwakku, P., Gossage, J.P., Trujillo, P.M., Buckley, D.G., Miller, J.H., Aragon, A.S., Khaole, N. (2005): A practical clinical approach to

diagnosis of fetal alcohol spectrum disorders: clarification of the 1996 institute of medicine criteria. Pediatrics, 115:39-47.

Jacobson, J.L., Jacobson, S.W. (2002): Effects of prenatal alcohol exposure on child development. Alcohol Research and Health, 26:282-286.

Jacobson S.W., Stanton M.E., Dodge N.C., Pienaar M., Fuller D.S., Molteno C.D., Meintjes E.M., Hoyme H.E., Robinson L.K., Khaole N. (2011): Impaired delay and trace eyeblink conditioning in school-age children with fetal alcohol syndrome. Alcoholism: Clinical and Experimental Research, 35(2):250-264.

Jacobson, J.L., Jacobson, S.W., Sokol, R.J. (1996): Increased Vulnerability to Alcohol-Related Birth Defects in the Offspring of Mothers Over 30. Alcoholism: Clinical and Experimental Research, 20:359-363.

Jacobson, S.W., Jacobson, J.L., Sokol, R.J., Chiodo, L.M., Corobana, R. (2004): Maternal age, alcohol abuse history, and quality of parenting as moderators of the effects of prenatal alcohol exposure on 7.5-year intellectual function. Alcoholism: Clinical and Experimental Research, 28:1732-1745.

Jacobson, S.W., Jacobson, J.L., Sokol, R.J., Martier, S.S., Ager, J.W. (1993): Prenatal alcohol exposure and infant information processing ability. Child development, 64:1706-1721.

Jacobson, S.W., Stanton, M.E., Dodge, N.C., Pienaar, M., Fuller, D.S., Molteno, C.D., Meintjes, E.M., Hoyme, H.E., Robinson, L.K., Khaole, N. (2011): Impaired Delay and Trace Eyeblink Conditioning in School-Age Children With Fetal Alcohol Syndrome. Alcoholism: Clinical and Experimental Research, 35:250-264.

Jacobson, S.W., Stanton, M.E., Molteno, C.D., Burden, M.J., Fuller, D.S., Hoyme, H.E., Robinson, L.K., Khaole, N., Jacobson, J.L. (2008): Impaired eyeblink conditioning in children with fetal alcohol syndrome. Alcoholism: Clinical and Experimental Research, 32:365-372.

Jones, K., Smith, D. (1973): Recognition of the fetal alcohol syndrome in early infancy. The Lancet, 302:999-1001.

Kaemingk, K.L., Mulvaney, S., Halverson, P.T. (2003): Learning following prenatal alcohol exposure: performance on verbal and visual multitrial tasks. Archives of Clinical Neuropsychology, 18:33-47.

Kalberg, W.O., Provost, B., Tollison, S.J., Tabachnick, B.G., Robinson, L.K., Eugene Hoyme, H., Trujillo, P.M., Buckley, D., Aragon, A.S., May, P.A. (2006): Comparison of motor delays in young children with fetal alcohol syndrome to those with prenatal alcohol exposure and with no prenatal alcohol exposure. Alcoholism: Clinical and Experimental Research, 30:2037-2045.

Kim, J., Wozniak, J.R., Mueller, B.A., Shen, X., Pan, W. (2014): Comparison of statistical tests for group differences in brain functional networks. NeuroImage, 101:681-694.

Kinney, H., Faix, R., Brazy, J. (1980): The fetal alcohol syndrome and neuroblastoma. Pediatrics, 66:130-132.

Kiviniemi, V., Kantola, J.H., Jauhiainen, J., Hyvärinen, A., Tervonen, O. (2003): Independent component analysis of nondeterministic fMRI signal sources. Neuroimage, 19:253-260.

Kodituwakku, P., Handmaker, N., Cutler, S., Weathersby, E., Handmaker, S. (1995): Specific impairments in self-regulation in children exposed to alcohol prenatally. Alcoholism: Clinical and Experimental Research, 19:1558-1564.

Lanphear, B.P., Dietrich, K., Auinger, P., Cox, C. (2000): Cognitive deficits associated with blood lead concentrations< 10 microg/dL in US children and adolescents. Public health reports, 115:521.

Lavond, D.G., Steinmetz, J.E. (1989): Acquisition of classical conditioning without cerebellar cortex. Behavioural brain research, 33:113-164.

Lebel, C., Rasmussen, C., Wyper, K., Andrew, G., Beaulieu, C. (2010): Brain microstructure is related to math ability in children with fetal alcohol spectrum disorder. Alcoholism: Clinical and experimental research, 34:354-363.

Lebel, C., Rasmussen, C., Wyper, K., Walker, L., Andrew, G., Yager, J., Beaulieu, C. (2008): Brain diffusion abnormalities in children with fetal alcohol spectrum disorder. Alcoholism: Clinical and Experimental Research, 32:1732-1740.

Lee, M., Smyser, C., Shimony, J. (2013): Resting-state fMRI: a review of methods and clinical applications. American Journal of Neuroradiology, 34:1866-1872.

Lemoine, P., Harousseau, H., Borteyru, J., Menuet, J. (1968): Children of alcoholic parents: Abnormalities observed in 127 cases. Ouest Medical, 21:476–482.

Li, L., Coles, C.D., Lynch, M.E., Hu, X. (2009): Voxelwise and skeleton-based region of interest analysis of fetal alcohol syndrome and fetal alcohol spectrum disorders in young adults. Human brain mapping, 30:3265-3274.

Logothetis, N.K., Wandell, B.A. (2004): Interpreting the BOLD signal. Annu. Rev. Physiol., 66:735-769.

Lowe, M., Mock, B., Sorenson, J. (1998): Functional connectivity in single and multislice echoplanar imaging using resting-state fluctuations. Neuroimage, 7:119-132.

Ma, X., Coles, C.D., Lynch, M.E., LaConte, S.M., Zurkiya, O., Wang, D., Hu, X. (2005): Evaluation of corpus callosum anisotropy in young adults with fetal alcohol syndrome according to diffusion tensor imaging. Alcoholism: Clinical and Experimental Research, 29:1214-1222.

MacKinnon, D.P., Lockwood, C.M., Hoffman, J.M., West, S.G., Sheets, V. (2002): A comparison of methods to test mediation and other intervening variable effects. Psychological methods, 7:83-104.

Madge, E. (1981): Manual for the junior South African individual scales (JSAIS) Part I: Development and Standardisation. Pretoria: Human Science Research Council.

Maldonado, G., Greenland, S. (1993): Simulation study of confounder-selection strategies. American journal of epidemiology, 138:923-936.

Margulies, E.H., Cooper, G.M., Asimenos, G., Thomas, D.J., Dewey, C.N., Siepel, A., Birney, E., Keefe, D., Schwartz, A.S., Hou, M. (2007): Analyses of deep mammalian sequence alignments and constraint predictions for 1% of the human genome. Genome research, 17:760-774.

Martin, J., Martin, D.C., Lund, C.A., Streissguth, A.P. (1977): Maternal alcohol ingestion and cigarette smoking and their effects on newborn conditioning. Alcoholism: Clinical and Experimental Research, 1:243-247.

Mattson, S.N., Crocker, N., Nguyen, T.T. (2011): Fetal alcohol spectrum disorders: neuropsychological and behavioral features. Neuropsychology review, 21:81-101.

Mattson, S.N., Goodman, A.M., Caine, C., Delis, D.C., Riley, E.P. (1999): Executive functioning in children with heavy prenatal alcohol exposure. Alcoholism: Clinical and Experimental Research, 23:1808-1815.

Mattson, S.N., Riley, E.P. (1998): A review of the neurobehavioral deficits in children with fetal alcohol syndrome or prenatal exposure to alcohol. Alcoholism: Clinical and Experimental Research, 22:279-294.

Mattson, S.N., Riley, E.P., Delis, D.C., Stern, C., Jones, K.L. (1996): Verbal learning and memory in children with fetal alcohol syndrome. Alcoholism: Clinical and Experimental Research, 20:810-816.

Mattson, S.N., Riley, E.P., Gramling, L., Delis, D.C., Jones, K.L., of Dysmorphology, T.D. (1997): Heavy prenatal alcohol exposure with or without physical features of fetal alcohol syndrome leads to IQ deficits. The Journal of pediatrics, 131:718-721.

Mattson, S.N., Riley, E.P., Jernigan, T.L., Ehlers, C.L., Delis, D.C., Jones, K.L., Stern, C., Johnson, K.A., Hesselink, J.R., Bellugi, U. (1992): Fetal alcohol syndrome: A case report of neuropsychological, MRI, and EEG assessment of two children. Alcoholism: Clinical and Experimental Research, 16:1001-1003.

Mattson, S.N., Riley, E.P., Jernigan, T.L., Garcia, A., Kaneko, W.M., Ehlers, C.L., Jones, K.L. (1994): A decrease in the size of the basal ganglia following prenatal alcohol exposure: a preliminary report. Neurotoxicology and teratology, 16:283-289.

May, P.A., Brooke, L., Gossage, J.P., Croxford, J., Adnams, C., Jones, K.L., Robinson, L., Viljoen, D. (2000): Epidemiology of fetal alcohol syndrome in a South African community in the Western Cape Province. American journal of public health, 90:1905.

May, P.A., Gossage, J.P. (2011): Maternal risk factors for fetal alcohol spectrum disorders: not as simple as it might seem. Alcohol Research & Health, 34:15.

May, P.A., Gossage, J.P., Kalberg, W.O., Robinson, L.K., Buckley, D., Manning, M., Hoyme, H.E. (2009): Prevalence and epidemiologic characteristics of FASD from various research methods with an emphasis on recent in-school studies. Developmental disabilities research reviews, 15:176-192.

McKeown, M.J., Makeig, S., Brown, G.G., Jung, T.-P., Kindermann, S.S., Bell, A.J., Sejnowski, T.J. (1998): Analysis of fMRI data by blind separation into independent spatial components. DTIC Document.

Meindl, T., Teipel, S., Elmouden, R., Mueller, S., Koch, W., Dietrich, O., Coates, U., Reiser, M., Glaser, C. (2010): Test–retest reproducibility of the default-mode network in healthy individuals. Human brain mapping, 31:237-246.

Mori, S., van Zijl, P. (2002): Fiber tracking: principles and strategies–a technical review. NMR in Biomedicine, 15:468-480.

Mukherjee, R.A., Hollins, S., Turk, J. (2006): Fetal alcohol spectrum disorder: an overview. Journal of the Royal Society of Medicine, 99:298-302.

Nardelli, A., Lebel, C., Rasmussen, C., Andrew, G., Beaulieu, C. (2011): Extensive deep gray matter volume reductions in children and adolescents with fetal alcohol spectrum disorders. Alcoholism: Clinical and Experimental Research, 35:1404-1417.

Ogawa, S., Lee, T., Kay, A.R., Tank, D.W. (1990): Brain magnetic resonance imaging with contrast dependent on blood oxygenation. Proceedings of the National Academy of Sciences, 87:9868-9872.

Ozer, E., Sarioglu, S., Güre, A. (2000): Effects of prenatal ethanol exposure on neuronal migration, neuronogenesis and brain myelination in the mice brain. Clinical neuropathology, 19:21-25.

Paolozza, A., Treit, S., Beaulieu, C., Reynolds, J.N. (2014): Response inhibition deficits in children with Fetal Alcohol Spectrum Disorder: Relationship between diffusion tensor imaging of the corpus callosum and eye movement control. NeuroImage: Clinical, 5:53-61.

Peiffer, J., Majewski, F., Fischbach, H., Bierich, J., Volk, B. (1979): Alcohol embryo-and fetopathy: Neuropathology of 3 children and 3 fetuses. Journal of the Neurological Sciences, 41:125-137.

Phillips, D., Krueger, S. (1992): Effects of combined pre-and postnatal ethanol exposure (three trimester equivalency) on glial cell development in rat optic nerve. International journal of developmental neuroscience, 10:197-206.

Power, J.D., Cohen, A.L., Nelson, S.M., Wig, G.S., Barnes, K.A., Church, J.A., Vogel, A.C., Laumann, T.O., Miezin, F.M., Schlaggar, B.L. (2011): Functional network organization of the human brain. Neuron, 72:665-678.

Ptak, R., Schnider, A. (2010): The dorsal attention network mediates orienting toward behaviorally relevant stimuli in spatial neglect. The Journal of Neuroscience, 30:12557-12565.

Raichle, M.E., MacLeod, A.M., Snyder, A.Z., Powers, W.J., Gusnard, D.A., Shulman, G.L. (2001): A default mode of brain function. Proceedings of the National Academy of Sciences, 98:676-682.

Rajaprakash, M., Chakravarty, M.M., Lerch, J.P., Rovet, J. (2014): Cortical morphology in children with alcohol-related neurodevelopmental disorder. Brain and behavior, 4:41-50.

Renwick, J., Asker, R.L. (1983): Ethanol-sensitive times for the human conceptus. Early human development, 8:99-111.

Riley, E.P., Mattson, S.N., Sowell, E.R., Jernigan, T.L., Sobel, D.F., Jones, K.L. (1995): Abnormalities of the corpus callosum in children prenatally exposed to alcohol. Alcoholism: Clinical and Experimental Research, 19:1198-1202.

Rosazza, C., Minati, L. (2011): Resting-state brain networks: literature review and clinical applications. Neurological Sciences, 32:773-785.

Rosazza, C., Minati, L., Ghielmetti, F., Mandelli, M., Bruzzone, M. (2012): Functional Connectivity during Resting-State Functional MR Imaging: Study of the Correspondence between Independent Component Analysis and Region-of-Interest-Based Methods. American Journal of Neuroradiology, 33:180-187.

Roussotte, F.F., Sulik, K.K., Mattson, S.N., Riley, E.P., Jones, K.L., Adnams, C.M., May, P.A., O'Connor, M.J., Narr, K.L., Sowell, E.R. (2012): Regional brain volume reductions relate to facial dysmorphology and neurocognitive function in fetal alcohol spectrum disorders. Human brain mapping, 33:920-937.

Santhanam, P., Coles, C.D., Li, Z., Li, L., Lynch, M.E., Hu, X. (2011): Default mode network dysfunction in adults with prenatal alcohol exposure. Psychiatry Research: Neuroimaging, 194:354-362.

Seeley, W.W., Crawford, R.K., Zhou, J., Miller, B.L., Greicius, M.D. (2009): Neurodegenerative diseases target large-scale human brain networks. Neuron, 62:42-52.

Seeley, W.W., Menon, V., Schatzberg, A.F., Keller, J., Glover, G.H., Kenna, H., Reiss, A.L., Greicius, M.D. (2007): Dissociable intrinsic connectivity networks for salience processing and executive control. The Journal of neuroscience, 27:2349-2356.

Shehzad, Z., Kelly, A.C., Reiss, P.T., Gee, D.G., Gotimer, K., Uddin, L.Q., Lee, S.H., Margulies, D.S., Roy, A.K., Biswal, B.B. (2009): The resting brain: unconstrained yet reliable. Cerebral cortex, 19:2209-2229.

Shulman, G.L., Fiez, J.A., Corbetta, M., Buckner, R.L., Miezin, F.M., Raichle, M.E., Petersen, S.E. (1997): Common blood flow changes across visual tasks: II. Decreases in cerebral cortex. Journal of cognitive neuroscience, 9:648-663.

Smith, S.M., Fox, P.T., Miller, K.L., Glahn, D.C., Fox, P.M., Mackay, C.E., Filippini, N., Watkins, K.E., Toro, R., Laird, A.R. (2009): Correspondence of the brain's functional architecture during activation and rest. Proceedings of the National Academy of Sciences, 106:13040-13045.

Smith, S.M., Jenkinson, M., Johansen-Berg, H., Rueckert, D., Nichols, T.E., Mackay, C.E., Watkins, K.E., Ciccarelli, O., Cader, M.Z., Matthews, P.M. (2006): Tract-based spatial statistics: voxelwise analysis of multi-subject diffusion data. Neuroimage, 31:1487-1505.

Smith, S.M., Jenkinson, M., Woolrich, M.W., Beckmann, C.F., Behrens, T.E., Johansen-Berg, H., Bannister, P.R., De Luca, M., Drobnjak, I., Flitney, D.E. (2004): Advances in functional and structural MR image analysis and implementation as FSL. Neuroimage, 23:S208-S219.

Sowell, E.R., Johnson, A., Kan, E., Lu, L.H., Van Horn, J.D., Toga, A.W., O'Connor, M.J., Bookheimer, S.Y. (2008): Mapping white matter integrity and neurobehavioral correlates in children with fetal alcohol spectrum disorders. The Journal of Neuroscience, 28:1313-1319.

Sowell, E.R., Mattson, S., Thompson, P., Jernigan, T., Riley, E., Toga, A. (2001a): Mapping callosal morphology and cognitive correlates Effects of heavy prenatal alcohol exposure. Neurology, 57:235-244.

Sowell, E.R., Thompson, P.M., Mattson, S.N., Tessner, K.D., Jernigan, T.L., Riley, E.P., Toga, A.W. (2001b): Voxel-based morphometric analyses of the brain in children and adolescents prenatally exposed to alcohol. Neuroreport, 12:515-523.

Sowell, E.R., Thompson, P.M., Mattson, S.N., Tessner, K.D., Jernigan, T.L., Riley, E.P., Toga, A.W. (2002a): Regional brain shape abnormalities persist into adolescence after heavy prenatal alcohol exposure. Cerebral Cortex, 12:856-865.

Sowell, E.R., Thompson, P.M., Peterson, B.S., Mattson, S.N., Welcome, S.E., Henkenius, A.L., Riley, E.P., Jernigan, T.L., Toga, A.W. (2002b): Mapping cortical gray matter asymmetry patterns in adolescents with heavy prenatal alcohol exposure. Neuroimage, 17:1807-1819.

Spadoni, A.D., McGee, C.L., Fryer, S.L., Riley, E.P. (2007): Neuroimaging and fetal alcohol spectrum disorders. Neuroscience & Biobehavioral Reviews, 31:239-245.

Spottiswoode, B.S., Meintjes, E.M., Anderson, A.W., Molteno, C.D., Stanton, M.E., Dodge, N.C., Gore, J.C., Peterson, B.S., Jacobson, J.L., Jacobson, S.W. (2011): Diffusion tensor imaging of the cerebellum and eyeblink conditioning in fetal alcohol spectrum disorder. Alcoholism: Clinical and Experimental Research, 35:2174-2183.

Stratton, K., Howe, C., Battaglia, F.C. (1996) Fetal alcohol syndrome: Diagnosis, epidemiology, prevention, and treatment. National Academies Press.

Stanton, M.E., Goodlett, C.R. (1998): Neonatal ethanol exposure impairs eyeblink conditioning in weanling rats. Alcoholism: Clinical and Experimental Research, 22:270-275.

Streissguth, A.P., Barr, H.M., Sampson, P.D. (1990): Moderate prenatal alcohol exposure: effects on child IQ and learning problems at age 7 1/2 years. Alcoholism: Clinical and Experimental Research, 14:662-669.

Streissguth, A.P., Bookstein, F.L., Sampson, P.D., Barr, H.M. (1989): Neurobehavioral effects of prenatal alcohol: Part III. PLS analyses of neuropsychologic tests. Neurotoxicology and Teratology, 11:493-507.

Stevens, M.C., Pearlson, G.D., Calhoun, V.D. (2009): Changes in the interaction of resting-state neural networks from adolescence to adulthood. Human brain mapping, 30:2356-2366.

Supekar, K., Musen, M., Menon, V. (2009): Development of large-scale functional brain networks in children. PLoS biology, 7:e1000157.

Taylor, P.A., Gohel, S., Di, X., Walter, M., Biswal, B.B. (2012): Functional covariance networks: obtaining resting-state networks from intersubject variability. Brain connectivity, 2:203-217.

Taylor, P.A., Jacobson, S.W., Van der Kouwe, A., Molteno, C.D., Chen, G., Wintermark, P., Alhamud, A., Jacobson, J.L., Meintjes, E.M. (2015): A DTI-based tractography study of effects on brain structure associated with prenatal alcohol exposure in newborns. Human brain mapping, 36:170-186.

Taylor, P.A., Saad, Z.S. (2013): FATCAT:(an efficient) functional and tractographic connectivity analysis toolbox. Brain connectivity, 3:523-535.

Thomason, M.E., Dennis, E.L., Joshi, A.A., Joshi, S.H., Dinov, I.D., Chang, C., Henry, M.L., Johnson, R.F., Thompson, P.M., Toga, A.W. (2011): Resting-state fMRI can reliably map neural networks in children. Neuroimage, 55:165-175.

Tisdall, M., Hess, A., Van der Kouwe, A. (2009): MPRAGE using EPI navigators for prospective motion correction. ISMRM.

Tomasi, D., Volkow, N.D. (2012): Resting functional connectivity of language networks: characterization and reproducibility. Molecular psychiatry, 17:841-854.

Tran, T., Thomas, J. (Perinatal choline supplementation mitigates trace eyeblink conditioning deficits associated with 3rd trimester alcohol exposure in rodents). In; 2007.

Treit, S., Lebel, C., Baugh, L., Rasmussen, C., Andrew, G., Beaulieu, C. (2013): Longitudinal MRI reveals altered trajectory of brain development during childhood and adolescence in fetal alcohol spectrum disorders. The Journal of Neuroscience, 33:10098-10109.

Van de Ven, V.G., Formisano, E., Prvulovic, D., Roeder, C.H., Linden, D.E. (2004): Functional connectivity as revealed by spatial independent component analysis of fMRI measurements during rest. Human brain mapping, 22:165-178.

Van der Kouwe, A.J., Benner, T., Salat, D.H., Fischl, B. (2008): Brain morphometry with multiecho MPRAGE. Neuroimage, 40:559-569.

Van Dijk, K.R., Hedden, T., Venkataraman, A., Evans, K.C., Lazar, S.W., Buckner, R.L. (2010): Intrinsic functional connectivity as a tool for human connectomics: theory, properties, and optimization. Journal of neurophysiology, 103:297-321.

Vincent, J., Patel, G., Fox, M., Snyder, A., Baker, J., Van Essen, D., Zempel, J., Snyder, L., Corbetta, M., Raichle, M. (2007): Intrinsic functional architecture in the anaesthetized monkey brain. Nature, 447:83-86.

Vincent, J.L., Kahn, I., Snyder, A.Z., Raichle, M.E., Buckner, R.L. (2008): Evidence for a frontoparietal control system revealed by intrinsic functional connectivity. Journal of neurophysiology, 100:3328-3342.

Weissman, D., Roberts, K., Visscher, K., Woldorff, M. (2006): The neural bases of momentary lapses in attention. Nature neuroscience, 9:971-978.

Winer, B.J., Brown, D.R., Michels, K.M. (1971) Statistical principles in experimental design. McGraw-Hill New York. 907 p.

Wisniewski, K., Dambska, M., Sher, J., Qazi, Q. (1983): A clinical neuropathological study of the fetal alcohol syndrome. Neuropediatrics, 14:197-201.

Woodruff-Pak, D.S., Disterhoft, J.F. (2008): Where is the trace in trace conditioning? Trends in neurosciences, 31:105-112.

Wozniak, J.R., Mueller, B.A., Bell, C.J., Muetzel, R.L., Hoecker, H.L., Boys, C.J., Lim, K.O. (2013): Global functional connectivity abnormalities in children with fetal alcohol spectrum disorders. Alcoholism: Clinical and Experimental Research, 37:748-756.

Wozniak, J.R., Mueller, B.A., Chang, P.N., Muetzel, R.L., Caros, L., Lim, K.O. (2006): Diffusion tensor imaging in children with fetal alcohol spectrum disorders. Alcoholism: Clinical and Experimental Research, 30:1799-1806.

Wozniak, J.R., Mueller, B.A., Muetzel, R.L., Bell, C.J., Hoecker, H.L., Nelson, M.L., Chang, P.N., Lim, K.O. (2011): Inter-Hemispheric Functional Connectivity Disruption in Children With Prenatal Alcohol Exposure. Alcoholism: Clinical and Experimental Research, 35:849-861.

Wozniak, J.R., Muetzel, R.L., Mueller, B.A., McGee, C.L., Freerks, M.A., Ward, E.E., Nelson, M.L., Chang, P.N., Lim, K.O. (2009): Microstructural corpus callosum anomalies in children with prenatal alcohol exposure: an extension of previous diffusion tensor imaging findings. Alcoholism: Clinical and Experimental Research, 33:1825-1835.

Xiong, L., Liu, K., Dai, X., Xu, C., Zhang, Q. (1999): Identification of genetic factors controlling domestication-related traits of rice using an F2 population of a cross between Oryza sativa and O. rufipogon. Theoretical and Applied Genetics, 98:243-251.

Yang, Y., Phillips, O.R., Kan, E., Sulik, K.K., Mattson, S.N., Riley, E.P., Jones, K.L., Adnams, C.M., May, P.A., O'Connor, M.J. (2012): Callosal thickness reductions relate to facial dysmorphology in fetal alcohol spectrum disorders. Alcoholism: Clinical and Experimental Research, 36:798-806.

Yeo, B.T., Krienen, F.M., Sepulcre, J., Sabuncu, M.R., Lashkari, D., Hollinshead, M., Roffman, J.L., Smoller, J.W., Zöllei, L., Polimeni, J.R. (2011): The organization of the human cerebral cortex estimated by intrinsic functional connectivity. Journal of neurophysiology, 106:1125-1165.

Zang, Y., Jiang, T., Lu, Y., He, Y., Tian, L. (2004): Regional homogeneity approach to fMRI data analysis. Neuroimage, 22:394-400.

Zang, Y., He, Y., Zhu, C., Cao, Q., Sui, M., Liang, M., Tian, L., Jiang, T., Wang, Y. (2007): Altered baseline brain activity in children with ADHD revealed by resting-state functional MRI. Brain and Development, 29:83-91.

Zhou, D., Lebel, C., Lepage, C., Rasmussen, C., Evans, A., Wyper, K., Pei, J., Andrew, G., Massey, A., Massey, D. (2011): Developmental cortical thinning in fetal alcohol spectrum disorders. Neuroimage, 58:16-25.

Zou, Q., Zhu, C., Yang, Y., Zuo, X., Long, X., Cao, Q., Wang, Y., Zang, Y. (2008): An improved approach to detection of amplitude of low-frequency fluctuation (ALFF) for resting-state fMRI: fractional ALFF. Journal of neuroscience methods, 172:137-141.

Zuo, X., Di Martino, A., Kelly, C., Shehzad, Z.E., Gee, D.G., Klein, D.F., Castellanos, F.X., Biswal, B.B., Milham, M.P. (2010a): The oscillating brain: complex and reliable. Neuroimage, 49:1432-1445.

Zuo, X., Kelly, C., Adelstein, J.S., Klein, D.F., Castellanos, F.X., Milham, M.P. (2010b): Reliable intrinsic connectivity networks: test–retest evaluation using ICA and dual regression approach. Neuroimage, 49:2163-2177.

Appendix

Appendix 1 Threshold volume for significant clusters in each network

	DMN	Salience	Ventral attention	Dorsal attention	R executive control
Size (mm^3)	324	324	270	297	324

Appendix 2.a Regions (size and peak coordinates in TT standard space) where connectivity was lower in children with FAS/PFAS compared to controls when voxelwise group comparisons were repeated with each potential confounder added separately into the model.

DMN

Predictor	Size (mm^3)	Peak coordinates		
		x	y	z
None	540	46.5	-31.5	44.5
Child's sex	351	46.5	-31.5	44.5
Child's age at scan	432	46.5	-28.5	44.5
Lead exposure	324	46.5	-31.5	47.5
Maximum displacement	432	46.5	-31.5	44.5
Maternal age	486	46.5	-31.5	44.5
Maternal education	324	46.5	-31.5	44.5
Smoking during pregnancy	324	46.5	-31.5	44.5

Salience

Predictor	Size (mm^3)	Peak coordinates		
		x	y	z
None	351	10.5	-1.5	59.5
Child's sex	297	10.5	1.5	56.5
Child's age at scan	459	10.5	-1.5	56.5
Lead exposure	567	10.5	1.5	56.5
Maximum displacement	378	10.5	-1.5	59.5
Maternal age	378	10.5	-1.5	56.5
Maternal education	297	10.5	-1.5	59.5
Smoking during pregnancy	297	10.5	-1.5	59.5

Ventral attention

Predictor	Size (mm^3)	Peak coordinates		
		x	y	z
None	729	43.5	1.5	44.5
Child's sex	378	46.5	-1.5	47.5
Child's age at scan	378	43.5	-1.5	47.5
Lead exposure	351	46.5	1.5	44.5
Maximum displacement	378	43.5	1.5	44.5
Maternal age	459	43.5	-1.5	44.5
Maternal education	378	46.5	-1.5	47.5
Smoking during pregnancy	594	43.5	-1.5	44.5

Dorsal attention

Predictor	Size (mm^3)	Peak coordinates		
		x	y	z
None	486	-31.5	-7.5	53.5
Child's sex	486	-31.5	-10.5	53.5
Child's age at scan	621	-28.5	-10.5	53.5
Lead exposure	486	-31.5	-7.5	53.5
Maximum displacement	594	-31.5	-7.5	53.5
Maternal age	324	-31.5	-7.5	50.5
Maternal education	594	-31.5	-7.5	53.5
Smoking during pregnancy	783	-28.5	-7.5	50.5

Right executive control

Predictor	Size (mm^3)	Peak coordinates		
		x	y	z
None	675	-10.5	-73.5	-30.5
Child's sex	378	-10.5	-76.5	-30.5
Child's age at scan	351	-13.5	-73.5	-30.5
Lead exposure	351	-10.5	-76.5	-30.5
Maximum displacement	378	-10.5	-73.5	-30.5
Maternal age	378	-10.5	-73.5	-30.5
Maternal education	567	-13.5	-76.5	-30.5
Smoking during pregnancy	567	-10.5	-76.5	-30.5

Appendix 2.b Regions (size and peak coordinates in TT standard space) where connectivity was lower in nonsyndromal heavily exposed children compared to controls when voxelwise group comparisons were repeated with each potential confounder added separately into the model.

DMN

Predictor	Size (mm^3)	Peak coordinates		
		x	y	z
None	405	52.5	-28.5	38.5
Child's sex	405	52.5	-28.5	38.5
Child's age at scan	459	52.5	-28.5	38.5
Lead exposure	432	52.5	-28.5	38.5
Maximum displacement	405	52.5	-28.5	38.5
Maternal age	324	52.5	-28.5	38.5
Maternal education	351	52.5	-28.5	38.5
Smoking during pregnancy	378	52.5	-28.5	38.5

Salience

Predictor	Size (mm^3)	Peak coordinates		
		x	y	z
None	891	7.5	1.5	53.5
Child's sex	756	10.5	-1.5	53.5
Child's age at scan	756	10.5	-1.5	53.5
Lead exposure	702	10.5	-1.5	53.5
Maximum displacement	702	7.5	1.5	53.5
Maternal age	891	10.5	-1.5	53.5
Maternal education	837	10.5	1.5	53.5
Smoking during pregnancy	891	10.5	-1.5	53.5

Ventral attention

Predictor	Size (mm^3)	Peak coordinates		
		x	y	z
None	513	40.5	-7.5	44.5
Child's sex	432	40.5	-7.5	44.5
Child's age at scan	324	43.5	-1.5	47.5
Lead exposure	405	40.5	-7.5	44.5
Maximum displacement	432	40.5	-7.5	44.5
Maternal age	405	40.5	-7.5	44.5
Maternal education	486	40.5	-7.5	44.5
Smoking during pregnancy	405	40.5	-7.5	44.5